UCLouvain

epl

École polytechnique de Louvain

Techno-economic study of grid-scale Carnot batteries

What techno-economic conditions enable grid-scale Carnot battery deployment?

Author: **Louis Gayina**
Supervisors: **Francesco Contino, Antoine Laterre**
Readers: **Emmanuel De Jaeger, Xavier Rixhon**
Academic year 2022–2023
Master [120] in Electro-mechanical Engineering

Contents

Acronyms

LAES Liquid Air Energy Storage.

PTES Pumped Thermal Energy Storage.

TI-PTES Thermally Integrated Pumped Thermal Energy Storage.

TI-CB Thermally Integrated Carnot Battery.

CB Carnot Battery.

TES Thermal Energy Storage.

VCHP Vapor Compression Heat Pump.

ORC Organic Rankine Cycle.

HP Heat Pump.

HS Heat Storage.

PV Photovoltaic.

CCGT Combined Cycle Gas Turbines.

WT Wind Turbines.

V2G Vehicle-to-grid.

PHS Pumped Hydro Storage.

Acknowledgments

I am profoundly grateful to the individuals who have supported and guided me throughout this journey, making the completion of this master's thesis possible. Their unwavering encouragement, expertise, and camaraderie have been instrumental in shaping this work.

In completing this master's thesis, I was fortunate to receive support, advice and inspiration from a diverse and remarkable group of people. I would like to thank Antoine Laterre, Xavier Rhixon, Diederik Coppitters and Gauthier Limpens for their contributions. They played an essential role in the realization of this work, and I am grateful for their presence on my journey.

I sincerely thank my professor, Prof. Francesco Contino, for your mentorship. Your willingness to fuel my intellectual curiosity and push me beyond my limits has been crucial to my academic development.

My gratitude extends to my beloved family and friends, whose unwavering support, encouragement and faith in my abilities have sustained me throughout this journey. Your presence, understanding and words of encouragement have been the foundation on which my success is built. I would especially like to thank Eva Kévers for her unconditional support.

A special thank you is reserved for my high school mathematics teachers, Mr. Alain Burton, Ms. Hélène Cochart and Ms. Virgine Genard, whose dedication to education and passion for mathematics ignited my fervor for engineering. Your teachings and your unshakeable faith in my abilities were the driving force behind my decision to obtain this university degree.

Finally, I'd like to thank Mr Novotny and Mr McTigue for the time they gave me when I reached out to them.

In closing, this master's thesis stands as a testament to the collective efforts of these extraordinary individuals. Their impact on my academic and personal growth has been immeasurable, and I am humbled by their unwavering support.

This work was written with the help of DeepL and chatGPT.

Abstract

This master's thesis offers an investigation into the techno-economic aspects and potential applications of three distinct Carnot batteries designed for daily energy storage purposes. The primary objective of this study is to enhance our comprehension of the potential framework within which Carnot batteries could be deployed.

Through the utilization of an energy system optimization model, the deployement costs of Carnot batteries on a grid scale are determined. This methodology serves to emphasize how the performance disparities among various technologies directly influence their deployment costs.

The findings of this research work provide a better understanding of how the Carnot battery would be used, and the costs at which the Carnot battery would prove to be the optimal solution in Belgium.

In summary, this master's thesis not only clarifies the economic and operational complexities associated with the integration of Carnot batteries, but also provides an assessment of their potential contributions to energy systems. The impact of the performance and discharge time of these machines on their deployment underlines the complex nature of energy storage planning, highlighting the need for meticulous deliberation and well-informed decision-making to move towards a sustainable and efficient energy future.

Introduction

Climate change is one of the most pressing challenges that humanity faces today. It is caused by the release of greenhouse gases into the atmosphere, primarily by the burning of fossil fuels for energy. The consequences of climate change are severe and far-reaching, including rising temperatures, more frequent and severe weather events and rising sea levels. As a result, renewable energy sources have been developing rapidly to replace fossil fuels and mitigate ongoing climate change.

Renewable energy sources are those that can be replenished naturally and are not finite in their availability. These include solar, wind, hydro, and geothermal power, among others. In recent years, there has been a significant increase in the adoption and development of renewable energy sources, driven by both environmental concerns and economic benefits. Renewable energy is often considered to be a cleaner and more sustainable alternative to traditional fossil fuel-based energy sources, which are a major contributor to greenhouse gas emissions.

However, the intermittency of renewable energy sources, largely attributed to the weather-dependent nature of solar and wind power, can lead to significant fluctuations in their power output. In some regions, this phenomenon is best exemplified by the "Duck curve" where solar production peaks during midday and drops off sharply in the evening as demand rises creating a load curve that looks like a duck. This can pose challenges for grid operators who must balance supply and demand to maintain grid stability. Energy storage can help balance the intermittency of renewable energy sources by capturing excess electricity during times of high production and releasing it during periods of low output. This not only helps maintain a stable grid but can also increase the utilization of renewable energy resources, leading to a more cost-effective and sustainable electrical system.

As the world transitions to a low-carbon energy system, the energy storage technologies are becoming increasingly important. However, not all storage systems are equivalent. Storage systems differ in a multitude of aspects including storage capacity and power, storage duration, efficiency, cost and environmental impact. For instance, pumped hydro storage has been widely used for many years and offers reliable long-duration storage. However, it requires specific geological features and can have significant environmental impacts. Meanwhile, lithium-ion batteries are gaining popularity due to their high energy density, fast response time, and modular design but these batteries are resource-intensive to produce and may not be able to provide electricity for extended duration. As a result, there is a growing need for energy storage technologies that can provide electricity for several hours or more.

It is therefore becoming increasingly important to assess the feasibility of different storage systems, taking into account the different factors that define them but also the context in which they fit. Analyzing the trade-offs and benefits of each technology in relation to these factors is essential to make informed decisions that optimize resource use and minimize environmental impact and costs.

In this study, the focus is on the integration of the Carnot battery within an energy system and exploring the techno-economical conditions that contribute to the potential of this technology. The research question that is covered is stated as follows : *what are the techno-economic conditions that allow the deployment of grid-scale Carnot batteries ?*

In order to answer this question, the work will be done using the EnergyScope TD tool and optimizing an energy system representing the Belgian energy system. The focus of the study will be on three promising Carnot battery technologies: a recuperated Brayton Carnot battery, a Thermally integrated Rankine Carnot battery, and a Carnot battery made from a retrofitted coal-fired power plant.

The work is organized into five chapters :

- **Chapter 1 - Literature review**
- **Chapter 2 - Methodology**
- **Chapter 3 - Results & Interpretation**
- **Chapter 4 - Discussion**
- **Chapter 5 - Conclusion**

Chapter 1

Literature review

The purpose of this chapter is to lay the foundation for the rest of this work. The chapter is structured into three sections. The first section provides a descriptive overview of the Carnot Battery (CB), including the principles of the Brayton and Rankine Pumped Thermal Energy Storage (PTES) cycles. The second section presents a literature review of the CB, highlighting the research gaps and questions that will be addressed. Finally, the third section will briefly describe EnergyScope, the tool used to answer the research questions.

1.1 What is a Carnot Battery?

The concept of CBs appeared for the first time in the literature in 1924 [29] but their interest has increased in recent years with the development of renewable energies in the context of the energy transition.

CBs are energy storage solutions where electricity is stored as thermal exergy. During charge, an electric input is used to produce thermal exergy which is stored in thermal reservoirs; the temperature difference then drives a power cycle for electricity production during discharge. Hence, CBs charge and discharge processes involve, respectively, forward and backwards conversion between electricity and heat, while the storage consists of a Thermal Energy Storage (TES) [44, 33, 10].

CBs include several technologies and configurations, but the fundamental principle remains the same: a CB is an electrical energy storage technology. Therefore, there must always be at least one electrical input and one electrical output [10]. However, a CB is capable of multi-vector integration, i.e., it is able to use and produce electricity and heat. This configuration is more commonly known as Thermally Integrated Pumped Thermal Energy Storage (TI-PTES). In this case, the use of additional heat streams to supply the Heat Pump (HP) increases the efficiency during charge and therefore offers a higher power-to-power efficiency. This technology associated with a residual heat source could therefore make it possible to recover this heat in order to store electricity with a higher efficiency. A classical representation of the CB is provided in figure 1.1.

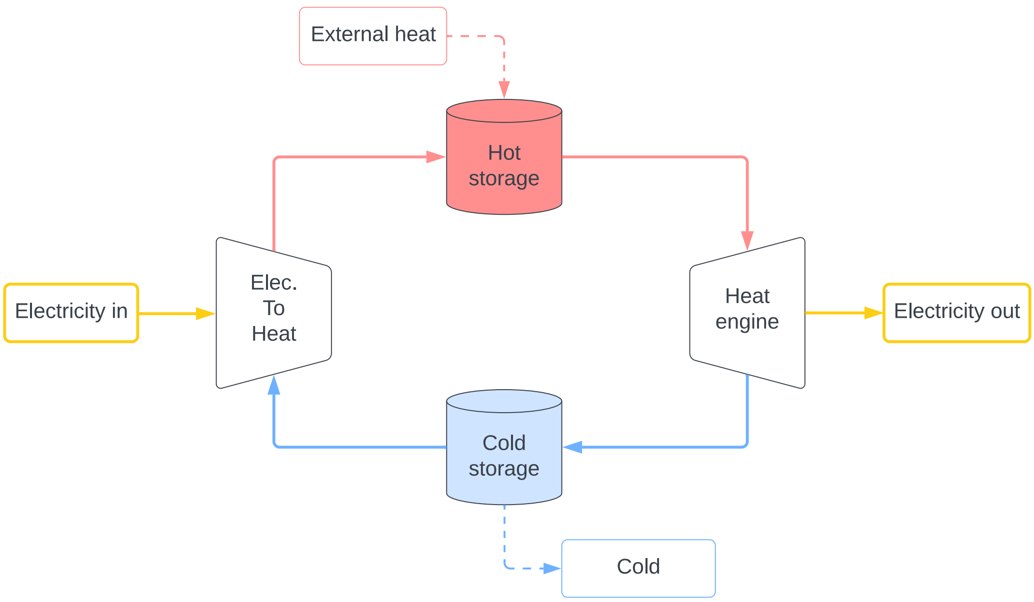

Figure 1.1: Carnot battery concept

It is important to note that there are many ways to make a Carnot battery. In the precedent representation, descriptive terms are chosen only to conceptualize the Carnot battery. In all generality, the CB can be broken down into three parts: The electricity to heat conversion machine, the Heat Storage (HS) and the heat to electricity conversion machine. These parts represent various technological elements and a choice can be made among them.

For example:

- **The electricity to heat conversion machine can be:** An electrical heater, a vapor compression heat pump, a super-critical heat pump, transcritical heat pump (which can be used for trigeneration systems) [44, 10].
- **The heat storage can be:** a Latent heat thermal storage, a sensible heat thermal storage and a thermochemical storage, although the latter will not be discussed in this study [44, 10].
- **The heat to electricity conversion machine can be:** A conventional steam Rankine cycle or an organic Rankine cycle, a gas turbine or a Stirling engine [44, 10].

Another advantage of the CB is that it is capable of reusing existing facilities and some countries (China, Chile, Germany, USA) are investigating the possibility of reusing their existing coal-fired power plants in order to convert them into CBs [2, 47, 20].

Because of the number of possible configurations, several categories of CBs are used: Liquid Air Energy Storage (LAES) and PTES [10, 44, 33]. In this study, only the PTES solution will be examined because, as mentioned in [19], these two technologies are competitive with each other but, in terms of power capital cost, LAES was already found to be more competitive than a variety of existing technologies. This is less clear for PTES.

Figure 1.2 shows this usual classification. The technologies excluded from further discussion are presented on the left side of the diagram, such as the Lamm-Honigmann process (Thermochemical energy storage) and LAES. While the right-hand side is dedicated to the technologies that are discussed and can be classified as PTES which are again divided in two subgroups: Brayton cycle and Rankine cycle.

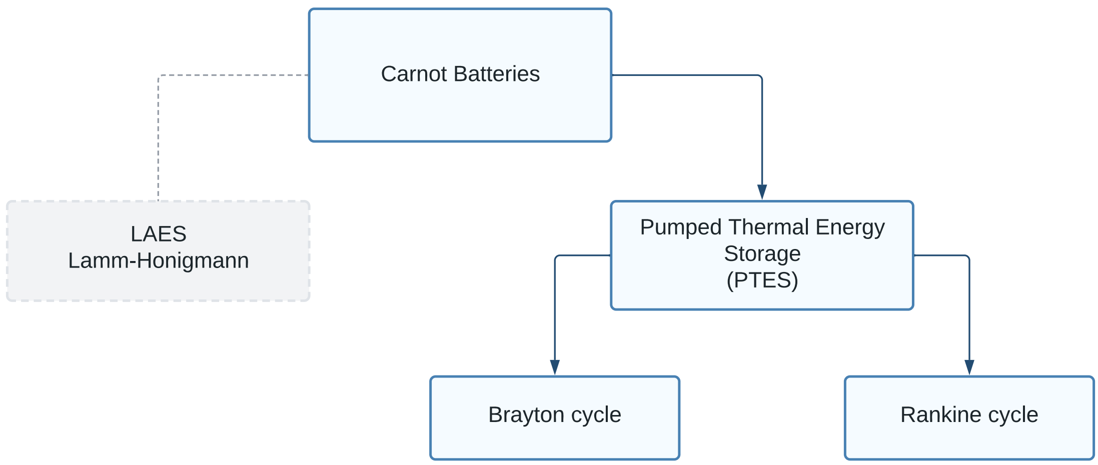

Figure 1.2: Classification of Carnot batteries in this study

1.1.1 Brayton cycle PTES

A Brayton CB, i.e., a Brayton PTES, is usually composed of a Brayton HP and a Brayton heat engine. The HP operation is based on an inverse closed Brayton cycle with two sensible heat thermal reservoirs (High temperature and Low temperature). Given this layout, the complete electrical energy storage usually contains two thermal reservoirs and four machines (two compressors and two expanders) [10].

Another way to approach PTES with Brayton cycles is to consider the cycle shown in figure 1.3, which uses reversible machines (an approach that is purely theoretical).

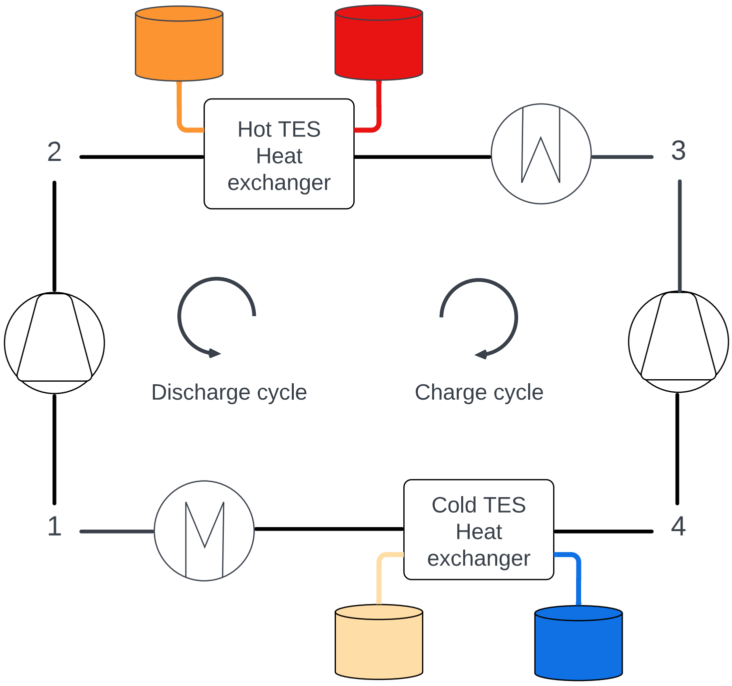

Figure 1.3: Process flow diagram for a Brayton cycle PTES

This layout reduces the total cost of the system but also reduces its overall performances. It should be noted that due to its cyclic operation and the irreversibilities caused by compression and expansion, it is usually impossible to perfectly match the inlet and outlet temperatures of compression and expansion between charge and discharge cycles. In this case, heaters and coolers can be used to adjust the output conditions of the machine. In this way, the heat generated by the irreversibilities is removed to the environment, and the storage can be operated cyclically, these heaters and coolers are also represented on figure 1.3 [44].

The process can be described as follows, when charging, the Brayton cycle CB operates in a clockwise direction. The working fluid in gaseous state is compressed (1-2), transferring the heat of compression to the hot TES (2-3). This is followed by gas expansion (3-4), which results in lower outlet pressure and temperature at point 4, leading to a decrease in the temperature of the cold TES (4-1). This establishes a positive temperature difference between the two thermal reservoirs. During discharge, the cycle is reversed, with heat transferred from the hot TES to the pressurized fluid (3-2) to drive turbine expansion (2-1), and cold energy used (1-4) to reduce compression work (4-3).

Brayton PTES cycles are usually considered as standalone units because of their high operating temperatures up to 1000 °C [44]. This kind of temperature level is the reason why CBs based on the Brayton cycle are not specifically studied for thermal integration since the waste heat is at much lower temperature levels. However, a trigenerative Brayton PTES system with heat exchangers providing heat and cold thermal energy could be capable of achieving higher electrical efficiencies when properly integrated [50].

The high temperatures reached by Brayton cycles allow typical configurations to produce between 5 to 50 MWe as per Vecchi et al.However, this margin could be extended from 1 to 100 MWe if the development of certain projects, such as the one proposed by Malta Inc. for the recovery of a coal-fired power plant using a 100 MWe Brayton cycle (referred to as the Malta heat engine), is relied upon. This would enable the reduction of investment costs for the project through the recovery of a portion of the previous installation's resources (Truong et al., 2022).

Based on the research conducted by White (2013) [48], it has been demonstrated that the efficiency of a system is primarily influenced by the temperature ratio, rather than the pressure ratio. When comparing the efficiency of CBs utilizing Brayton and Rankine cycles, it has been observed that the former generally achieves a higher round-trip efficiency, mainly due to its higher temperature levels. However, there are instances, such as in Thermally Integrated Carnot Batteries (TI-CB), where the Rankine cycle may outperform the Brayton cycle in terms of power-to-power efficiency.
In the literature, round-trip efficiencies ranging from 40 to 70% are observed [10]. The high values of 60-70% are calculated with very high compressor/turbine polytropic efficiencies, which are over 90% [10], this fact must be taken into account when making a more simplistic model of a CB because these results are optimistic, such values will probably not be reached in reality.

Packed beds thermal reservoirs are mostly considered for this application due to lower cost and larger operating temperature; typical solid storage media include gravel, magnetite and limestone [44]. With a packed bed, TES can be either indirectly linked to the cycle via a coupling heat exchanger [7] or can be directly crossed by the working fluid [46]. This latter option allows for better heat transfer, but the TES containment tank must be able to withstand pressures of 20 to 30 bar[10]. In addition to the above-mentioned pressure problem, packed beds TES systems have some drawbacks. For instance, they demand a considerable installation space and possess relatively low heat transfer rates, which can impede their efficiency. Moreover, the materials used in these systems usually necessitate frequent maintenance or replacement due to wear and tear caused by frequent changes in pressure and temperature. Additionally, these systems often need to be cleaned regularly to remove accumulated sediment, which can affect their long-term efficiency [3]. In contrast, molten salt TES systems have attracted significant attention in recent years as a promising alternative for packed bed systems in high-temperature applications, particularly concentrated solar power [28, 35]. Molten salt systems offer some notable advantages, such as high energy density and good heat transfer characteristics as well as temperature stability, which can significantly enhance their performance and reduce the overall system cost. Furthermore, molten salt systems can withstand high-temperature cycling and have longer cycle lives compared to conventional packed bed systems, which tend to lose their efficiency over time due to sediment accumulation [3]. However, molten salt HS systems come with certain drawbacks, such as their cost or the technical challenges associated with their high melting temperature, which can lead to issues with the solidification of molten salts within the pipes [36]. Finally, combined storage or storage of high-temperature phase-change materials alone are interesting solutions, but these solutions must be studied in greater depth [26].

The above discussion suggests that molten salt storages offer certain advantages over packed bed storages. However, the use of molten salt storage requires ensuring that it remains above a minimum temperature within the cycle to prevent it from returning to the salt's freezing point. To address this issue, some authors have proposed the use of a recuperator within a Brayton cycle [24, 30]. This cycle has the added benefit of having a higher efficiency compared to a conventional Brayton cycle and makes use of molten salts. Further details regarding this cycle will be expounded upon in the subsequent chapter.

It must also be mentioned that the combination of electric heating and a gas cycle has also been considered, but with rather low round trip efficiencies(40-50%) [5]. This is one reason why this layout will not be considered in this study.

1.1.2 Rankine cycle PTES

The second branch of PTES technology is based on Rankine cycles, i.e., a Rankine PTES. Rankine PTES could be a valid alternative to the Brayton cycle and usually stores energy at a much lower temperature [10].

A Rankine CB, is usually comprised of a vapor compression heat pump and a power recovery unit based on a Rankine cycle, plus a TES section. For a resistive heating system, the HP is replaced by a resistive heater [44]. A process flow diagram of a Rankine PTES is shown in figure 1.4.

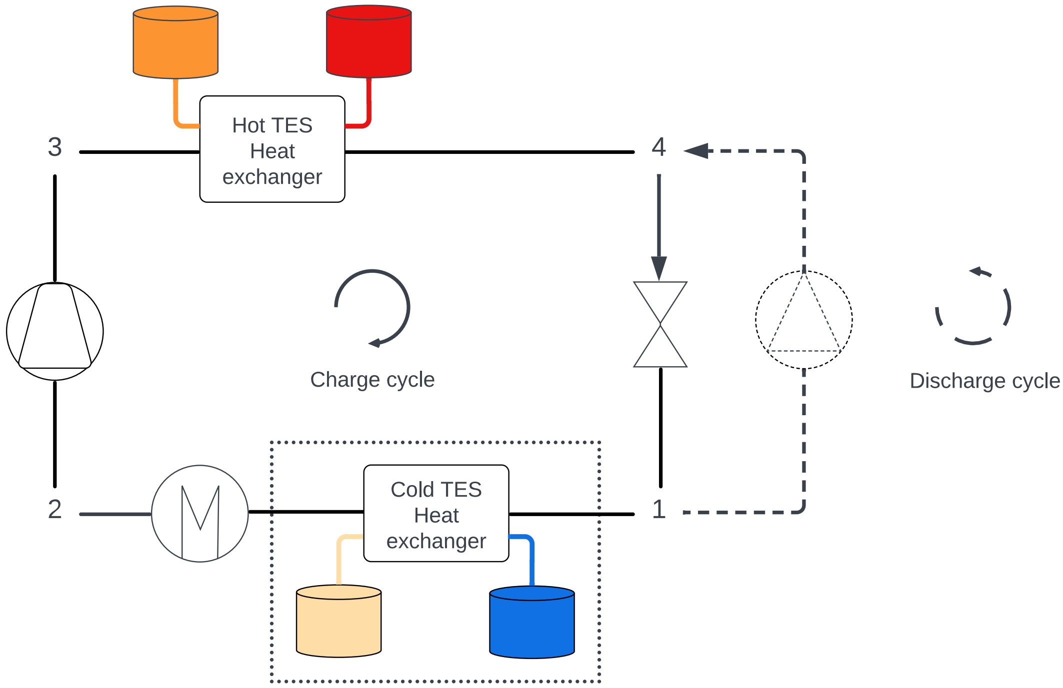

Figure 1.4: Process flow diagram for a reversible Rankine cycle

During charge, the working fluid is evaporated (1–2) and then compressed to high pressures and temperatures (2–3), releasing both sensible and latent heat to the hot storage unit during condensation (3–4) and is finally expanded to low pressures (4–1). For discharging or power production, the liquid fluid is pumped to a high pressure (1-4), evaporated with energy from the TES (4-3) and expanded in a turbine (3-2). It is finally condensed through an auxiliary heat exchanger and the cold storage (2-1) [44].

A common Rankine PTES system layout has only a hot reservoir and uses the ambient as the cold sink/source, which is practical and inexpensive. Water (pressurised, if necessary) is widely adopted for the hot TES, due to material abundance, high energy density and low cost [44]. If a cold TES is considered, an ice slurry is a popular choice, mostly applied to CO_2-based Rankine PTES [44].

Rankine PTES solutions studied in the literature include the steam Rankine cycle [45] and Organic Rankine Cycle (ORC)[22, 9]. The choice of the working fluid is driven by the scale and temperature levels throughout the process[44, 26]. These choices include organic refrigerants, non-organic refrigerants, water, ammonia, and ethanol. Frate et al. [16] showed how different fluids maximize different performance indicators (e.g. power density vs exergy efficiency) [44]. Water is selected for cycle temperatures above 200 °C, which is not the case unless an external heat source is available [44]. In the range below 150 °C, R1233zd (E) is generally preferred, as it enables efficient cycle operation, is cost effective due to reduced equipment sizing and because it gives good performance at a small pressure ratio [26, 15, 44].

The actually considered Rankine cycle PTES has a limited span between the highest and lowest cycle temperatures. This limitation has several implications. First, it produces, on average, lower efficiencies compared to Brayton cycles (Mean value of 61.6% for Brayton PTES and 52.8% for Rankine PTES are observed) [44]. Second, it results in a lower power range.

Nevertheless, the limited temperature span allows for thermal integration with external heat sources (Waste heat sources in particular). By integrating waste heat streams, the power-to-power efficiency can be raised above 100%, assuming a free waste heat stream [44, 10, 17]. TI-PTES is one area with high research interest and will be discussed in this study.

Finally, with the gradual phasing out of coal-fired power plants and the transition to renewable energy resources underway, retrofitting these power plants with the storage technology is a promising approach. One option is to retrofit steam Rankine cycles, which have been used in power generation in most of coal-fired power plants. The retrofit can involve a replacement of firing chambers with Renewable Energy Sources-powered TES and has the potential to bring existing conventional power plants in line with net-zero carbon policy objectives. Moreover, reusing existing equipment such as suitable steam turbines, heat recovery steam generators or heat exchangers is characterized by significant potentials for higher cost-effectiveness [44]. Retrofitting existing power plants with this technology has the potential to contribute to the reduction of greenhouse gas emissions, extend the operational lifespan of current infrastructure, and aid the transition to a more sustainable energy system. Additionally, this approach may have environmental advantages as it involves reusing existing equipment and may require less harmful materials than other technologies, such as Li-Ion batteries, or cause less environmental damage than Pumped Hydro Storage (PHS).

1.2 Literature review

In recent years, there has been a significant expansion of research on CBs, with several studies exploring the latest developments and trends in this field. Notably, the state-of-the-art reviews by Novotny et al. and Vecchi et al. [33, 44] have identified similar research directions and highlighted specific types of CBs that have shown promise.

The studies suggest that two main types of CBs have emerged as leading candidates: LAES and PTES. The aforementioned category can be classified into two distinct types, namely Brayton and Rankine PTES. Vecchi et al. highlighted that although these technologies span a vast range of layouts and commercial scales [44], the vast range of application of this technology makes it challenging to determine the suitable charge and discharge times for integrating these machines into an energy grid. As a result, there is currently no definitive guidance on the appropriate charge and discharge times when integrating these machines into an energy system. Additionally, the authors note that there is little scientific discussion around concepts based on electrical resistances, despite the fact that numerous industrial projects such as [42, 1] are based on this technology [33, 44].
According to Vecchi's research on CBs, the technology has the potential to serve needs that PHS and Lithium-ion batteries cannot fulfill [44]. Meanwhile, McTigue et al. noted in their study that Brayton PTES could prove more advantageous than a Lithium-ion battery for discharge periods exceeding 6 hours [30].

In recent years, a trend has emerged among industries in various countries such as Germany, China, the US, and Chile, to retrofit coal-fired power plants in order to reduce capital costs [42, 1]. To do this, the industries are developing conceptual plans to reuse equipment from former coal-fired power generation sites, reusing the existing Rankine steam cycle and other equipment on site. The existing steam cycle could be connected to a HS system which would be charged by a new electrical resistor or heat pump. Despite this growing interest, there is still a scarcity of studies on this subject and industry documents are not readily available to the research community, despite the call for transparency of technical and economic data [44]. It should be noted that some companies are considering the use of HPs to improve power-to-power efficiency, although electrical resistance-based retrofits remain a cheaper option [42].

Frate and Dumont are among the authors who have investigated TI-CB from a research perspective [18, 17, 8, 9]. The idea behind these batteries is to use waste heat as a means to improve the power-to-power efficiency of the machine. This concept is promising as several initiatives including "The heat roadmap" are trying to promote a decarbonisation of the heat and cooling sector, a good way to achieve this would be to reuse the waste heat available in large quantities in Europe [21].

However, as Dumont mentions [10], only a few studies have examined TI-PTES integration in terms of the actual availability of waste heat streams to be exploited. In other words, given that the available heat stream is set by the upstream system (e.g., an industrial facility for waste heat), how large can the electrical storage system be? Is the amount of waste heat sufficient to deploy the thermally integrated Carnot battery?

This study aims to address various questions that surfaced during the literature review, which are as follows: *At what cost does this technology become attractive, and what impact does efficiency have on its implementation? What role will the technology play in the Belgian energy system once deployed? How does the discharge time, and therefore, the energy to power capacity ratio of these technologies affect their deployment and the energy system in which they are integrated? Specifically to thermally integrated Carnot battery, what amount of heat is necessary to have a deployment of the technology?*

These questions can be summarized in a more global question: *What techno-economic conditions enable grid-scale Carnot battery deployment?*

1.3 EnergyScope

For the purpose of this study, the energy system was modeled and cost-optimized using EnergyScope TD - an ESOM (Energy System Optimization Model) that enables the modeling and optimization of energy systems. This tool is an open model that optimizes the design and operation of an urban or regional energy system considering all energy carriers and demand with hourly resolution over a target year. The objective of the tool is to study the interactions between sectors and the implementation of promising technologies, such as storage, during the energy transition [27].

Description of the tool

The tool operates in two stages. The initial phase involves preprocessing input data such as time series, scenarios, and technologies, followed by solving a mixed-integer linear programming (MILP) problem. This process determines the appropriate set of typical days used to represent a full year. These typical days are generated to simulate electricity and space heating demand as well as weather conditions (solar irradiance, onshore wind speed and offshore wind speed).

The second step is the main energy model: it identifies the optimal design and operation of the energy system over the selected set of typical days, i.e. technology selection, sizing and operation for a target future year under CO_2 emission constraints [27]. The model's second phase involves optimizing the overall annual cost. The objective function, which needs to be minimized, is expressed as:

$$min\ C_{tot} = min\ (\sum_{j\ in\ TECH} (C_{inv}(j)\tau_j + C_{maint}(j)) + \sum_{i\ in\ RES} C_{op}(i))$$

with:

- TECH and RES are sets including respectively the conversion technologies and resources,
- $C_{inv}(j)\tau_j$ is the annualised investment cost of technology j expressed in M€,
- $C_{maint}(j)$ is the operating and maintenance cost of technology j expressed in M€,
- $C_{op}(i)$ is the operating cost of resource i expressed in M€.

This cost function is restricted by a GWP (Global Warming Potential) limitation for the entire energy system, which cannot be exceeded:

$$gwp_{limit} \geq \sum_{i\ in\ RES} GWP_{op}(i) + \sum_{j\ in\ TECH} \frac{GWP_{constr}(j)}{lifetime(j)}$$

where:

- TECH and RES are sets including respectively the conversion technologies and resources,
- gwp_{limit} is the maximum allowed amount of yearly emissions expressed in $ktCO_{2eq}/y$,
- $GWP_{op}(i)$ is the amount of emissions due to the resource i expressed in $ktCO_{2eq}$,
- $\frac{GWP_{constr}(j)}{lifetime(j)}$ is the amount of emissions resulting from the production and dismantling of technology j throughout its lifespan, expressed in $ktCO_{2eq}/y$.

Figure 1.5 depicts the two-step process outlined in this description.

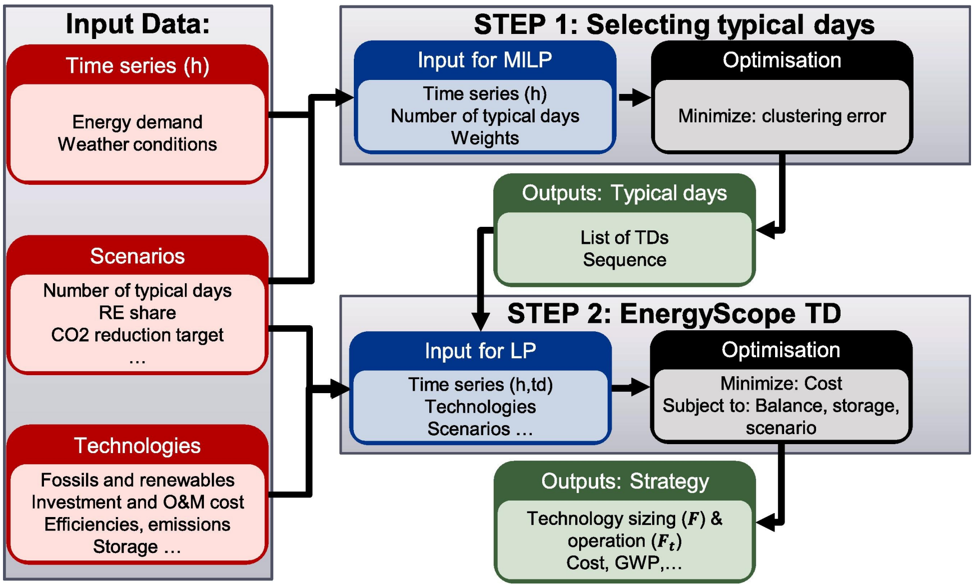

Figure 1.5: Overview of the 2 step process [27]

How does the tool work?

The proposed modelling framework is a simplified representation of an energy system accounting for the energy flows within its boundaries. Its primary objective is to satisfy the energy balance constraints, meaning that the demand is known and the supply has to meet it. The input for the proposed modelling framework is the End Use Demand (EUD) in energy services, represented as the sum of four energy-sectors: electricity, heating, mobility and non-energy demand. Heat is divided in three End Use Types (EUTs): high temperature heat for industry, low temperature for space heating and low temperature for hot water. Mobility is divided in two EUTs: passenger mobility and freight. Non-energy demand is, based on the IEA definition, "fuels that are used as raw materials in the different sectors and are not consumed as a fuel or transformed into another fuel." [27]. The energy system encompasses all the energy conversion technologies needed to transform resources and supply the EUD. These technologies are used to supply *layers*. *Layers* are defined as all the elements in the system that need to be balanced in each time period; they include resources and EUTs. As an example, the electricity layer must be balanced at any time, meaning that the production and storage must equal the consumption and losses. These layers are connected to each other by technologies. Three types of technologies are defined:

- **Technologies of end-use type** can convert the energy (e.g. a fuel resource) from one layer to an EUT layer, such as a combined heat and power unit that converts natural gas into heat and electricity.
- **Storage technologies** convert energy from a layer to the same one, such as TS that stores heat to provide heat.
- **Infrastructure technologies** gather the remaining technologies, including the networks, such as the power grid and District Heating Networks, but also technologies linking non end-use layers, such as methane production from wood gasification or hydrogen production from methane reforming.

Implementing the technologies

Details regarding the implementation of technologies within EnergyScope are provided here, as they were necessary for the completion of the work. For each technology that was implemented, the corresponding values are to be specified:

Design variable	Generation assets Corresponding unit	Storage assets Corresponding unit
c_{inv}	[Meuro/GW]	[Meuro/GWh]
c_{maint}	[Meuro/GW/y]	[Meuro/GWh/y]
gwp_{constr}	[$ktonCO2_{e}q$/GW]	[$ktonCO2_{e}q$/GWh]
Lifetime	[Years]	[Years]
c_p	/	/
$f_{min,perc}$	%	%
$f_{max,perc}$	%	%
f_{min}	[GW]	[GWh]
f_{max}	[GW]	[GWh]

Table 1.1: Generation and storage assets input data

For storage technologies, the following values also have to be provided:

Design variable	Corresponding unit
τ_{charge}	h
$\tau_{discharge}$	h
storage$_{availability}$	/
storage$_{losses}$	%/h

Table 1.2: Storage assets input data

Finally, the technologies (Generators and storage units) should interact with layers and vice versa, to do that, efficiencies are used in matrixes linking technologies to layers.

Limitations of EnergyScope TD

EnergyScope TD is not a predictive model, but rather an optimization model that aims to provide the optimal energy system design while considering assigned constraints. Its primary objective is to minimize system costs, but it does not take into account certain parameters such as risk and failure, geopolitical factors, and environmental impacts. While policymakers can use this type of model, they should be aware that it has limitations and should be complemented with additional constraints beyond its scope.

It is essential to note that EnergyScope TD focuses equally on different energy usage domains, such as mobility, power, heating, and Non-Energy Demand. The model is designed to operate on a large scale, such as national and annual scales, which sometimes results in a lack of precision. This makes it challenging to analyze at smaller scales, such as hourly market price variability and single building focus. Overall, EnergyScope TD should be considered a tool for devising potential strategies for future energy system design investment rather than a predictive model.

Additionally, it is worth noting that as EnergyScope TD is a linear optimization tool, the accuracy of its results heavily relies on the quality of the data inputted into the optimization problem. To enhance the precision of the results, researchers can use a robust optimization approach that takes into account the uncertainty of the parameters inserted into the model. To enhance the accuracy of the results of this study, exploring this idea could be considered in future research.

A small introduction to the tool's outputs

In this section, an optimization performed by EnergyScope TD is presented to enable the reader to gain a better understanding of the results that will be discussed in upcoming sections. The system introduced here will be utilized extensively throughout the work and is therefore instrumental in comprehending the subsequent stages of this study.

The system presented here is EnergyScope's reference system when subjected to emissions constraints of up to 25 $MtCO_{2eq}$. To delve into EnergyScope's outcomes, the tool provides a means to visually depict the system through a Sankey diagram. The Sankey diagram associated with this system is provided in Figure 1.6 as an illustrative example.

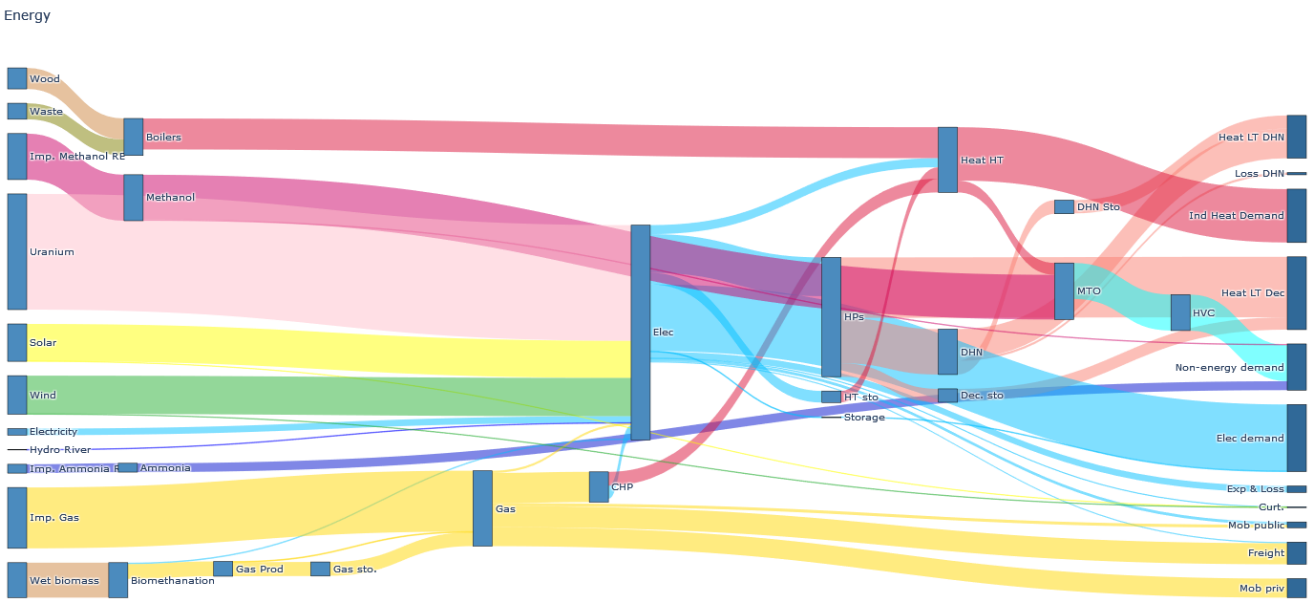

Figure 1.6: Illustrative example: Sankey diagram - 25 $MtCO_{2eq}$ energy system

This figure precisely illustrates the functioning of the energy system and also enhances our comprehension of how EnergyScope operates: Based on the system's demand (right-hand side of the figure), EnergyScope optimizes resource consumption (left-hand side) as well as the technologies to be deployed (conversion between resources and demand) to minimize the total costs of the system while staying within the imposed constraints. As an example, the sankey diagram can be read as follows: Electricity demand is mainly met by resource conversion units (such as solar panels, which convert solar resources into electricity). It is shown that a large proportion comes from nuclear power, followed by renewable energies and finally, a fraction of the electricity generated comes from imported gas. However, note that all the electricity generated can be used in other sectors, such as high-temperature heat production or meeting the demand for public mobility.

In this work, the system will be subject to minor deviations; that's why it's necessary to present, in figure 1.7, a visualization that helps understand the behavior of the typical days generated by EnergyScope. In the positive power values, there are production technologies such as photovoltaic (PV) panels, Combined Cycle Gas Turbines (CCGT) , Wind Turbines (WT), and more.

In the negative power values, there are consumption technologies, such as electric heaters that generate industrial heat or electricity consumption (This is 'End use').

In this work, the use of this visualization will primarily be employed to understand how the typical days are influenced by the CB, as the behavior of the studied machine can be directly observed in the daily view, enabling a more effective understanding of its role.

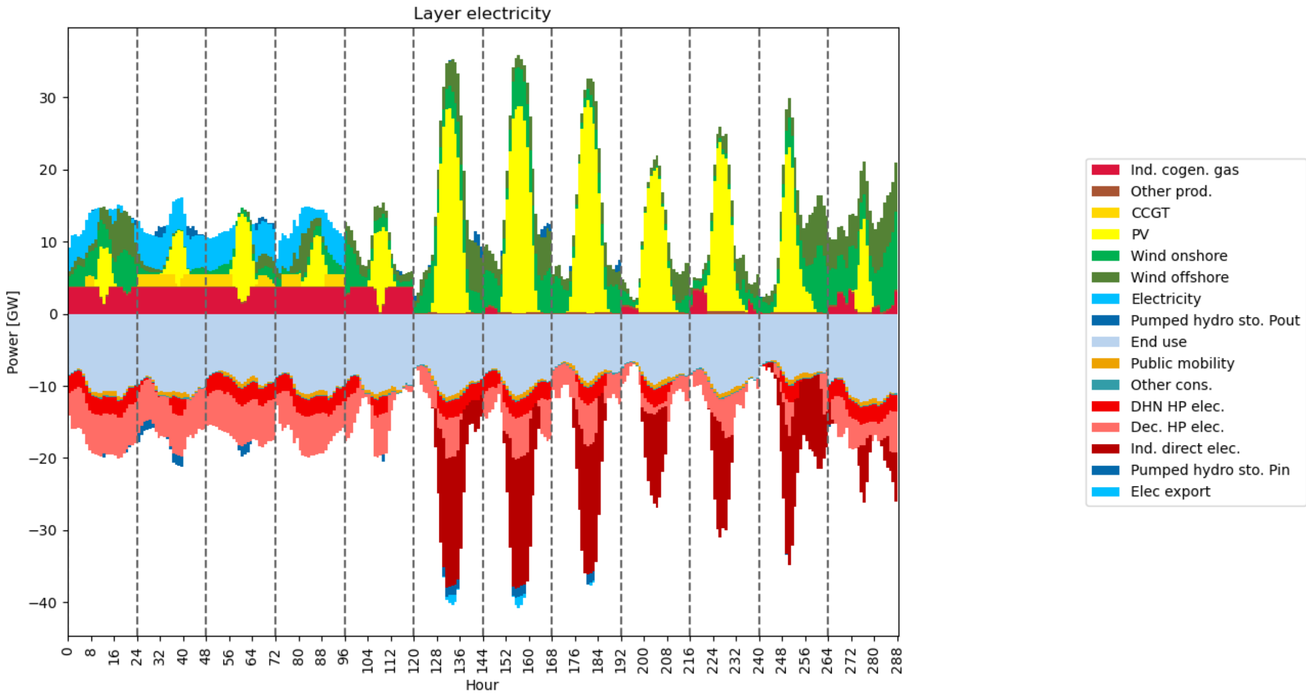

Figure 1.7: Illustrative example: Energy system behavior - 25 $MtCO_{2eq}$ constraint

Chapter 2

Methodology

This chapter presents the methodology used to conduct a techno-economic study of Carnot batteries. The research design involved the utilization of an Energy System Optimization Model (ESOM) to analyze the three types of CBs: Recuperated Brayton CB, Thermally integrated Carnot battery (TI-CB) and Retrofitted coal-fired power plants. The following sections outline the key stages of our methodological approach, including Model review, configuration of the optimization model, and analysis scenarios.

2.1 Model review - Standalone Brayton Cycle

The first considered configuration is a standalone Brayton cycle, more precisely a recuperated Brayton cycle. The cycle comes from a study provided by McTigue et al. [30]. The flow diagram of this cycle is presented in figure 2.1.

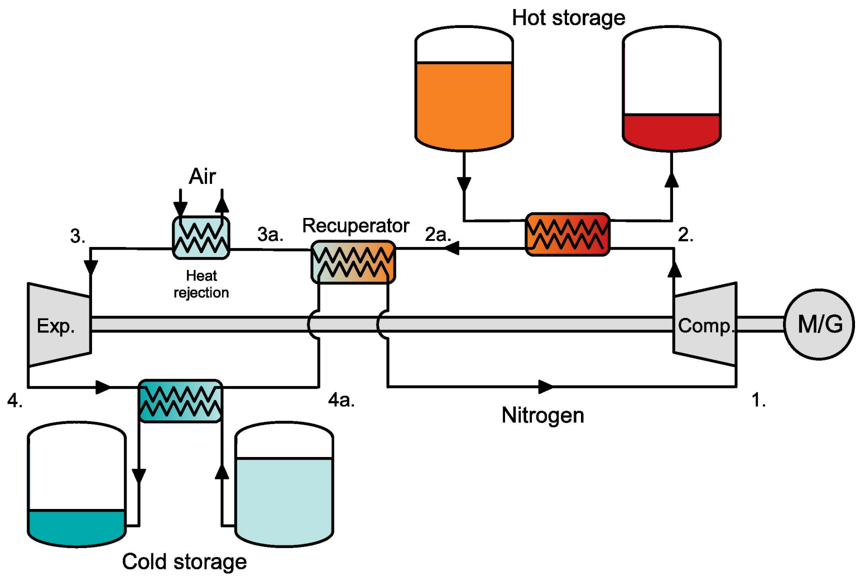

Figure 2.1: Process flow diagram of the recuperated Brayton cycle presented in [30]

The reason for selecting this specific Brayton cycle is partly due to its compatibility with the use of molten salt HS. While packed bed HS may seem appealing due to their lower initial costs, prolonged use of packed bed HS may lead to decreased efficiency and increased maintenance costs. By incorporating molten salts HS in the cycle for high temperature HS, T_3 must be maintained above the freezing point of the salt. Although a simple Joule-Brayton cycle without a recuperator is a viable option, the turbine's work during charge becomes a relatively high fraction of the compression work, resulting in low round-trip efficiencies of approximately 35%, as illustrated in [37]. The cycle proposed by McTigue et al. incorporates a recuperator, which allows the cycle to respect the condition on T_3 by ensuring that T_3 remains above the freezing point of the salt. This, in turn, enables the use of molten salts in the cycle for hot storage, while also improving the cycle's efficiency compared to a simple Brayton cycle. As a result, this cycle appears to be a promising solution in terms of efficiency and maintenance costs associated with the machine.

McTigue's study initially proposes a nominal model for his study, which is then used to perform multi-objective optimization between the cost and efficiency of the proposed nominal machine for two different salts, chloride and nitrate salts. The study of McTigue then focuses on one of the optimized models called 'N2' (Using Nitrate salts), this model will be used for this study since it has low costs for a high efficiency relative to other results proposed in the paper.

The technical and economic parameters of this machine will be presented in the following subsection. Additionally, an estimation of the parameter related to the CO_{2eq} emission constraint resulting from the construction of the machine will also be provided. Then, the methodology used to answer the research question is described, presenting the values used.

Techno-economic parameters

To begin, let's consider the technical parameters of the reference machine that was used. In the study conducted by McTigue et al. [30], the 'N2' machine is thoroughly described in a parametric manner, allowing for an analysis of its integration into the energy system through the manipulation of its parameter values. The parameters used in the modeling are summarized in table 2.1:

Time of charge [h]	Time of discharge [h]	Efficiency	Daily Losses	Availability	Lifetime
10	2-14	59%	5%	1	25

Table 2.1: Technical parameters of the machine[30]

It is important to mention here that the round trip efficiency value is in this case optimistic, the author having used a polytropic efficiency value of 90%. Furthermore, the efficiency is also assumed to be constant in this study although the author shows that the efficiencies are sensitive to the ratio of charge and discharge times.

Let us then examine the economic parameters derived from this parametric model. The study proposes a cost per unit of storage of 260 ± 70 $/kWh [30].

While the value used in this study is assumed to remain constant with respect to discharge time, it should be noted that this assumption does not reflect real-world conditions. Nevertheless, the author acknowledges that no existing research has identified any correlations that would necessitate adjustments for cost variations. Additionally, the costs utilized in this study exhibit a significant degree of variance and are intended solely as a preliminary reference for further investigation.

The costs will be multiplied by a factor of 0.951 Euro / USD in order to be reused in the units of EnergyScope [43].

Global warming potential

The carbon footprint of the system under consideration will be estimated by integrating carbon dioxide emissions from the construction and dismantling phases of a CCGT with the carbon footprint of a molten salt HS system. This approach is adopted due to the lack of a specific life cycle assessment for this technology and the similarities between the machines involved.
Two sources of information were used for the calculations: a National Renewable Energy Laboratory [38] report and an Environmental Science and Technology article [6]. The report quantifies emissions generated during construction and decommissioning as $2\,gCO_{2,eq}/kWh$, while the article finds that the TES alone contributes $4.02\,gCO_{2,eq}/kWh$ to the carbon footprint of the overall system. Combining these values, the emissions related to the technology are estimated to be approximately $6\,gCO_{2,eq}/kWh$. It is worth noting that the calculations were based on a 30-year lifespan of the machines, and the TES was assumed to contribute significantly to the overall carbon footprint.

Model implementation

Based on the previously mentioned data, an electricity storage model can be implemented on EnergyScope. A visual representation of this EnergyScope implementation is provided in Figure 2.2.

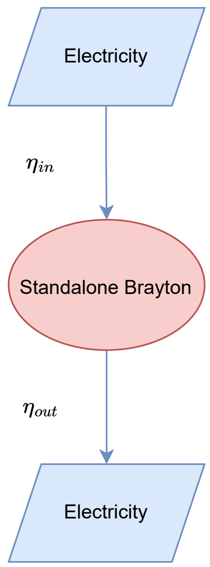

Figure 2.2: Schematics of the recuperated Brayton PTES implementation

Since storage is modeled in terms of a cost per unit of storage and a predefined round-trip efficiency, the technology is considered as a single storage technology that charges and discharges by exchanging electricity with the layer associated with that resource. This technology is considered to be a daily storage technology capable of discharging at a maximum power given by the ratio between the installed storage capacity divided by its discharge time ($P = \frac{f}{\tau_{discharge}}$).

2.2 Model review - Thermally Integrated Rankine cycle

The second solution studied is the thermally integrated Rankine Cycle CB. One key motivation for exploring this concept is the potential to reuse waste heat, which is generated by a range of industrial processes and is often released into the environment as a byproduct. By harnessing this waste heat and converting it into useful energy, the TI-CB can improve the efficiency of energy conversion.
The cycle considered for the TI-PTES is a cycle based on a Vapor Compression Heat Pump (VCHP), an ORC and a thermal storage based on pressurized water. The flow diagram of this cycle is presentend in figure 2.3.

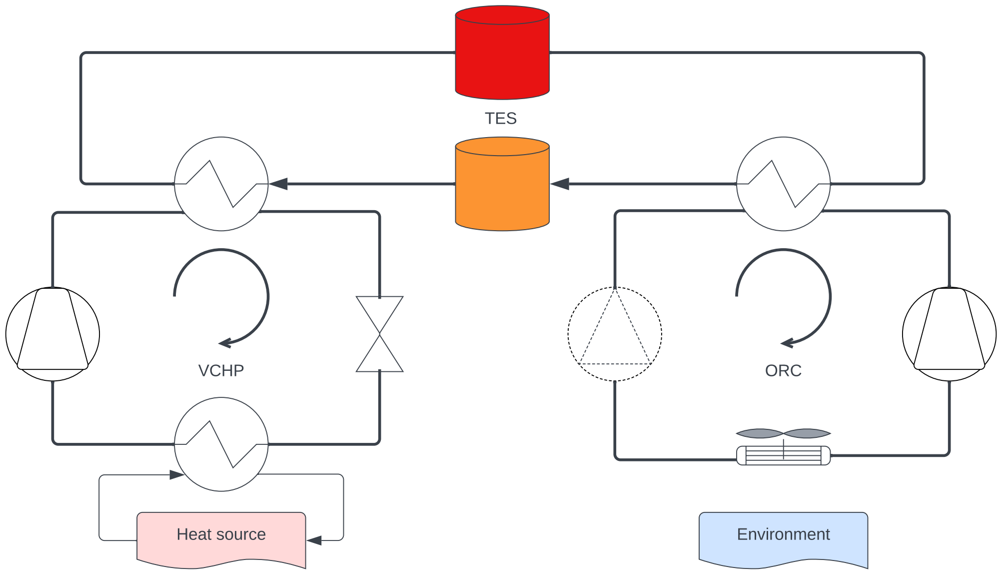

Figure 2.3: Process flow diagram for an Organic Rankine Cycle TI-PTES

The selection of this cycle was primarily motivated by the desire to achieve higher efficiencies while simultaneously reducing system costs. Integration of thermal energy can significantly enhance the overall technology efficiency and facilitate the coupling between electricity and heat. However, in this study, emphasis will be placed on prioritizing electrical energy storage over heat utilization. Heat will be employed to increase the electrical efficiency of the system but will not be utilized to produce heat for a district heating application.

The use of a VCHP is grounded on the underlying objective of reusing waste heat at low temperatures, typically ranging between 40 °C and 90 °C, where alternative heat recovery technologies may be less effective. The primary aim is to elevate the thermal energy from the low-temperature source to higher temperature regimes, typically ranging from 70 °C to 130 °C, where it can be employed for useful purposes.

Technical parameters

In order to comprehensively assess the technical parameters of the machine under consideration, it is imperative to split it into three distinct components. Namely the VCHP, the thermal storage system, and the ORC.

Vapor Compression Heat Pump:

The coefficient of performance (COP) of the VCHP can be computed using a fraction of the carnot efficiency :

$$\text{COP} = \text{Fo}C_{hp} \cdot \frac{T_{tes}}{T_{tes} - T_{source}}$$

Here, the carnot coefficient $\text{Fo}C_{hp}$ is assumed to be 0.4, as per Frate et al. [15]. By varying the source temperature for different storage temperatures, the corresponding COP values can be computed and visualized in Figure 2.4.

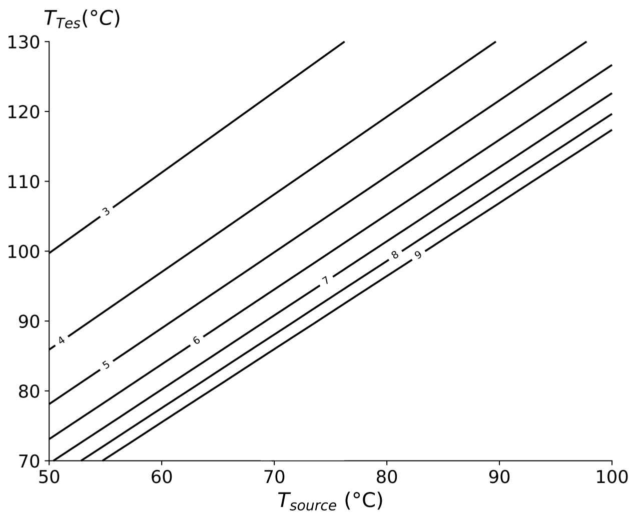

Figure 2.4: COP of the VCHP

Pressurized water thermal energy storage:

Additionally, the use of pressurized water as the storage medium offers a cost-effective, environmental friendly and easily scalable solution that is well-suited for this application [26, 32]. The storage is considered to have daily thermal losses of 5% and efficiencies between storage and created layers are unitary. These losses are not taken into account in round-trip efficiency of the machine even if a 5% loss could potentially impact the storage temperature level, consequently influencing the efficiency of the ORC. Here, these effects are neglected.

Organic Rankine Cycle:

The ORC is chosen due to its higher efficiency at low to medium temperatures, as compared to a conventional steam Rankine cycle. The efficiency of the ORC can be determined using the following equation:

$$\eta = FoC_{orc} \cdot \frac{T_{tes} - T_0}{T_{tes}}$$

where $T_0 = 0\,°C$ is the environment temperature and FoC_{orc} is a fraction of the Carnot efficiency assumed to be 0.35, as per Ohman et al. [34]. The results obtained using this value are presented in Figure 2.5.

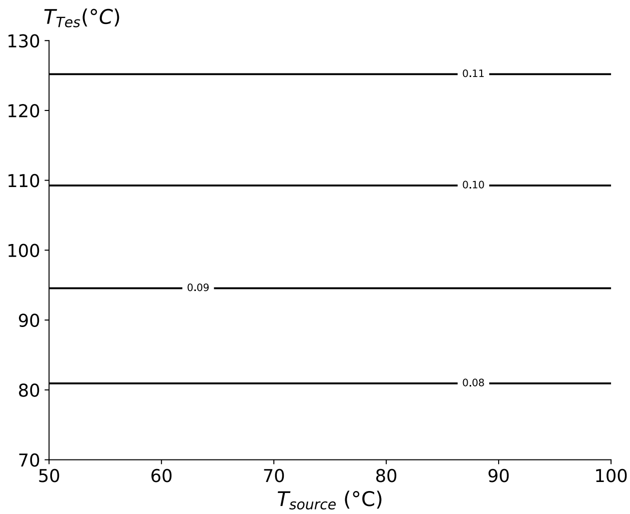

Figure 2.5: ORC efficiency

Round-trip efficiency

The round-trip efficiency η_{RT} will be computed as the product of the ORC efficiency and the coefficient of performance of the heat pump :

$$\eta_{RT} = \eta \times \text{COP}$$

The mapping of this efficiency is presented in Figure 2.6.

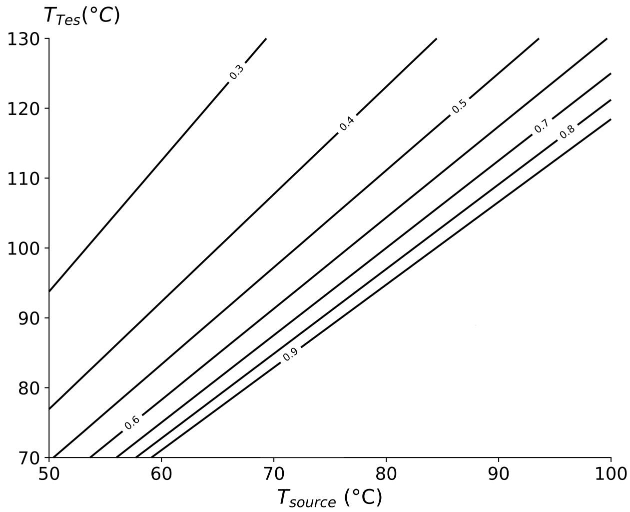

Figure 2.6: Round-trip efficiency for $T_0 = 0\,°\text{C}$

Summary

Finally, after the introduction of these relationships, the remaining parameters are presented, and the technical parameters of the machine are grouped together. The lifetime is based on the lifetime of the HP which is generally considered to be 25 years [40].

$\tau_{charge}(h)$	$\tau_{discharge}(h)$	COP	Daily losses	η_{ORC}	Lifetime	Availability
10	2-14	$\text{COP}(T_{source}, T_{tes})$	5%	$\eta_{ORC}(T_0, T_{tes})$	25	1

Table 2.2: Technical parameters

To the author knowledge, there has been no indication of a minimum discharge time for this machine. A permissible margin of 2 to 14 hours is allowed. Lastly, the COP and η_{ORC} values are computed using $T_{source} = 50$ and $70\,°\text{C}$ while $T_{tes} = 90\,°\text{C}$ giving COP values equal to 3.632 and 7.263 with η_{ORC} constant and equal to 0.087. Finally leading to $\eta_{RT} = 0.63$ and $\eta_{RT} = 0.315$.

Economical parameters

The economic aspect of this concept also needs to be modeled. To achieve this, a decomposition into three components was performed, taking into account the VCHP, the thermal storage, and the ORC separately. For each component, a cost per unit of power (or energy) was determined. The yearly maintenance costs are assumed to be 5% of the investment costs. The methodology is presented below.

Vapor Compression Heat Pump:

In order to determine the costs associated with HPs, a series of manufacturers' technical datasheets showing a price margin per kW of heat [4]. The cost used is 500 €/kW, chosen to reflect the average of the given prices. All the costs of the HPs are shown in the appendix 5.

Pressurized water thermal energy storage:

In accordance with a study conducted by Espagnet et. al [12], cost values for storage per unit of stored energy are suggested, with the following values cited:

Energy stored [kWh]	Cost [€]	Cost per unit of energy [€/kWh]
500	4002.87	8.01
5000	40028.69	8.01
50 000	159725.89	3.19
500 000	5548752.75	11.1

Following this data table, a cost of 10 €/kWh is considered.

Organic Rankine Cycle:

Finally, the costs associated with the ORC are estimated using the module costing technique. This method is useful for making preliminary estimates within precision margins of -20% to +30% [25]. This method applied by Lemmens et al. enables us to find a cost per unit of power of the order of 1843.44 €/kW

Waste heat

EnergyScope currently lacks the functionality to account for various temperature levels when incorporating waste heat, limiting its ability to optimize with a realistic waste heat scenario. To address this limitation, a more comprehensive approach can be taken by conducting an exergy analysis to quantify the available heat resources in Belgium. This analysis begins with estimating the total waste heat potential in Belgium, drawing from sources such as [39] and [11]. The estimated range of available waste heat energy in Belgium falls between 68 TWh and 86.7 TWh.

By using the upper-bound value along with insights from studies like [14] and [39], we can establish an upper limit on the exergy potential inherent in Belgium's waste heat resources.

To proceed, we identify the sources of this waste heat, as categorized by [39]. Grouping thermal power and waste-to-energy under the umbrella of 'electricity generation,' while maintaining industry as a distinct category, we find that 55.59% of waste heat emissions originate from the electricity generation sector, whereas the industrial sector contributes 44.09%.

Further insights from [14] allow us to determine temperature thresholds associated with each sector. Specifically, the research indicates that 88% of waste heat from power generation and 42% from the industrial sector exhibit temperatures below 100°C.

Lastly, the exergy content of this waste heat can be calculated using the Carnot efficiency equation:

$$\eta_C = 1 - \frac{T_{low}}{T_{high}}$$

In this context, T_{low} corresponds to the heat collection temperature of the HP, while T_{high} is considered to be 100 °C. This equation provides a valuable tool for evaluating the potential efficiency and utilization of the available waste heat resources.

We finally obtain the results from table 2.3 :

Table 2.3: Available exergy from waste heat in Belgium

	Electricity	Industrial	Total	Units
$T_{low} = 50\,°C$	5683.3	2151.3	7834.5	GWh/year
$T_{low} = 70\,°C$	3410.0	1290.8	4700.7	GWh/year

Model implementation

Based on the previously mentioned data, an electricity storage model can be implemented on EnergyScope. A visual representation of this EnergyScope implementation is provided in Figure 2.7.

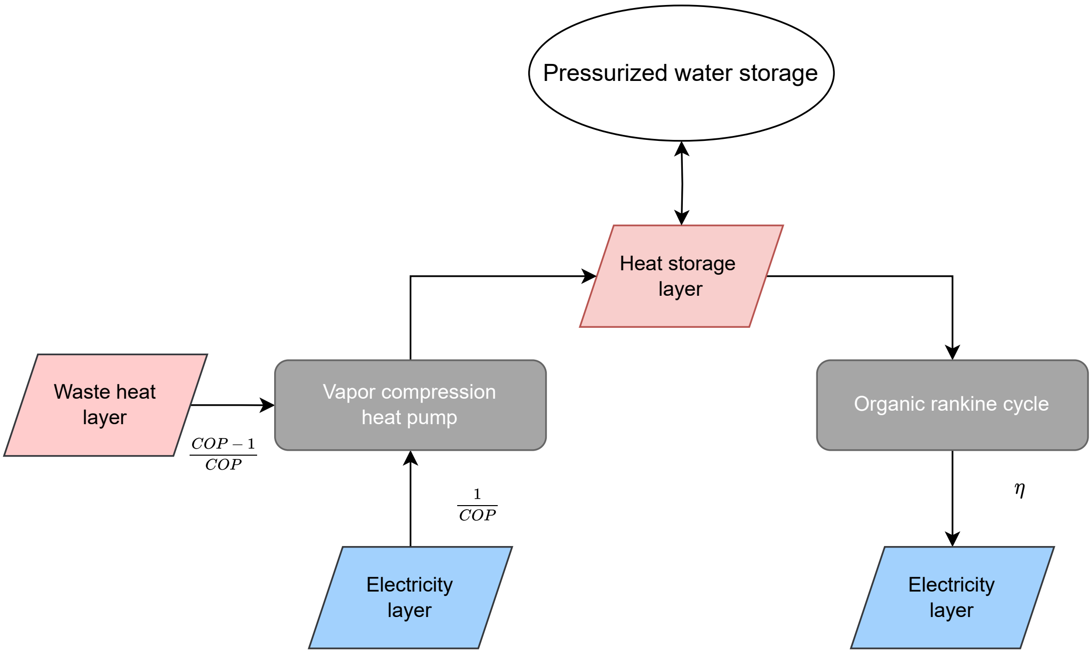

Figure 2.7: Schematics of the recuperated Brayton PTES implementation

The advantage of this method is its capability to work with cost units in relation to both energy and storage.

2.3 Model review - Retrofitted coal-fired power plants

The final solution examined involves retrofitting a coal-fired power plant. This concept holds an interesting characteristic: the possibility of reducing battery costs through the utilization of the steam cycle in an existing coal-fired power plant. In this approach, the burner in the current plant is substituted with an electricity-to-heat conversion and storage system. For our specific case, these components will be represented by an electrical resistor and a molten-salt HS system. A process flow diagram of this technology is proposed in figure 2.8

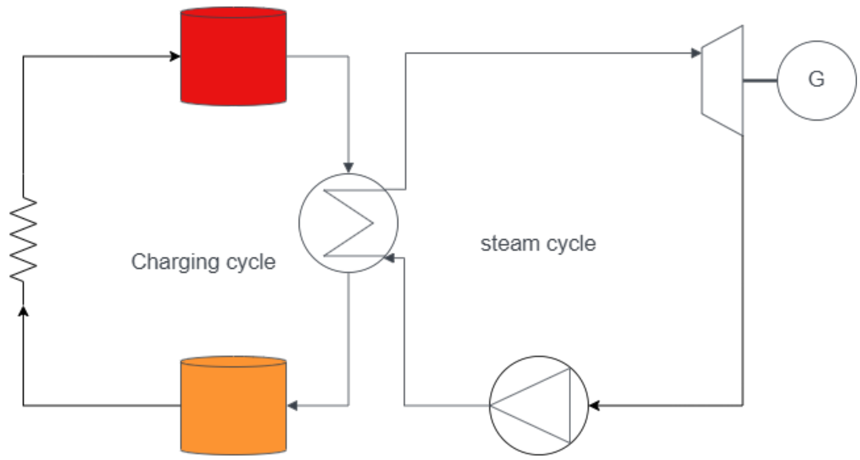

Figure 2.8: Process flow diagram for a retrofitted coal-fired power plant

The choices made in modeling this concept are based mainly on the results of available studies and industrial work [42, 1, 49]. Many of these rely on electric resistors to convert electricity into heat, for simplicity and low cost. It should be noted that some manufacturers propose alternatives using HPs to slightly improve the efficiency of the overall installation. This alternative has not been explored, however, due to a lack of literature and economic data on these potential HPs.

Techno-economic parameters

In order to comprehensively evaluate the technical and economical parameters of the machine under study, it is imperative to divide it into three distinct components. An industrial electrical resistor, thermal storage in the form of molten salts and a steam cycle (Rankine cycle).

Electrical resistor

The electric resistance is modeled based on economic data from a document produced by the European Commission [13], which provides cost projections for heating elements. In this document, the investment cost of the electric resistance is estimated at 120 €/kW. The maintenance cost is low, at 0.7 €/kWy.

Efficiency	Inv. cost [€/kW]	Maint. cost [€/kWy]	Availability	Lifetime [y]
1	120	0.7	1	15

Table 2.4: Parameters of the electrical resistor

Molten salt heat storage

We examine the molten salt HS, taking into account an investment cost of 30 €/kWh$_{th}$[41], a maintenance cost of 5%, and a lifespan of 25 years. The estimation of this lifespan is derived from the characterization of a high-temperature HS system modeled on Energyscope. Once more, the storage is assumed to experience a daily loss of 5%. Efficiencies between storage and created layers are unitary.

Steam Rankine cycle

Finally, the steam cycle is recovered from an existing coal-fired power plant. The technology is considered to have a conventional efficiency of 40% and an investment cost of 0 €/kW. Maintenance costs are assumed to be equal to those of a CCGT and they are kept constant [40].

Model implementation

Based on the previously mentioned data, an electricity storage model can be implemented on EnergyScope. A visual representation of this EnergyScope implementation is provided in figure 2.9.

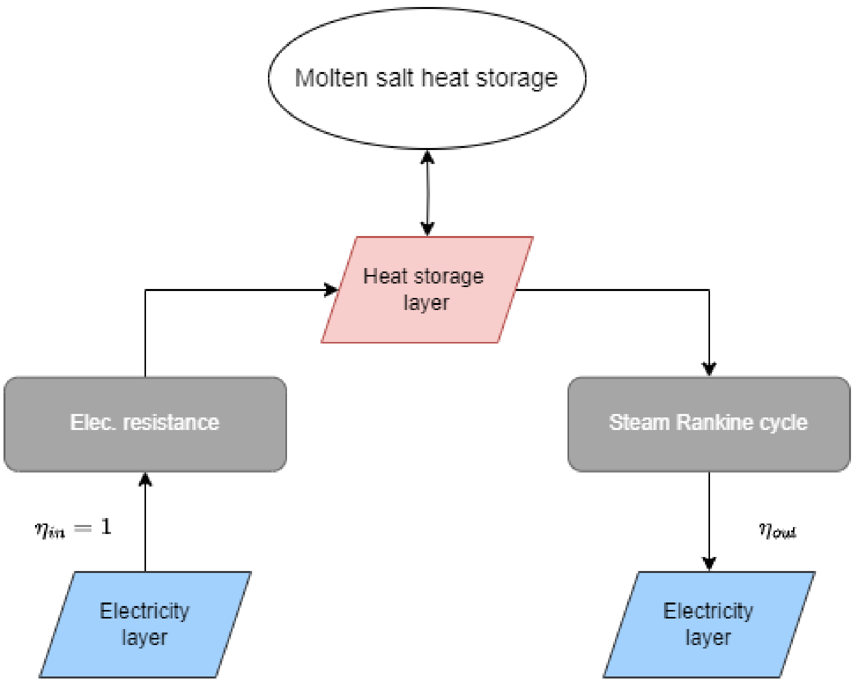

Figure 2.9: Schematics of the retrofitted coal fired power plant

To the author knowledge, there has been no indication of a minimum discharge time for this machine. A permissible margin of 2 to 14 hours is allowed. Lastly, the COP and η_{ORC} values will be provided later in the description of the scenarios.

2.4 Optimizer Configuration

Having established the parameters for the machines, it is now necessary to elaborate on the parameters of the system within which they function. This system specifically represents the energy system of Belgium in the year 2020. The data used in this work are given in appendix B.

It is then necessary to add to this data, the 3 technologies we described above. To do this, we need to create and modify 3 distinct environments. An environment hosting the recuperated Brayton CB. A second environment for the TI-CB, and a final environment for the retrofitted CB. The modifications made to the tool environments are also detailed in the appendix C. **It is important to note that CBs are, in this work, considered as daily storage units. This has a major impact on the obtained results.**

2.5 Identified scenarios

In order to carry out our studies, two steps need to be considered. These are described in this section.

First scenario - Operating zone

The aim of the first step is to determine the operating "zone" of the CB concept in terms of machine efficiency and costs. On the basis of these mappings, it will then be interesting to know how the energy system is constituted and to understand how the CB is used, and what the differences are in the use of these technologies according to their performance. In addition, it will be useful to understand which technology is prioritized among the 4 cases proposed.

Since the CB is a storage technology, the first parameter to iterate on is the system's CO2 emissions constraint. This constraint is essential in order to force EnergyScope to provide a system dependent on renewable energies and, in the long term, a system dependent on electricity and HS. The CO_2 constraints will evolve according to a simple linear constraint represented in the figure 2.10.

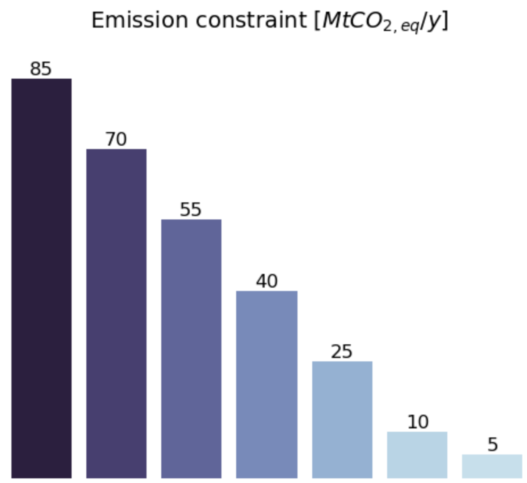

Figure 2.10: Evolution of the CO_2 emission constraint

Then, due to the high cost of the CB compared to other technologies, it will be necessary to iterate on the costs of the technologies that make it up. To achieve this, the author arbitrarily chooses to take percentages of the costs (Investment costs and maintenance costs) found in the literature cited above. These percentages are chosen to be all cost fractions above 5% of the initial cost until we have deployment of the CB. This same method will be used in 2 different ways for each CB. The first, referred to as 'Mapping', will have combinations of the various available cost fractions taken. By this method, different evolution scenarios and cost combinations can be taken into account. A second method, known as the 'even cost reduction approach', will have certain systems studied under the assumption that costs will evolve in the same manner.

The way costs evolve can be written as follows, with x being the cost fraction:

$$\begin{aligned} c_{inv}(x) &= x \times (\text{Init. Inv. cost}) \\ c_{maint}(x) &= 5\% \times c_{inv}(x) \quad \text{or} \\ c_{maint}(x) &= x \times (\text{Init. Maint. cost}) \end{aligned}$$

However, it is not the case for the retrofit CB's discharge cycle which had a fixed investment cost and therefore, a fixed maintenance cost. This is formulated as:

$$\begin{aligned} c_{inv} &= 0[€/kW] \\ c_{maint} &= 20.92[€/kWy] \end{aligned}$$

Second scenario - Impact of the time of discharge

In order to answer the research question concerning the CB's energy to power ratio, a CB with a low enough cost to observe its deployment is selected and optimization scenarios are carried out by decreasing/increasing the machine's imposed minimum discharge time. This analysis will highlight the energy to power ratio of the machines, and the evolution of the system cost as a function of this discharge time (and therefore, indirectly, of this ratio).

Chapter 3

Results & Interpretation

This chapter gives an overview of the results obtained from several optimization scenarios carried out with EnergyScope. The review begins with a broader study aimed at contextualizing the use of the Carnot battery within the tool and understanding the implications of its insertion and how the tool uses this battery. In these first sections, the energy systems are compared to reference systems. These systems are presented and explained in Appendix D.

The costs associated with the deployment of the various CBs implemented will then be quantified, and an attempt will be made to explain the influence of the various components, particularly in the case of the thermally integrated battery and the coal-fired plant retrofit battery, as their implementation is the most relevant to this study. Subsequently, a more comprehensive mapping will be presented, which relates the investment costs of the CB to its installed capacity.

Finally, the study will explain in greater detail the use made of these batteries and the impact of the CB's discharge time (i.e. its power output) on deployment.

3.1 Conditions for deployment

In this initial section, the focus is on understanding the deployment of the different CBs and their operation within multiple different energy systems.

First, we explore the initial costs that allow the deployment of the technologies by reducing the investment and maintenance costs by fractions of their initial costs. The interest of this approach is to be able to have a feeling on the deployment and to understand in what kind of system it fits in difficult economic conditions.
Then, we continue to deepen the feasibility study by continuing to reduce these costs in order to highlight reasons that would prevent the deployment of the battery.

In this first part of the work, the discharge times of the CBs are fixed with a value of 6 h and the percentages shown in the graphs are even cos fractions of the technologies respective costs. This discharge time is chosen based on the findings of McTigue et al. [30]. In their study, a minimum discharge time of 6 hours is shown to be competitive compared to lithium-ion batteries. The investigation of different discharge times will be proposed in the subsequent sections.

Highest feasible costs

Now, let's analyze the four subsequent figures presented in Figure 3.5, which illustrate the installation of CBs with a storage capacity exceeding 1 GWh_e for each technology.

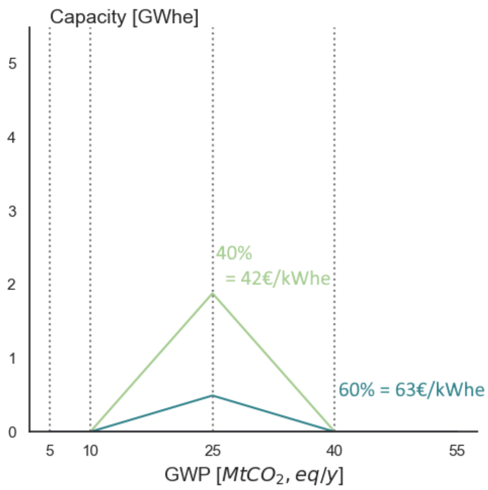

Figure 3.1: (a) Retrofit - $\eta = 40\%$

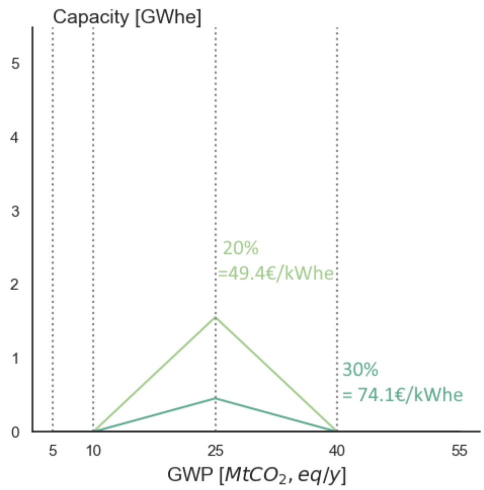

Figure 3.2: (b) Brayton - $\eta = 59\%$

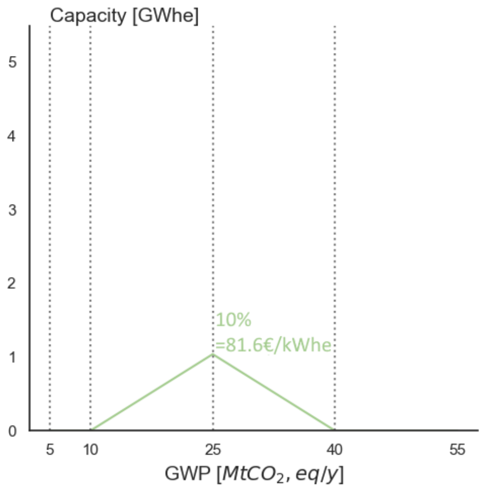

Figure 3.3: (c) TI - $\eta = 63.2\%\%$

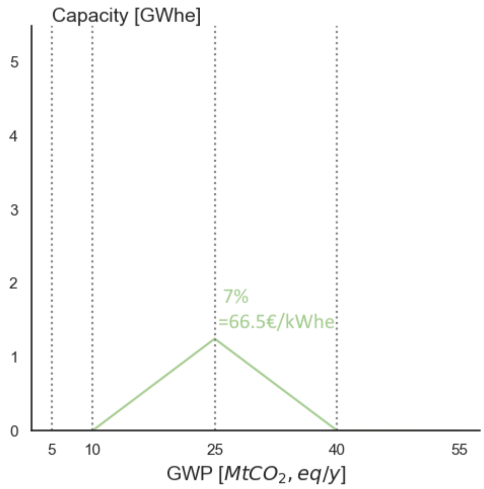

Figure 3.4: (d) TI - $\eta = 31.6\%$

Figure 3.5: Capacity with respect to GWP constraint - Percentages are initial cost fractions

The preceding illustration underscores three significant elements. First, CBs must reduce their cost in relation to their respective efficiency and their respective initial cost. The most "accessible" CB, therefore requiring a smaller cost reduction, is the retrofitted battery, followed by the Brayton battery with a higher efficiency, and finally the thermally integrated batteries where it is shown that efficiency plays an important role in the deployment of these batteries. The second element highlighted is that these batteries are first used with a CO_2 emissions constraint of 25 $MtCO_{2eq}$. This second element is explained by two factors in the next paragraph. Finally, these figures show that for a lower efficiency, the highest investment cost for deployment of the thermally integrated battery is higher than for the recovery battery. This is due to the maintenance costs of its discharge cycle. This aspect is discussed later and fully explained in the appendix E.

We discuss now the two factors that explain why the deployment of CBs mainly occurs with a CO_2 emissions constraint of 25 $MtCO_{2eq}$. The first factor is related to the way in which the transition of an energy system is achieved by EnergyScope. If we start with a fossil fuel-dependent energy system, EnergyScope will mitigate emissions by specifically targeting reductions in the electricity and heat sectors. To achieve this, a significant amount of renewable energy sources (onshore/offshore WTs and PV panels) and technologies that generate high-temperature heat with reduced or no emissions (electric resistors for industrial heating) are decided to be deployed by EnergyScope. As a result, a high electricity demand during the day (matching the production of solar electricity to the production of high temperature heat) and storage requirements are experienced by the system. Hence, the deployment of HS (high-temperature HS) and electricity storage (Carnot battery, when cost allows it) takes place. The advantage of CBs is that the system can have the duration of high-temperature heat production extended, thereby reducing the maximum power required for installation. If the cost of the CB is sufficiently low, a decrease in the overall system cost can be achieved. The shift from a fossil fuel-based system to one reliant on electricity and renewable fuels is the second key factor explaining why deployment only takes place when reaching a level of 25 $MtCO_{2eq}$. This transition emphasizes the significance of technology efficiency in generating and storing high-temperature heat. Consequently, interest in the CB diminishes as the system progressively electrifies. The adoption of CBs is additionally impacted by the vehicle-to-grid potential of electric vehicles, which play a role in decarbonizing the transportation sector but also creates additional electricity storage.

In the following sections of this study, the impact of deploying these technologies on the energy system will be further examined. To achieve this, scenarios (representing fractions of the initial cost) that enable technology deployment at the grid-scale level (on the order of GWh_e) are selected. Specifically, the focus is on the technologies depicted by the green lines in figure 3.5, which are:

- The retrofit battery at 40% of its initial cost (42 €/kWhe).
- The Brayton battery at 20% of its initial cost (49.4 €/kWhe).
- The thermally integrated battery with a high coefficient of performance (COP) at 10% of its initial cost (81.6 €/kWhe).
- The thermally integrated battery with a low COP at 7% of its initial cost (66.5 €/kWhe).

Impact of the Carnot battery on resource consumption

Figure 3.10 illustrates the impact of integrating a CB on the resource consumption, compared to a scenario without a CB (The reference system with a constraint 25 $MtCO_{2eq}$ is described in the appendix D).

The impact of CBs on resource consumption is minimal, with initial consumption in the range of dozen of TWh. However, they contribute to a reduction in gas consumption, favoring solar energy. This reduction primarily comes from a decrease in controllable power required by the energy system, as the CB provides this controllable power (It allows to shift the production of high temperature heat).

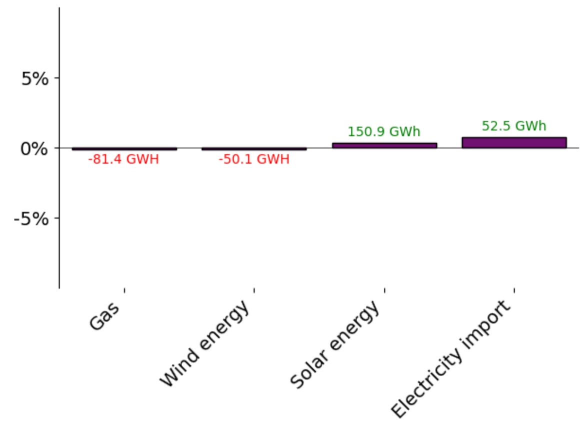

Figure 3.6: (a) Retrofit - $\eta = 40\%$

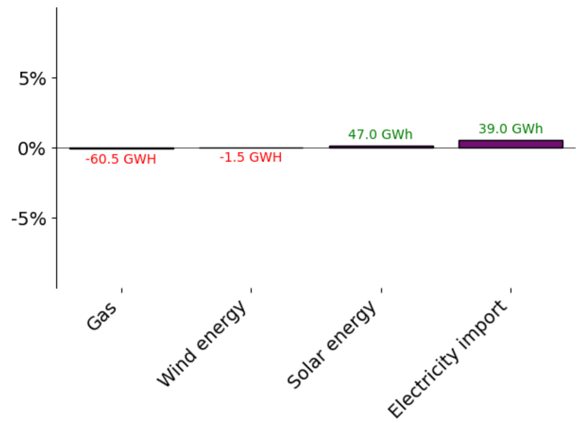

Figure 3.7: (b) Brayton - $\eta = 59\%$

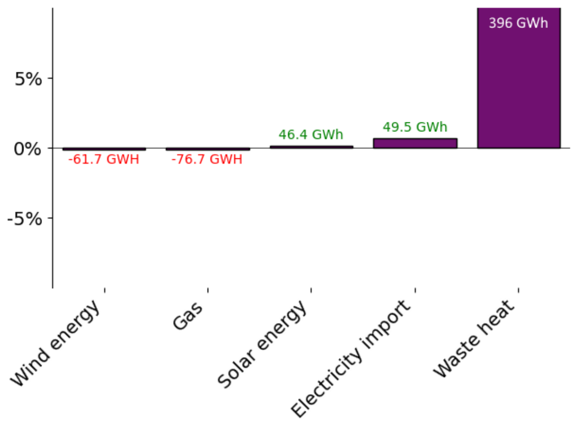

Figure 3.8: (c) TI - $\eta = 63.2\%\%$

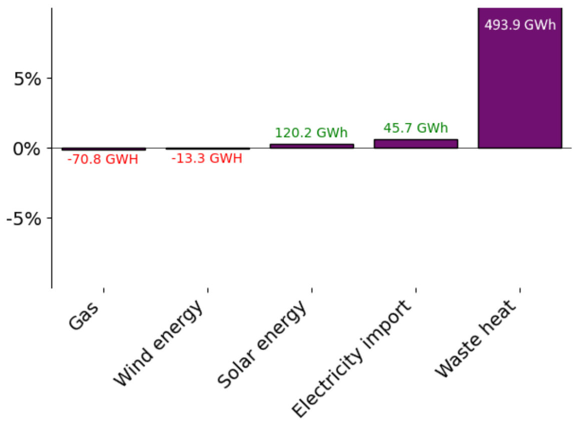

s

Figure 3.9: (d) TI - $\eta = 31.6\%$

Figure 3.10: Difference in resource consumption due to Carnot battery insertion

Additionally, wind energy is less used with most technologies. This can be attributed to the CB's behavior, which charges during the day, benefiting from solar energy, and discharges in the evening to meet the increasing electrical demand. This may lead to a shift away from wind power consumption.

Finally, we can see that TI-CBs consumed waste heat. The waste heat consumption is higher in the case of the thermally integrated with a lower COP. This is attributed to differences in efficiency and storage capacity of the second system. (To supply the same amount of electricity to the system, it will have to consume more electricity and therefore more waste heat.)

Impact of the Carnot battery on the generation and storage assets

In Figure 3.15, the impact of the CB on the deployed electricity generation technology capacities can be observed.

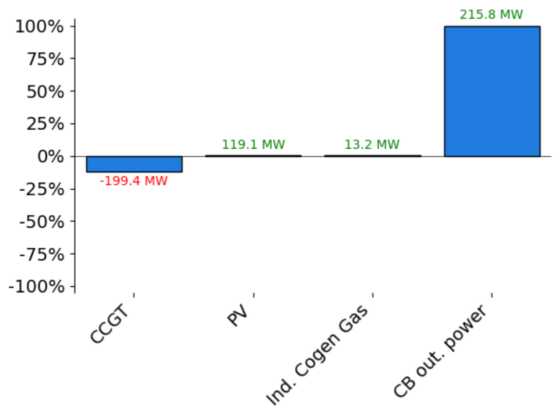

Figure 3.11: (a) Retrofit - $\eta = 40\%$

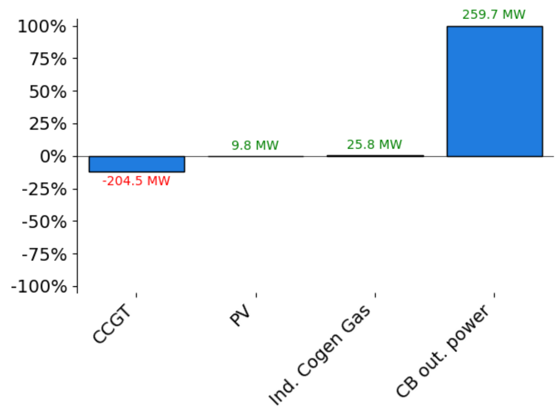

Figure 3.12: (b) Brayton - $\eta = 59\%$

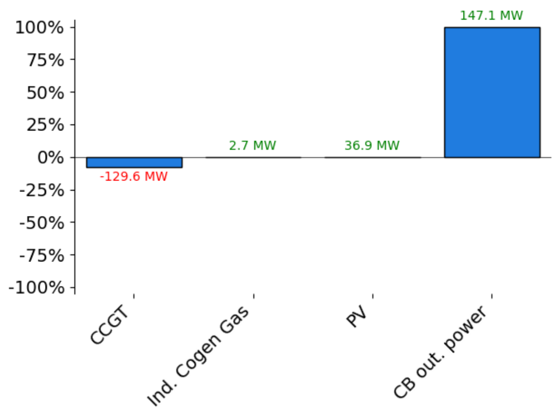

Figure 3.13: (c) TI - $\eta = 63.2\%\%$

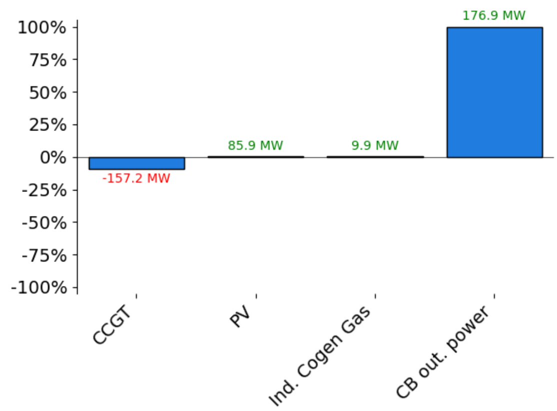

Figure 3.14: (d) TI - $\eta = 31.6\%$

Figure 3.15: Difference in technology capacities due to Carnot battery insertion

It is shown that the installed capacity of CCGTs is reduced by the CB insertion. The installed capacity of CCGTs is intended to support production by generating the necessary electricity when solar power is insufficient. (During morning and evenings in winter). Additionally, the power of solar PV increases slightly to take full advantage of the daily storage provided by the CB during the summer. Finally, a slight increase in installed gas fired co-generation capacity allows for a reduction in electricity imports and production of high-temperature heat. This comes from the emission constraint as we have just reduced its consumption through the installed CCGT capacity. Overall, this still leads to a reduction in gas consumption.

This section has highlighted the main impacts on the electricity sector of the energy system, as the CB ultimately interacts only with the electricity sector. However, there are effects on how the system responds to its demand, particularly in the way it produces industrial heat. This is demonstrated by examining the assets for high-temperature heat generation and the associated storage methods for this sector. This is figure 3.20 and 3.25.

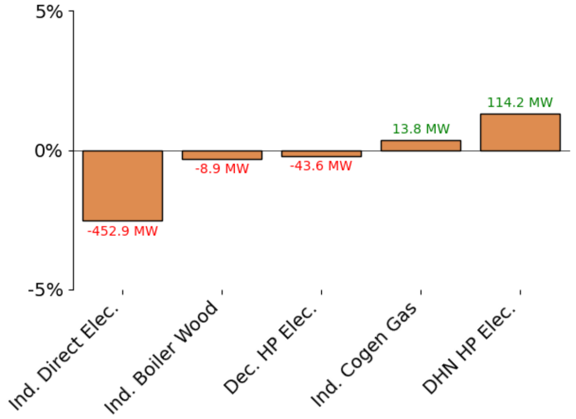

Figure 3.16: (a) Retrofit - $\eta = 40\%$

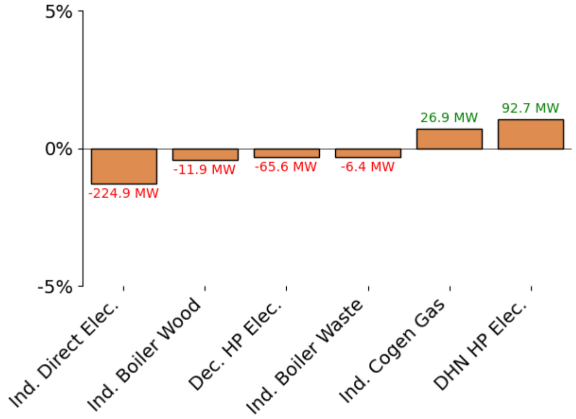

Figure 3.17: (b) Brayton - $\eta = 59\%$

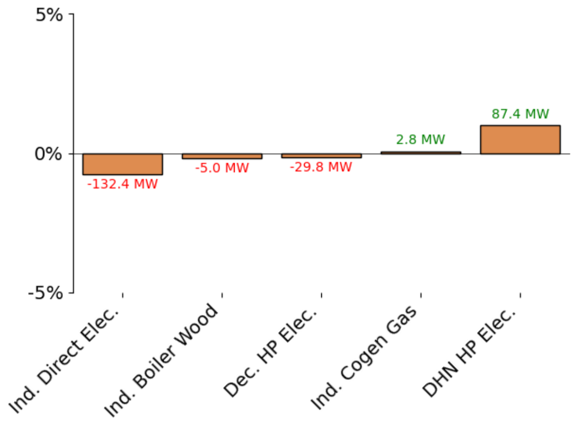

Figure 3.18: (c) TI - $\eta = 63.2\%\%$

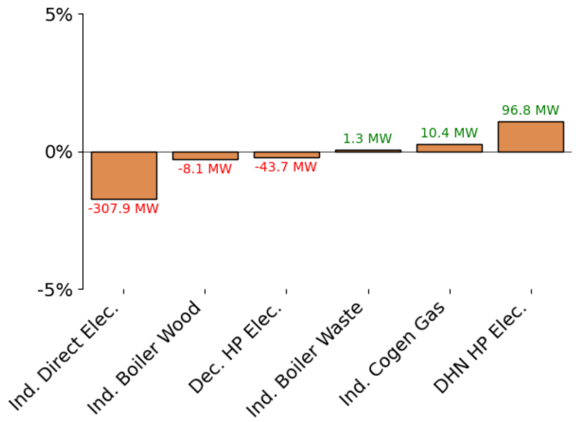

Figure 3.19: (d) TI - $\eta = 31.6\%$

Figure 3.20: Difference in technology capacities due to Carnot battery insertion

As can be seen in Figure 3.20, the installed capacity of industrial direct electricity heat generation varies based on the installed capacity of the CB.

This reduction, as shown in Figure 3.25, results in a decrease in the required amount of high-temperature HS. This is because the CB now serves as a storage capacity, instead of producing a large amount of high-temperature heat during sunlight hours, heat production is spread throughout the day, leading to a decrease in the total installed power and the storage capacity needed to meet overnight industrial heat demand.

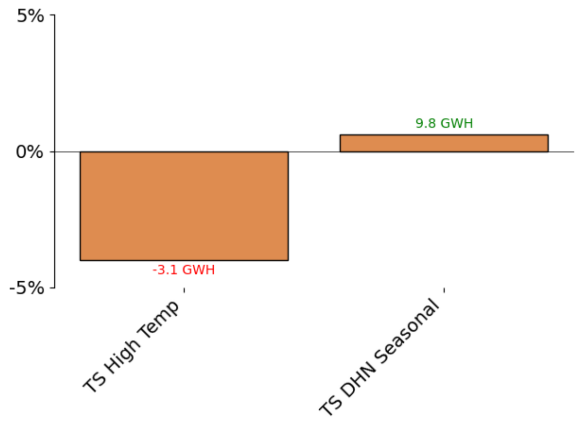

Figure 3.21: (a) Retrofit - $\eta = 40\%$

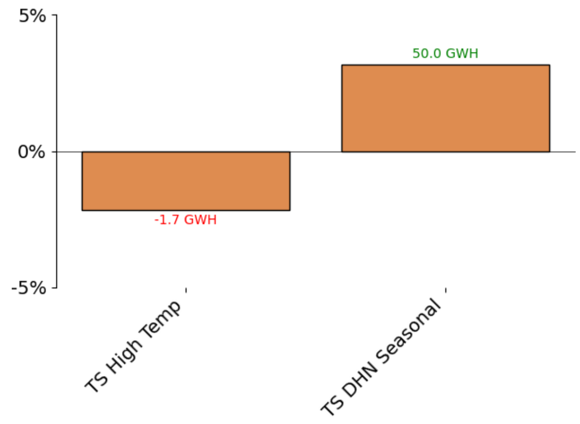

Figure 3.22: (b) Brayton - $\eta = 59\%$

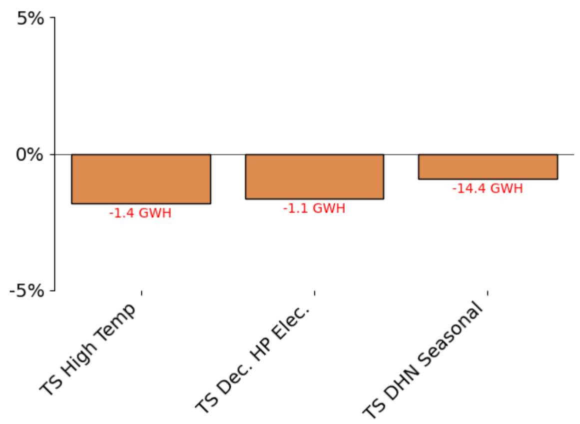

Figure 3.23: (c) TI - $\eta = 63.2\%\%$

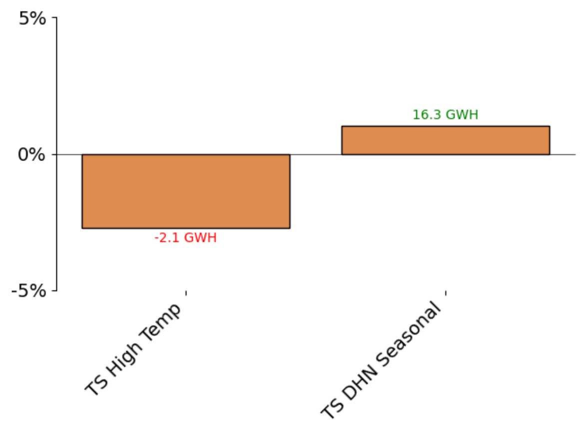

Figure 3.24: (d) TI - $\eta = 31.6\%$

Figure 3.25: Difference in technology capacities due to Carnot battery insertion

As a result, a different approach is now taken for low-temperature heat production. This is characterized by larger district heating networks with increased HS capacity and higher heat power output. Regarding the higher efficiency thermally integrated system, there is no significant increase in seasonal storage. Instead, the energy system fulfills directly the demand using DHN gas cogeneration.

In order to better visualize these changes, here's a chart showing the system's behavior on some typical days.

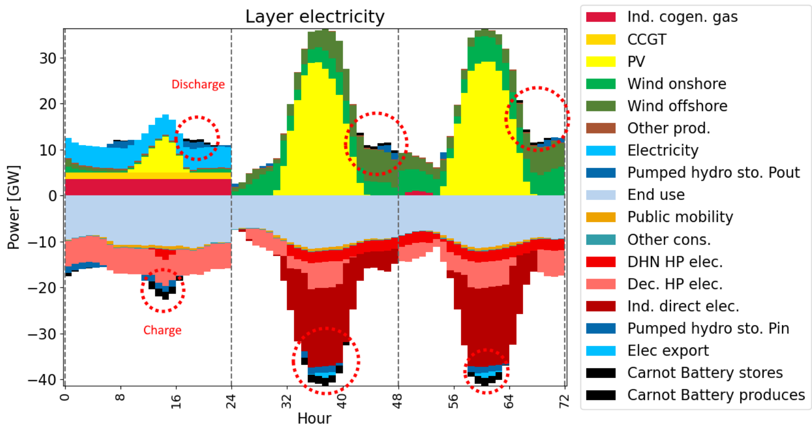

Figure 3.26: System behavior with Carnot battery

It's a little difficult to compare this chart with the reference one. Here's another way of looking at things, showing the differences between the new and the reference systems. This allows us to better understand the differences between the two systems.

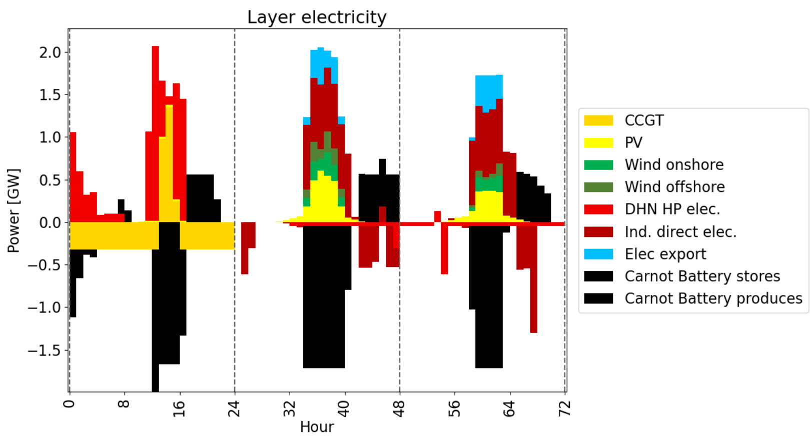

Figure 3.27: Differences in system behavior

The diagram illustrates several aspects: a decrease in production using the CCGT, alterations in heat production behavior via heating networks, higher electricity generation from PV panels and WTs, and the CB's utilization for balancing industrial heat production through industrial electrical heating. It also shows that electricity exports are actually reduced on these typical days.

3.2 Conditions for deployment - Further lowering the costs

An exploratory work is now being conducted to understand how the CB could be used by the tool if the technology is deployed under lighter cost conditions, enabling a more widespread deployment of it. This exploration also highlights the reasons why the CB is not deployed as the CO_2 emission constraint is reduced.

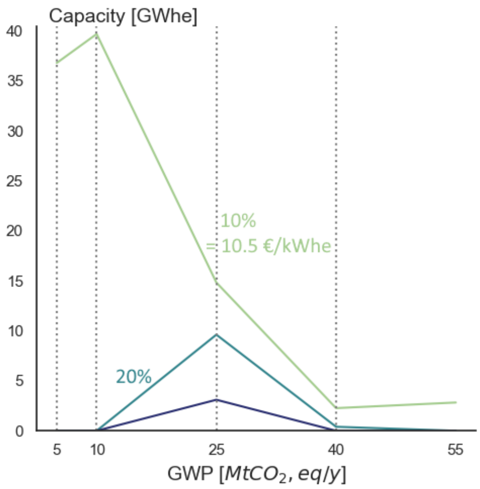

Figure 3.28: (a) Retrofit - $\eta = 40\%$

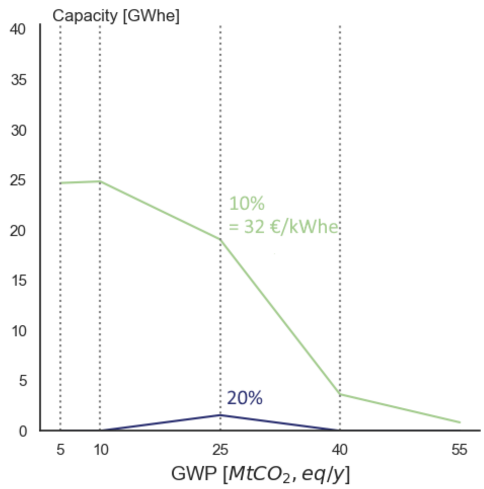

Figure 3.29: (b) Brayton - $\eta = 59\%$

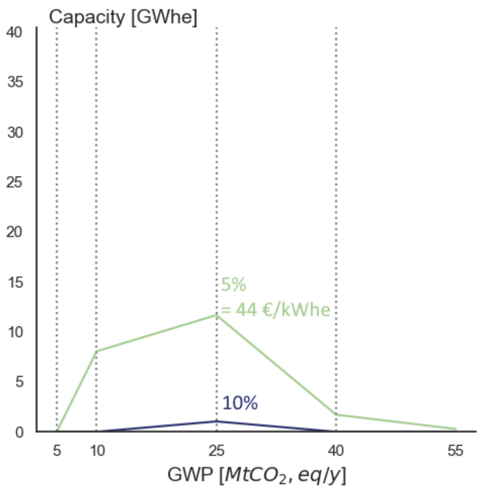

Figure 3.30: (c) TI - $\eta = 63.2\%\%$

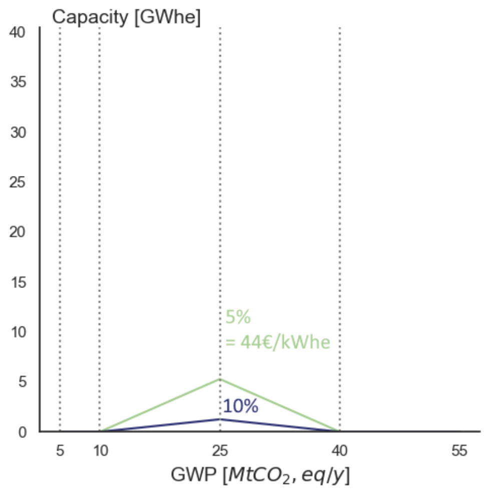

s

Figure 3.31: (d) TI - $\eta = 31.6\%$

Figure 3.32: Capacity with respect to GWP constraint - Percentages are initial cost fractions

An order in the deployments of the four models can now be observed in Figure 3.32. It is evident that the retrofit battery has the highest potential due to its lower initial cost, followed by the Brayton battery, and ultimately, the thermally integrated battery, which is deployed more extensively when its efficiency is higher. The diagram also shows the fact that, as the CO2 emission constraint becomes stricter, the CB tends to experience a decrease in installed capacity. This is primarily due to the efficiency of the batteries and the increased implementation of electrified systems. Indeed, in order to minimize the total cost of the system, the latter tries to minimize resource consumption. This constraint is all the more true when the resources in question are renewable fuels, and therefore more expensive. This constraint is especially strong when the geographical area studied (Belgium) is densely populated and does not possess excessive quantities of renewable resources such as sun or wind (in comparison with other countries such as Chile).

An attempt is made to understand, for systems with stricter CO_2 emissions constraints, what are the roles of the CBs in energy systems at 10 and $5MtCO_{2_{eq}}$. The system of reference are described in the appendix D.

The following subsections will now present the energy systems that are being integrated with the following technologies:

- The retrofit battery at 10% of its initial cost (10.5 €/kWhe).
- The Brayton battery at 10% of its initial cost (32 €/kWhe).
- The thermally integrated battery with a higher coefficient of performance (COP) at 5% of its initial cost (44 €/kWhe).
- The thermally integrated battery with a higher coefficient of performance (COP) at 5% of its initial cost (44 €/kWhe).

As the installed capacity of the last CB is zero for the last two constraints, no changes occur in the energy system compared to the initial system.

Carnot battery with constraint at $10\,\mathrm{MtCO_{2eq}}$

We start by describing the impact of the different CBs in the $10\,\mathrm{MtCO_{2eq}}$ energy system presented in the appendix D. In this system, the electrification of vehicles takes place. This electrification partly explains why the CBs are not deployed at this global warming potential constraint as the electric vehicles can provide storage through Vehicle-to-grid (V2G) capabilities.

Impact of the Carnot battery on resource consumption

The impact of each CB on the energy system resource consumption is illustrated in Figure 3.37. It can be observed that the CBs enable a reduction in the consumption of renewable ammonia and gas while increasing the use of renewable energy sources. Again,it is shown that the deployment of the CBs requires increased electricity imports.

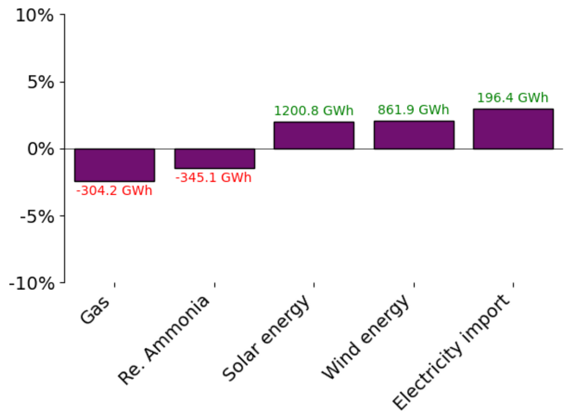

Figure 3.33: (a) Retrofit - $\eta = 40\%$

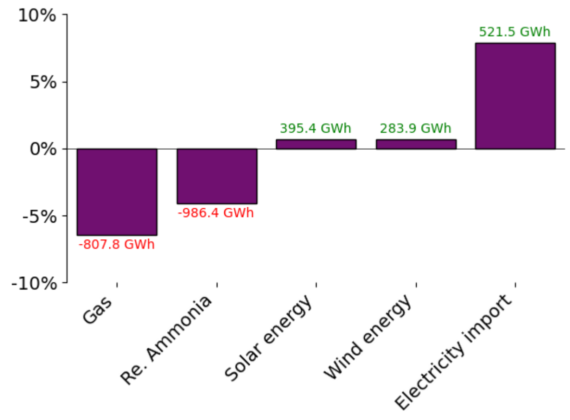

Figure 3.34: (b) Brayton - $\eta = 59\%$

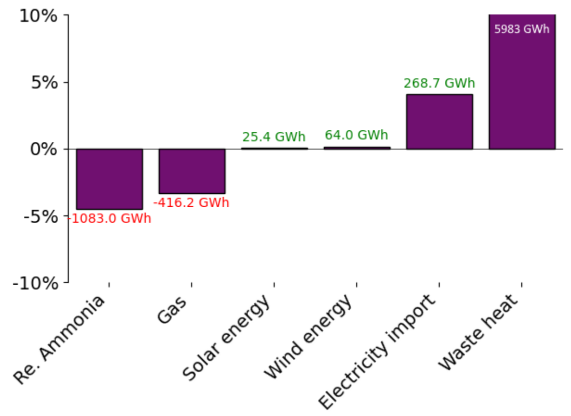

Figure 3.35: (c) TI - $\eta = 63.2\%\%$

Installed capacity < 1 GWhe

Figure 3.36: (d) TI - $\eta = 31.6\%$

Figure 3.37: Difference in resource consumption due to Carnot battery insertion

Impact of the Carnot battery on the generation and storage assets

Figure 3.42 displays the impact of the CB deployment on the energy system under a stricter constraint. It can be observed that a slight reduction in the installed capacity of CCGTs and a slight increase in industrial gas cogeneration are observed as a result of the CB deployment. These changes are attributed to the reasons mentioned earlier. Additionally, despite the significant output power of the CB, it does not have a substantial impact on electricity generation assets.

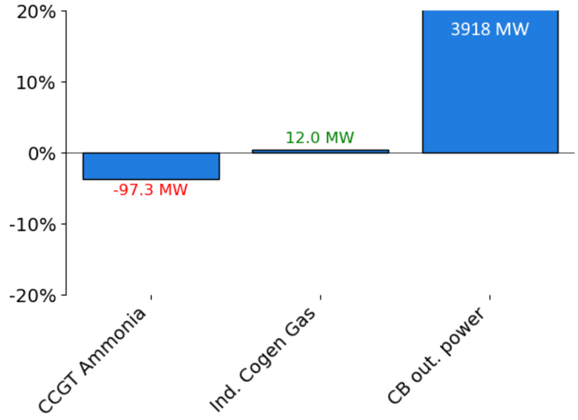

Figure 3.38: (a) Retrofit - $\eta = 40\%$

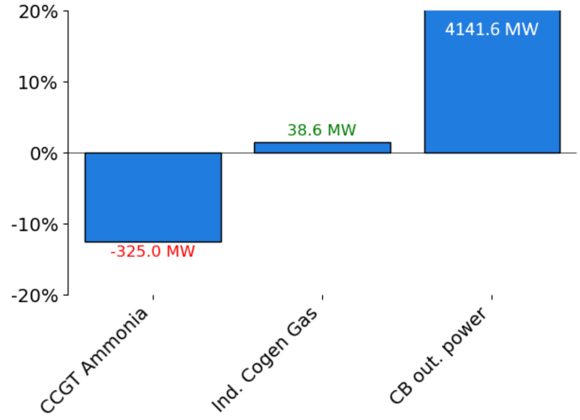

Figure 3.39: (b) Brayton - $\eta = 59\%$

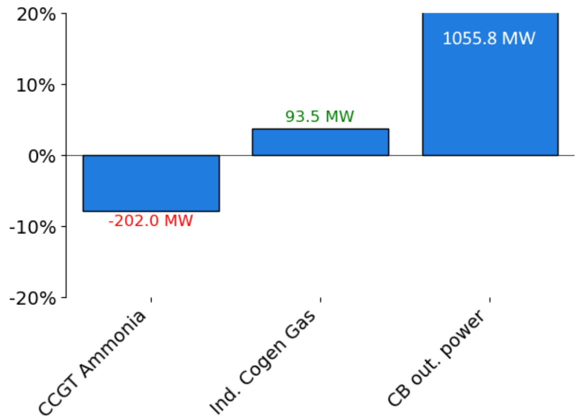

Figure 3.40: (c) TI - $\eta = 63.2\%$

Installed capacity < 1 GWhe

Figure 3.41: (d) TI - $\eta = 31.6\%$

Figure 3.42: Difference in technology capacities due to Carnot battery insertion

It should be noted that the output power of the CBs possesses unique characteristics. As a result of their implementation, the output power of the Brayton CB is determined as one-sixth of its installed capacity, considering the time of discharge (it is therefore dependant on the capacity of the battery). On the other hand, the retrofit CB exhibits a big output power since it incurs no investment cost.

Furthermore, the insertion of the CB is observed as an additional electrification of the energy system, reducing its dependence on (e-)fuels. This electrification facilitates the deployment of more battery electric vehicles, which are charged using the CB during the afternoons, as depicted in Figure 3.43. This is the main reason for a decrease in gas consumption as we decrease the number of natural gas cars.

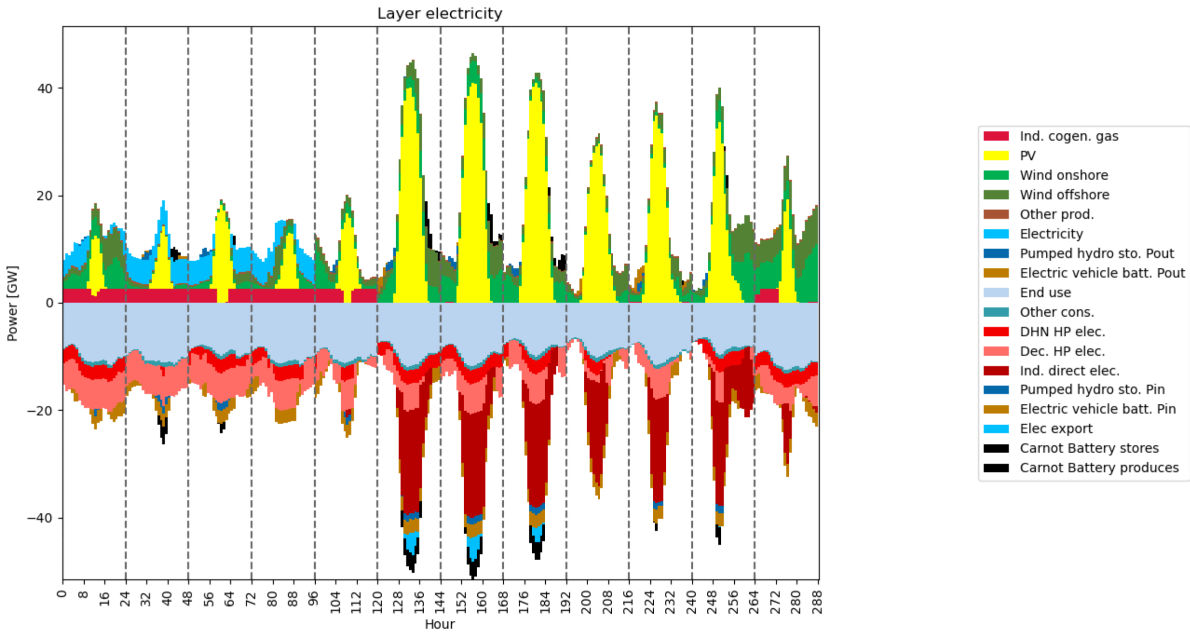

Figure 3.43: Carnot battery behavior over the 12 typical days

Similar to the previous observations, a reduction in the installed capacity of direct electricity to industrial heating conversion technology is observed in the heating sector. However, this graph is excluded as the behavior is similar to the previous graph shown when describing the impact of the CB on a 25 $MtCO_{2eq}$ system. Interested parties will still find these graphs in Appendix F

Carnot battery with constraint at $5\,\mathrm{MtCO_{2eq}}$

Now, the focus shifts to the impact of the CB on the $5\,\mathrm{MtCO_{2eq}}$ system presented in Appendix D. In this system, the main difference is found in the use of renewable fuels and the increased electrification of the system.

Impact of the Carnot battery on resource consumption

In this system, renewable gases are employed in the heat sector instead of the CB due to their superior efficiency. For the CB to be implemented, a lower cost and high efficiency are needed. However, these conditions are not met for the TI-CBs. Consequently, the preference is to minimize gas usage in the Combined Heat and Power (CHP) system, using direct solar production to generate and then store the high-temperature heat.

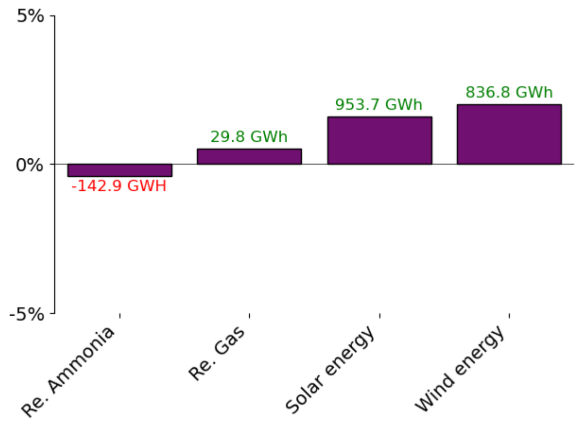

Figure 3.44: (a) Retrofit - $\eta = 40\%$

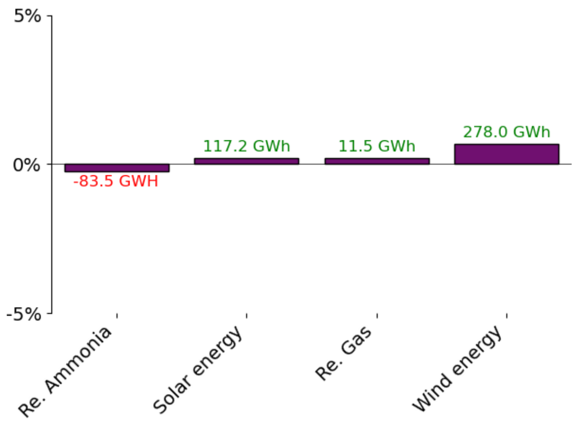

Figure 3.45: (b) Brayton - $\eta = 59\%$

Figure 3.46: Impact of the Carnot batteries on the resource consumption

In the cases where the CBs are actually deployed, figure 3.46 demonstrates a reduction in ammonia consumption alongside an increase in solar, wind, and renewable gas consumption, attributable to the implementation of the CB. This time, the increase in energy consumption linked to the insertion of the CB is much greater, thanks on the one hand to the large capacities installed in these scenarios, and on the other hand to the low efficiency of these batteries. In this scenario, the CB has a limited impact on the electricity sector. It mainly makes it possible to reduce the installed capacity of electrical resistance for the production of industrial high-temperature heat. This reduction is accompanied by a reduction in storage capacity. It is important to highlight that, in this particular scenario, gas consumption exhibits an increase. This deviation can be attributed to the absence of a reduction in gas consumption within the mobility sector, coupled with an increase in the heating sector. These factors account for the reversed trend observed in the system. Again, as the behavior is similar in this system, the corresponding figures can be seen in the appendix F.

3.3 Techno-economic analysis - Mapping

This section focuses on the technical and economic aspects of CBs. First, the costs per unit of energy and per unit of power required to deploy CBs 1 GWh_e - 100 MW_e are quantified. Then, for technologies involving multiple components (TI-CB and Retrofitted CB), the share of investment and maintenance costs is presented. The amount of waste heat consumed by the two thermally integrated systems is then quantified, and the number of cycles achieved by these systems is discussed, providing a better understanding of their behavior. Lastly, the impact of time of discharge on the CB will be studied through its impact on the total system cost.

First, a mapping of optimization scenarios allowing different combinations of cost fractions and different discharge times is presented. The results are based on optimization at the most favorable constraint for technology deployment, that is a GWP of 25 $MtCO_{2eq}$.

Investment costs per unit of energy

This section is dedicated to the comparison of all the CBs based on their respective cost per unit of energy. It is important to highlight that this comparison evaluates the CBs concerning their electricity storage capacities, which is calculated by multiplying their (Thermal) capacities by their output efficiencies. It begins with an examination of the storage cost of the CBs. Figure 3.47 presents the installed capacity of the CBs in relation to their cost per unit of storage.

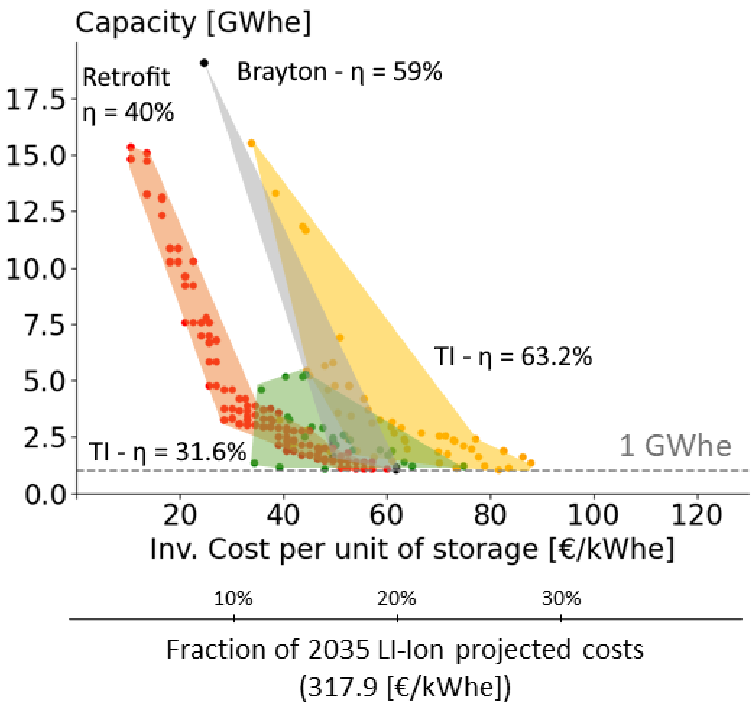

Figure 3.47: Cost per unit of storage of deployed Carnot batteries

The graph reveals that the deployment of CBs occurs at costs below 90 €/kWhe, with the highest efficiency technology being the first to be deployed ($\eta = 63.2\%$).

It is shown that investments are not 'all-or-nothing' investments where the battery is suddenly deployed on a large scale. Instead, the various batteries are deployed gradually and, depending on their price, different adaptations are made to the system, notably by changing the installed capacities of PVs and CCGTs. Therefore, the presence of trade-offs arises due to the interaction between the installed capacities of generation units and the installed capacities of CBs.

Finally, the figure demonstrates that the lowest efficiency CB is deployed at higher prices per unit of storage compared to the Brayton and retrofit options, which have higher efficiencies. This inconsistency can be explained by the maintenance costs associated with the retrofit battery. Indeed, the maintenance costs of the retrofit battery, and in particular of its discharge cycle, have been considered to be much higher than those of other technologies, and constant; this leads the technology to be less attractive compared to other technologies. A full explanation of this result is provided in a specific appendix, the appendix E.

Investment costs per unit of power

Now, the cost per unit of power of the machines deployed by EnergyScope is being examined. The figure 3.48 provides a visualization of the deployment of CBs based on their costs per unit of power.

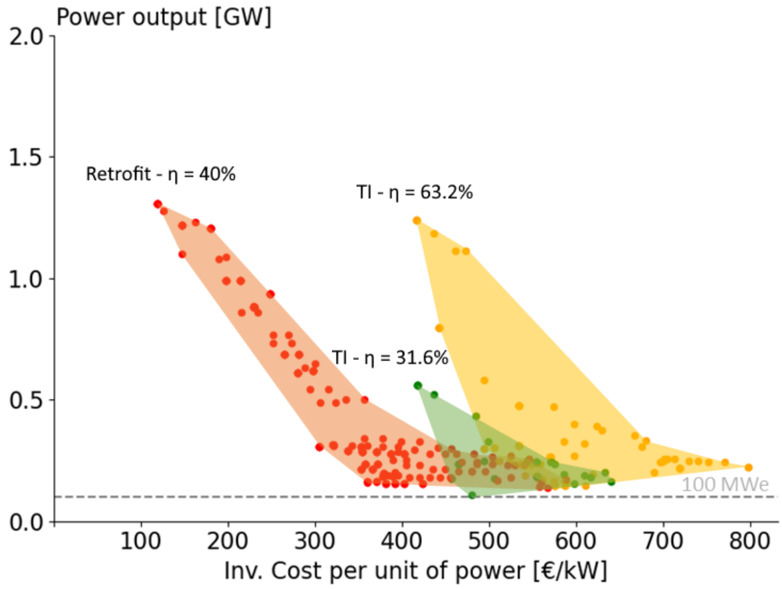

Figure 3.48: cost per unit of power of deployed Carnot batteries

The figure displays the deployment of CBs with varying costs per unit of power. For the TI-CBs, the deployment cost can reach up to ±800 €/kW, while for the same technology at a lower efficiency, the cost is ±640 €/kW. On the other hand, the retrofit CB has the lowest cost per unit of power, with a maximum of ±600 €/kW. This lower cost is attributed to its free discharge cycle and higher maintenance costs, resulting in reduced total investment costs, and ultimately leading to a lower investment cost per unit of power. The Brayton implementation is not shown on this graph as its implementation lacks of proper discharge cycle, rendering the data points misleading and nonsensical.

3.4 Techno-economic analysis - Even Cost Reduction Approach

The work is now being continued with the assumption that costs are going to decrease in similar/even ways. This big assumption results in a lot of uncertainty in the results, but it is a necessary step to make some sense of the provided results. The results are based on optimization at the most favorable constraint for technology deployment, that is a GWP of 25 $MtCO_{2eq}$. This section starts by examining the investment shares in the TI-CBs and the retrofitted CBs.

Cost shares

First, the examination is conducted on the investment shares achieved in the different TI-CB configurations (here, all cost percentages less than or equal to 10% and 7% are shown, they correspond to the cost fractions enabling deployment of the battery with poor and good performance, respectively).

Figure 3.49 shows that for a discharge time of 6h, the investment mainly comes from the charge cycle. The figure that follows, figure 3.50, shows that increasing the discharge time only slightly changes this investment pattern, and the charging cycle remains the largest part of the investment in the technology. In particular, a reduction in investment in the discharge cycle is reflected in an increase in investment in the charge cycle and thermal storage. This analysis also applies to all discharge times between 6h and 14h.

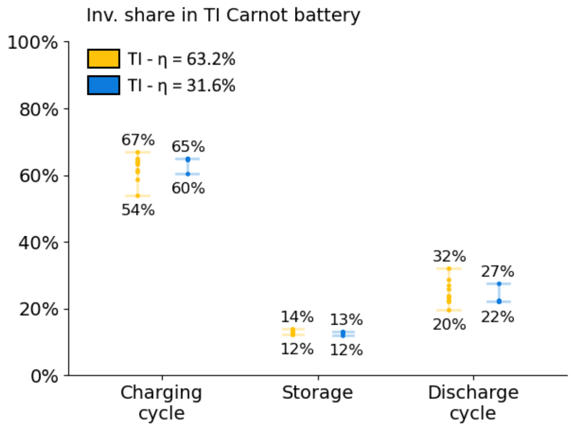

Figure 3.49: Discharge time of 6h

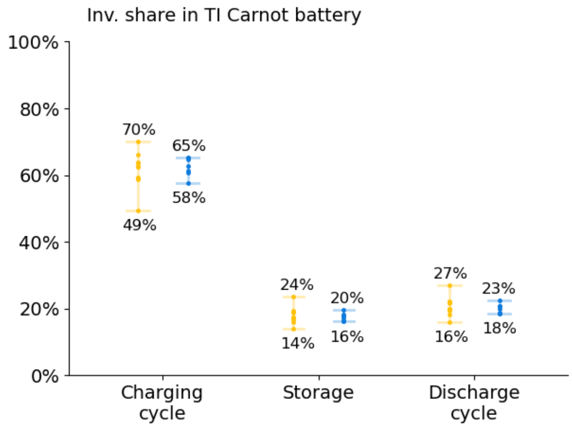

Figure 3.50: Discharge time of 14h

Figure 3.51: Investment shares in thermally integrated Carnot batteries

For the implementation of this battery, maintenance costs are proportional to investment costs, so the breakdown of maintenance costs is similar.

The investments and maintenance shares made for the retrofit battery are then examined. Figure 3.52 shows that the primary investment lies in molten salt HS. Due to the implementation of this CB, the investment distribution is not affected by the discharge time, nor is it affected by the reduction in component costs. However, because of the assumptions made, a significant proportion of the machine's cost is reflected in the maintenance cost of its discharge cycle. This is shown in figure 3.55. (This is also one of the reasons why this assumption is not fundamentally wrong, since high maintenance costs can be expected on pre-existing systems).

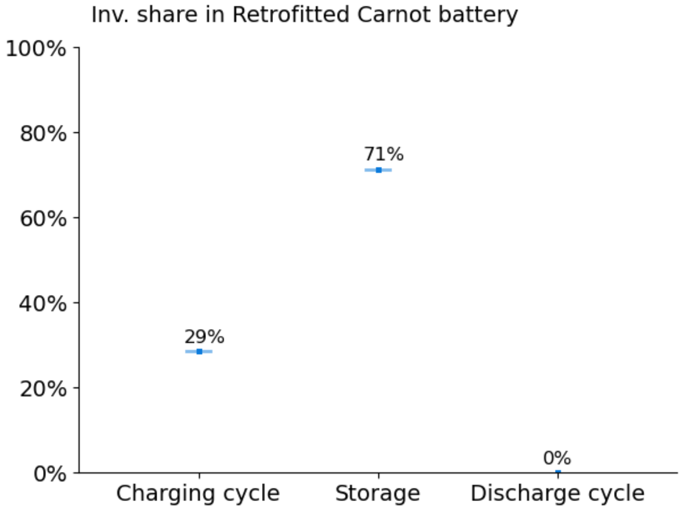

Figure 3.52: Investment shares in Retrofitted Carnot batteries - Constant for all discharge time

Because the maintenance cost of the discharge cycle is fixed, these maintenance costs vary according to cost fractions. As the maintenance costs of the charge cycle and storage decrease, the fraction represented by the discharge cycle increases. As the discharge time increases, the installed discharge cycle capacity decreases, reducing the maintenance costs share associated to the discharge cycle of the battery.

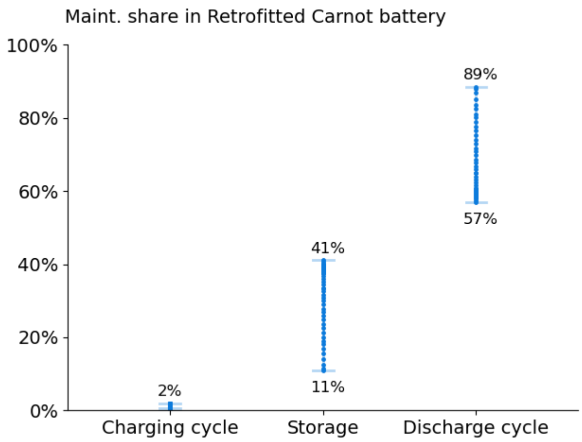

Figure 3.53: Discharge time of 6h

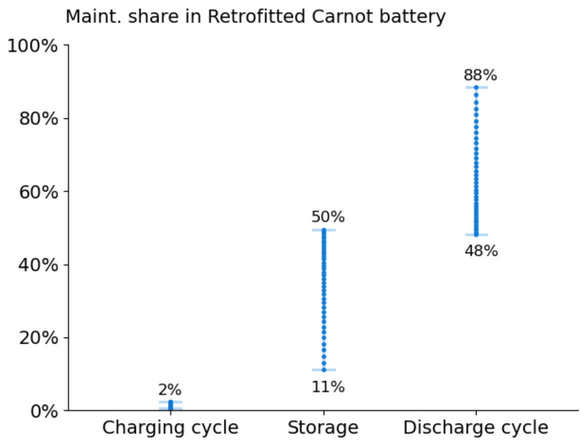

Figure 3.54: Discharge time of 14h

Figure 3.55: Maintenance shares in Retrofitted Carnot batteries

Waste heat consumption

In this section, the variations in heat consumption for thermally integrated batteries are illustrated. The relationship between heat consumption and storage capacity, particularly with a discharge duration of 6 hours, is depicted in Figure 3.56. A nearly linear trend in consumption under the condition of a fixed discharge time is revealed by the data when these CBs are deployed. This linear trend suggests a consumption of 475 GWh per GWh_e of storage for the battery consumming waste heat at a temperature above 70 °C. This is 354 GWh per GWh_e of storage for the second battery. These values decrease to 290 and 236 GWh of waste heat per GWh_e of storage once the discharge time is increased to 14 h.

Furthermore, we observe a limitation in the capacity of thermally integrated batteries due to the availability of waste heat. The highest efficiency battery has a restricted capacity of approximately 10 GWhe, whereas the second battery, which trades off some efficiency for the use of lower temperature heat, is constrained to about 20 GWhe of storage capacity. However, these limitations are subject to considerable uncertainties due to the way in which waste heat is estimated.

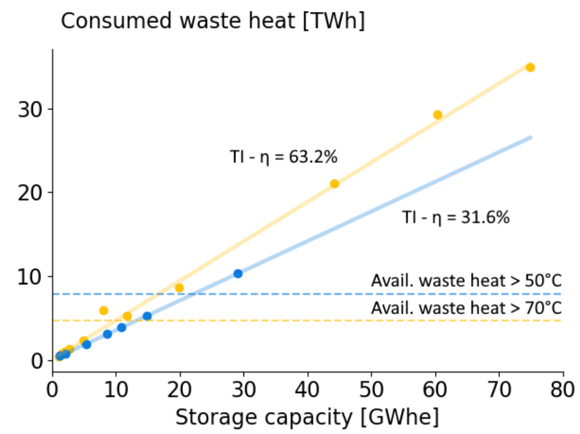

Figure 3.56: Discharge time of 6h

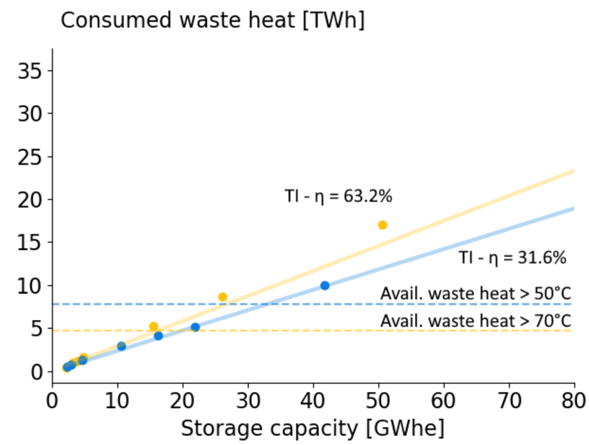

Figure 3.57: Discharge time of 14h

Figure 3.58: Heat consumption with respect to storage capacity

When the allowed discharge time is increased, it is observed that the heat consumption per storage unit decreases, as demonstrated in the right-hand side figure 3.57. The reason behind this result comes from the relationship between battery discharge time and the number of full cycles performed by the battery. As the discharge time increases, the number of cycles decreases, reducing the amount of stored electricity.

Number of cycles

In the previous section, the number of cycles performed by the TI-CBs and the influence of discharge time on this quantity were briefly discussed. In this section, for systems with similar cost reductions, the effect of discharge time on the number of cycles carried out by the CB throughout the year is presented. The number of cycles achieved by the different batteries is shown in Figure 3.61.

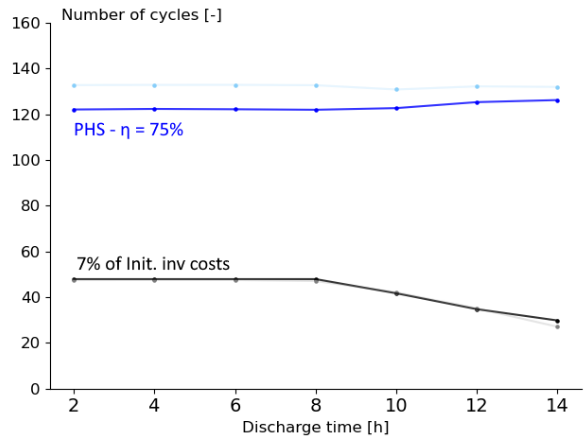

Figure 3.59: (c) TI - $\eta = 63.2\%\%$

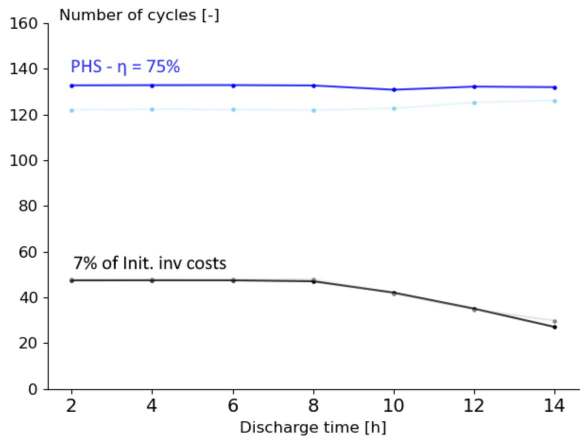

Figure 3.60: (d) TI - $\eta = 31.6\%$

Figure 3.61: Number of cycles performed by Carnot batteries according to their discharge time

It is shown that the number of cycles achieved by the TI-CBs revolves around 35 to 50 complete cycles per year. These cycles are mainly performed on sunny summer days to take advantage of PV panels production. One can compare this number of cycle to the number of cycles achieved by the deployed 6 GWh PHS. The observation reveals that PHS undergoes a greater number of cycles throughout the simulated year, owing to its superior efficiency compared to all implemented technologies. Consequently, it is favored for charging electricity, while CBs come into play for storing leftover electricity. It should be noted that when the efficiency of a CB is lower, a greater number of cycles are accomplished by hydroelectric pumped storage. Finally, an extended discharge period diminishes the annual number of cycles and also influences the operation of the PHS which tends to increase its number of cycles. In Appendix F.3, the number of cycles related to other CBs are proposed. The order of magnitude of the number of cycles achieved by these batteries is similar to those presented here.

Impact of Carnot battery on total system cost

In this concluding section, the impact of the discharge duration in the overall reduction of the system's costs is highlighted. As shown in Figure 3.66 below, the cost reduction achieved by CBs is portrayed. As before, the batteries featured here represent those with the highest feasible cost (with equal percentages for the two thermally integrated batteries to ensure a fair comparison between them).

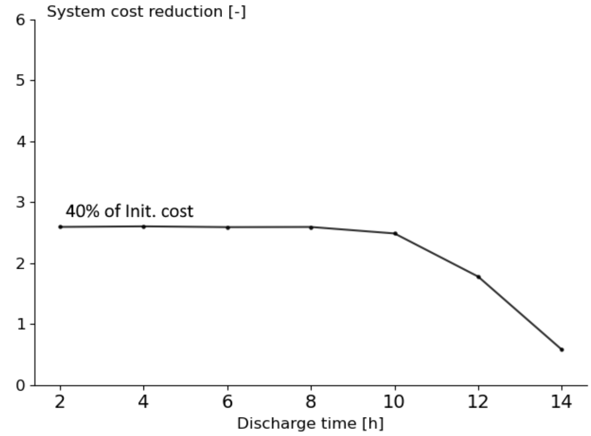

Figure 3.62: (a) Retrofit - $\eta = 40\%\%$

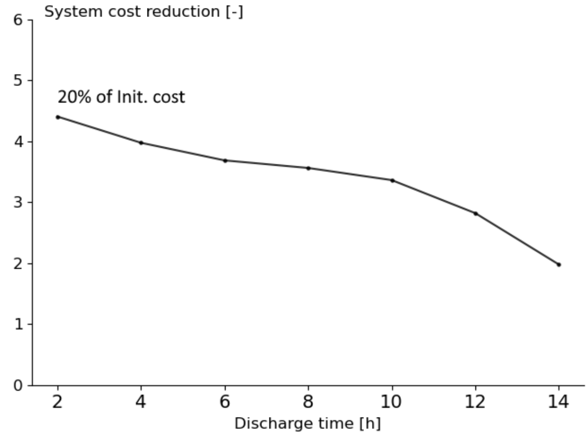

Figure 3.63: (d) Brayton - $\eta = 59\%$

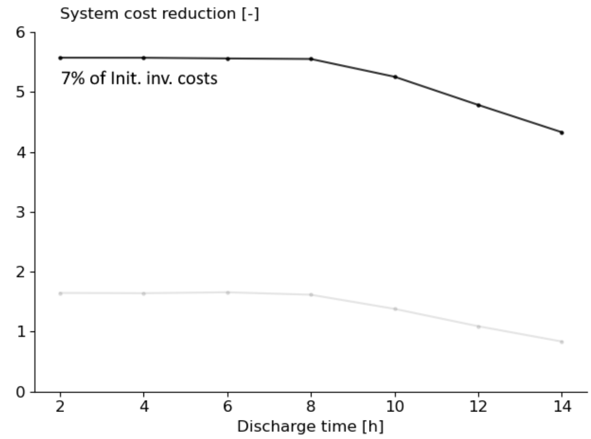

Figure 3.64: (c) TI - $\eta = 63.2\%\%$

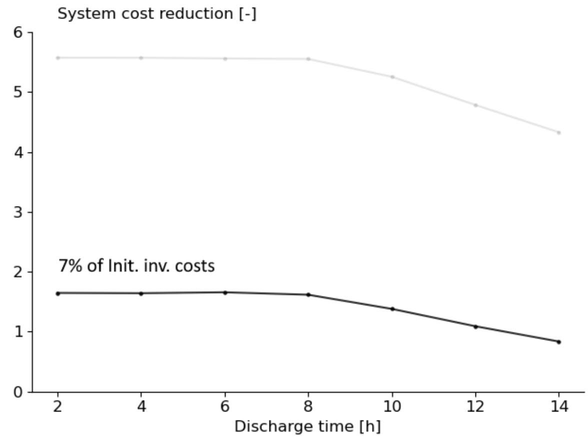

Figure 3.65: (d) TI - $\eta = 31.6\%$

Figure 3.66: Energy system cost reduction with discharge time

In these graphs, the primary observation is that shorter discharge times and consequently lower energy-to-power ratios (high power systems) minimize system costs. This hypothesis is confirmed when we look at the implementation of the Brayton battery, which does not take into account the costs of its discharge cycle. Indeed, in his case, the minimum cost is obtained for an energy-to-power ratio of 2h. Because of the assumption made regarding the maintenance costs of the retrofit battery's discharge cycle, its energy-to-power ratio is extended to over 9 hours. If an assumption similar to other batteries had been made (considering its maintenance cost as 5% of its investment cost), then a result similar to the Brayton battery would be expected.

Finally, for TI-CBs, it is demonstrated that the cost reduction of the system is unaffected by the discharge time as long as it falls within the range of 2 to 8 hours. This is attributed to the higher investment cost per unit of their discharge cycles. As a result, systems designed by EnergyScope tend to have energy-to-power ratios greater than what is permissible.

These results are significantly influenced by one of the parameters imposed on EnergyScope, which forces the implementation of daily storage. Nevertheless, this constraint can be removed, and a similar experiment can be conducted to explore storage possibilities that extend beyond the daily timeframe.

In order to better understand how discharge time can influence system cost, a comparison between 2 energy systems, one with a 6h discharge time battery and the other with a 14h discharge time battery, is proposed in the appendix F.4. The main difference is a reduction in CB power output and behavioral adjustments. Small recharges are added in some typical days and some small discharges during synthetic nights, thus showing a prolonged use of the battery. This prolonged use also leads to energy losses through heat losses in the thermal storage.

Chapter 4

Discussion

In this discussion section, the limitations of the various models that have been produced, as well as the methodological constraints, will be pointed out. Additionally, the model results will be contextualized in relation to reality, and potential areas for additional research questions or avenues of improvement for future work will be highlighted.

4.1 Discussing the models

The discussion will start by introducing the three implemented models. These models are the Carnot Brayton battery, the Thermally Integrated Carnot battery, and the Retrofitted coal-fired power plant Carnot battery.

Recuperated Brayton

The first implementation was the recuperated Brayton Carnot battery. Readers will notice that the cost per unit of power (both for the charging and discharging cycles) is not taken into account by this implementation. It is crucial to have these costs to quantify the power capacities that these batteries can provide.
During this study, an attempt was made to consider the machine costs based on the discharge time (and hence, the cost per unit of power). However, this approach led to results that were challenging to analyze. The method used was as follows.

McTigue et al. [30] provide a cost curve per unit of power concerning the machine's discharge time, similar to Figure 4.1 below:

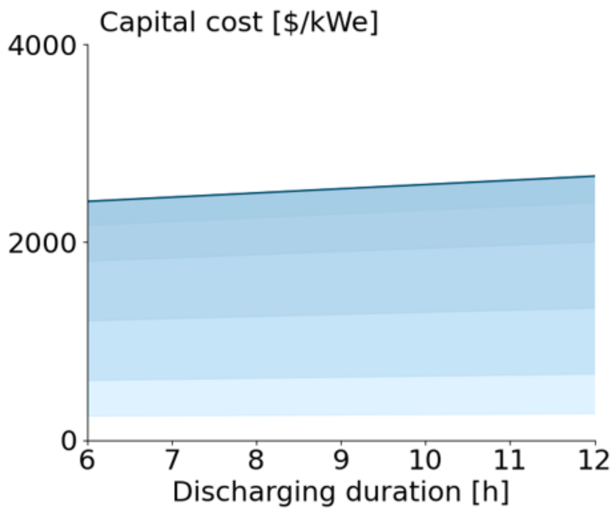

Figure 4.1: Cost per unit of power according to the time of discharge

In the same study, the author determines the cost per unit of energy by simply dividing the machine's cost per unit of power by its discharge time. Performing this operation using the preceding figure yields the following figure, which allows to associate a specific cost per unit of energy value with a particular discharge time. This approach would have enabled to consider the cost of the discharge cycle, and consequently, for longer discharge times, the cost would be lower since the discharge cycle (which is generally more expensive than storage) is reduced. This is illustrated in Figure 4.2 below.

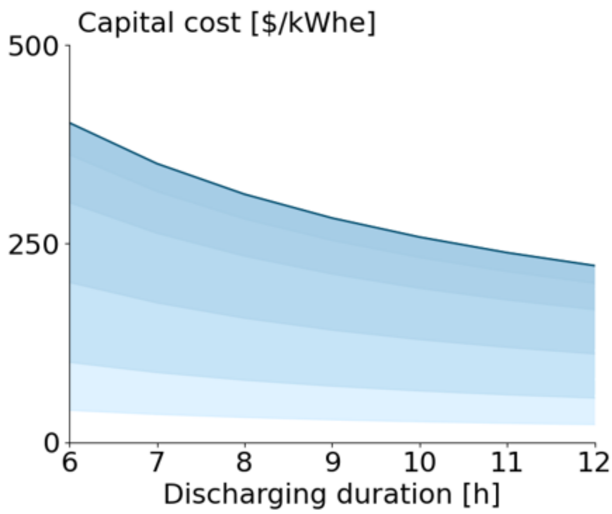

Figure 4.2: Cost per unit of energy according to the time of discharge

The model's results obtained from EnergyScope were difficult to comprehend and lacked coherence. Consequently, the methodology was abandoned in favor of adopting a fixed-cost approach. Within this study, the presentation of results related to the power cycle of this machine was deliberately avoided to prevent the display of inconsistent information.
For future research, one could revisit McTigue et al.'s thermodynamic model [31] and use it to develop a new model that evaluates costs per unit of energy based on the discharge time.

Multi-component models

Multi-component models do not include heat exchangers. This option was chosen due to the challenge of accurately modeling these elements in terms of cost and efficiency, considering the varying admissible scale of Carnot batteries. It was therefore preferable not to take them into account in the various models.

Retrofitted coal-fired power plant

In the retrofit battery model, it's important to mention that due to a lack of data from manufacturers, the cost associated with electrical resistance may be slightly out of line. The costs chosen come from a study aimed at forecasting future heat production system costs, and originate from the European commission [13]. In this document, the investment and maintenance costs of the electric resistance are given with a margin of uncertainty. The problem with this electrical resistance model is that its cost is not adapted to the scale of the machines studied in this work.

Retrofitted coal-fired power plant, in Belgium?

The main purpose of modeling this concept was comparative. To better understand the technical potential of this technology. But an existential question had to be asked. How do you renovate a coal-fired power plant when there are none currently in operation in Belgium? The author believes that it will only be a few years before existing CCGTs (which are also retrofits) have to be renovated. Although the application is not to be prioritized, there will come a day when the primary cycle of these plants will also have to be replaced/renovated due to their age. There is therefore a potential window of opportunity to use one of these power plants for a grid-scale battery. Of course, this is the opinion of a young engineering student, and some technical constraints might escape his notice.

Available amount of waste heat and exergy content

In chapter 2, a quantity of waste heat was calculated using the available means at our disposal, serving as an upper limit for the realization of this work. However, these results should be approached with caution due to the high level of uncertainty associated with this outcome. This is because the presented data are first calculated based on information from two different studies. Furthermore, the data provided in [14] are aggregated to represent a global average rather than specifically reflecting Belgium itself. Finally, the amount of heat at a temperature level below 100 °C does not reveal the exact fraction of this heat that is at precisely 100 °C; it is possible that 90% of this quantity is actually at 25 °C, for example. A dedicated study is necessary to better quantify this waste heat. Based on these findings, it would be interesting to assess whether integrated thermal battery technology remains a deployable solution in Belgium.

Data used and representative demand

The data used in this study dates back to 2020. These data have been used to reduce the uncertainty already present in this work. Indeed, it is quite difficult to predict how the costs of certain technologies will evolve, and the author found it judicious to use data from the past to build his work. These data are also accompanied by a demand corresponding to the year 2020, and it is worth noting that this demand will change in the future.

4.2 Discussing the methodology

In this section, the methodology employed will be addressed and critiqued in order to put the study's results into perspective with reality.

Reducing the costs of the Carnot batteries

To achieve feasible scenarios, it was deemed necessary to reduce the costs of components in each of the Carnot batteries. Ideally, cost projections for these components would have been preferred, but due to limited data and scarce projections, it was necessary to rely on fractions of their respective costs to identify study scenarios. (Also, it is worth noting that if projections had been used, they might not have produced any results.) These reductions were assumed to be bounded by a cost fraction of 5% for all components. This method has enabled us to obtain results for this work, but in no way constitutes proof that these conditions will ever be met. Take the electrical resistor as an example; although projections indicate stable costs for this component, it was assumed otherwise in this study.

Maintenance costs assumptions

For many components, it was assumed that their yearly maintenance costs are fractions (5%) of their investment costs (this is the case for the thermally integrated battery and the Brayton battery), due to the lack of data. Where data was found, it was assumed that the yearly maintenance cost varied with the investment cost. These costs are therefore also reduced as investment costs are reduced. These costs can be formulated as follows, with x being the cost fraction:

$$\begin{aligned} c_{inv} &= x\% \times (\text{Init. Inv. cost}) \\ c_{maint} &= 5\% \times c_{inv} \quad \text{or} \\ c_{maint} &= x\% \times (\text{Init. Maint. cost}) \end{aligned}$$

However, it is not the case for the retrofit Carnot battery's discharge cycle which had a fixed investment cost and therefore, a fixed maintenance cost. This is formulated as:

$$\begin{aligned} c_{inv} &= 0[€/\text{kW}] \\ c_{maint} &= 20.92[€/\text{kWy}] \end{aligned}$$

This method is debatable and is the reason for the disturbing retrofitted coal-fired power plant battery results. This doesn't mean that the results are all wrong, but it is important to keep in mind that the costs attributed to this technology are different, and can therefore lead to 'unexpected' results. This is why the obtained results should be taken with an informed understanding of the hypothesis.

For a deeper explanation of the impact of the hypothesis on the results, an appendix, appendix E is provided. This appendix illustrates the causal factors behind the results and presents additional outcomes, enhancing the author's ability to visualize the hypothesis's impact.

4.3 Discussing the results

The results presented in this study suggest that the viability of employing Carnot batteries on a daily basis for grid scale electricity storage arises when the cost of these batteries reaches a threshold of approximately ±90 €/kWh$_e$ for the firsts GWh$_e$ and ±800 €/kW$_e$ for the first 100 MW$_e$ of power output. These threshold move according to the efficiency of the different Carnot batteries and also depend on the maintenance costs of these technologies. This feasibility is especially relevant for energy systems reliant on renewable sources. Additionally, the study reveals that the integration of Carnot batteries into the Belgian energy system is restrained by their efficiency. Consequently, the Belgian energy system would find greater benefit in direct electricity consumption to minimize losses. These findings need to be contextualized within the specific country under investigation. Belgium, characterized by its high population density, unfortunately lacks substantial renewable energy resources to fulfill its energy requirements.

These results require nuance. It should be aware that the outcomes of an optimization tool warrant cautious consideration. The nature of this study is essentially deterministic and depends heavily on the quality of the data used, necessitating a significant degree of caution prior to making any assertions regarding the implementation of the Carnot battery. Furthermore, the translation of optimization model results into real-world implications is not automatic. While EnergyScope excludes lithium-ion batteries from its energy system considerations, it's important to note that this technology is currently undergoing significant global development (it's worth noting that some lithium-ion battery projects are already underway in Belgium). Thus, the outcomes presented in this context do not amount to a condemnation of the Carnot battery.

This work also demonstrates that the deployment of an integrated Carnot battery requires a significant cost reduction (cost reduction by a factor of 10) and that this reduction is not the sole constraint for its deployment. Indeed, even though the amount of waste heat presented in this study is sufficient for battery integration, the estimations of this quantity remain vague once again, and additional efforts could be undertaken to more accurately quantify these values. This, in turn, would facilitate a better understanding of the potential role of the thermally integrated battery.

Regarding the investment shares in thermally integrated Carnot batteries, it's important to consider that the costs will not evolve in the same manner as proposed in this study. The investment shares are thus highly sensitive to these developments. Nevertheless, the study already reveals two trends. If batteries are developed in alignment with EnergyScope's proposed usage (10-hour charge time, discharge time of approximately ± 8 hours), the thermally integrated battery will gain a substantial advantage from reducing its charging cycle and storage costs (although a cost reduction in the organic Rankine cycle will also enable more powerful systems). As for the retrofit battery, the projected cost of electrical resistance show no signs of decreasing[13]. However, costs associated with molten salt storage could decrease in the coming years (given the technology's increasing use in solar towers and even certain nuclear power plant technologies). Consequently, due to their lower initial costs, these technologies have a higher likelihood of being deployed. (And this is confirmed by the presence of numerous projects currently under consideration in Chile.[23])

The technology's role in extending renewable generation and mitigating daytime power peaks is indicated by the number of cycles and the evolution of its costs in relation to discharge time. This function arises due to the daily constraint imposed. Nevertheless, considering the energy-to-power ratios established by EnergyScope for thermally integrated batteries, it would be interesting to analyze the batteries behavior in the absence of this constraint. Exploring a potential long-term storage role might offer greater utility for these technologies. As for the retrofit battery, the existing discharge cycles present an opportunity to create a storage system designed for daily use but once again, this will depend on the evolution of costs related to these technologies. Future work could provide more information on this question.

4.4 Reflections & Future work

In this section, some of the author's thoughts and ideas for improvement and further development are presented.

Concerning the Carnot batteries, it would be interesting to find or carry out studies to better define the investment or maintenance costs of the machines used in this work. As the assumption concerning the maintenance costs are an order of magnitude, it would be interesting to be able to better quantify them for each machine. Improvements in the modeling of the Brayton battery would also be welcome.

With regard to the energy system modeled, improvements can be achieved by constraining the energy system with regard to the quantities of renewable fuels (ammonia, hydrogen, natural gas). In this work, all these quantities are assumed to be unlimited. Gaining insight into how this constraint influences the deployment costs of the Carnot batteries would be of interest, as this could have a positive influence on its deployment. It would also be interesting to do the same with the available amount of waste heat.

Sensitivity analysis could be carried out on the energy model studied. Here are a few ideas that the author would have liked to address in the continuation of this work:

1. The impact of relaxing the daily use constraint would have on the results proposed in this work.
2. The impact of a nuclear phase-out on Carnot's battery deployment costs.(To make this analysis realistic, we may need to constrain the availability of resources such as ammonia, renewable natural gas and hydrogen.)
3. Analyses of the cost of resources and technologies that interact with the Carnot battery during its deployment, such as the investment cost of photovoltaic panels, wind turbines, industrial resistors or various heat storage systems.
4. During this work, the author also considered the idea of making a comparison between several storage technologies, including the Carnot battery, but this time taking into account the CO_2 emissions involved in the construction, use and decommissioning of all technologies. Lithium-ion batteries are being developed rapidly, and the technology could play an important role in daily electrical storage. However, the massive deployment of this storage medium overlooks the importance of planetary limits. It would be interesting to compare these systems with a global approach taking these limits into account.
5. In this work, thermal integration was only partially achieved, since waste heat consumption was only a pretext to increase the electrical efficiency of the Carnot battery. However, the technology could have a role to play when integrated into a heating network. An implementation enabling this integration would be worth considering to realize the impact this could have on its deployment cost.
6. Finally, it would be interesting to study the integration of these technologies in other countries, in order to understand the extent to which renewable resources such as sun, wind and hydroelectricity enable the integration of this technology.

Chapter 5

Conclusion

At a time when the world needs to make an energy transition in order to combat climate change, it is now necessary to carry out studies into the techno-economical feasibility of the technologies that will power tomorrow's world. These studies focus in part on storage technologies, and among them is the Carnot battery. It is in this work that the techno-economic feasibility of this technology is studied in the context of daily electricity storage in Belgium. This work has addressed the following questions:

At what costs do these technologies become attractive? And what is the impact of efficiency on these costs?

The most efficient technology, the thermally integrated battery with an efficiency of 63.2%, has a cost per unit of energy and power of less than 90 €/kWh_e and 800 €/kW_e. These costs decrease as the efficiency of Carnot batteries decreases. These costs are obtained with a maintenance cost equivalent to 5% of the investment cost.

What role will the technology play in the Belgian energy system once deployed?

Carnot batteries, when competitive, are used when the system is constrained by its CO_2 emissions, in order to extend the use of renewable energies such as solar photovoltaic and wind power. This reduces the peak power required for industrial heat production, which in turn reduces the need for industrial heat storage.

How does the discharge time, and therefore, the energy to power ratio of these technologies affect their deployment and the energy system in which they are integrated ?

For daily electricity storage, EnergyScope shows that minimizing the energy to power ratio maximizes the cost reduction of the system in which the battery is integrated. However, this result must take into account that discharge cycle costs tend to increase this ratio due to their discharge cycle cost. A future study could investigate these same systems by removing this daily constraint to determine if another optimum exists.

Specifically to thermally integrated Carnot battery, what amount of heat is necessary to have a deployment of the technology ?

This study demonstrates that achieving high-efficiency thermally integrated daily electrical storage necessitates 475 GWh of waste heat per GWh_e of installed capacity, while a lower-efficiency system would lower this requirement to 354 GWh of waste heat per GWh_e of capacity.

In summary, this study demonstrates that the investigated Carnot batteries have a journey ahead before reaching cost optimality in Belgium. The key takeaway remains unchanged.

The best energy is the energy we do not consume

Bibliography

[1] *200928-GIZ-Chile-ExecSummary-v6-English-corrected.pdf*. URL: https://4echile.cl/wp-content/uploads/2020/09/200928-GIZ-Chile-ExecSummary-v6-English-corrected.pdf (visited on 02/12/2023).

[2] *201112-MG-Chile-Carnot-Batteries-_Webinar.pdf*. URL: https://4echile.cl/wp-content/uploads/2020/11/201112-MG-Chile-Carnot-Batteries-_Webinar.pdf (visited on 02/12/2023).

[3] Guruprasad Alva, Yaxue Lin, and Guiyin Fang. "An overview of thermal energy storage systems". In: *Energy* 144 (Feb. 1, 2018), pp. 341–378. ISSN: 0360-5442. DOI: 10.1016/j.energy.2017.12.037. URL: https://www.sciencedirect.com/science/article/pii/S036054421732056X (visited on 02/19/2023).

[4] *Annex 58*. Annex 58. URL: https://heatpumpingtechnologies.org/annex58/ (visited on 06/23/2023).

[5] Kevin Attonaty et al. "Thermodynamic analysis of a 200MWh electricity storage system based on high temperature thermal energy storage". In: *Energy* 172 (Apr. 1, 2019), pp. 1132–1143. ISSN: 0360-5442. DOI: 10.1016/j.energy.2019.01.153. URL: https://www.sciencedirect.com/science/article/pii/S0360544219301690 (visited on 02/19/2023).

[6] John J. III Burkhardt, Garvin A. Heath, and Craig S. Turchi. "Life Cycle Assessment of a Parabolic Trough Concentrating Solar Power Plant and the Impacts of Key Design Alternatives". In: *Environmental Science & Technology* 45.6 (Mar. 15, 2011). Publisher: American Chemical Society, pp. 2457–2464. ISSN: 0013-936X. DOI: 10.1021/es1033266. URL: https://doi.org/10.1021/es1033266 (visited on 03/17/2023).

[7] Tristan R. Davenne and Benjamin M. Peters. "An Analysis of Pumped Thermal Energy Storage With De-coupled Thermal Stores". In: *Frontiers in Energy Research* 8 (2020). ISSN: 2296-598X. URL: https://www.frontiersin.org/articles/10.3389/fenrg.2020.00160 (visited on 02/22/2023).

[8] O. Dumont and V. Lemort. "Mapping of performance of pumped thermal energy storage (Carnot battery) using waste heat recovery". In: *Energy* 211 (Nov. 15, 2020), p. 118963. ISSN: 0360-5442. DOI: 10.1016/j.energy.2020.118963. URL: https://www.sciencedirect.com/science/article/pii/S0360544220320703 (visited on 11/21/2022).

[9] Olivier Dumont, Antonios Charalampidis, and Vincent Lemort. "Experimental Investigation Of A Thermally Integrated Carnot Battery Using A Reversible Heat Pump/Organic Rankine Cycle". In: (2021).

[10] Olivier Dumont et al. “Carnot battery technology : a state-of-the-art review”. In: *JOURNAL OF ENERGY STORAGE* 32 (2020). ISSN: 2352-152X. DOI: 10.1016/j.est.2020.101756. URL: http://hdl.handle.net/1854/LU-8675786 (visited on 10/24/2022).

[11] DG Energy’s. “• 12th warmest of EU28 • 6th warmest among the 14 HRE countries”. In: (2020).

[12] Alberto rossi Espagnet. “Techno-Economic Assessment of Thermal Energy Storage integration into Low Temperature District Heating Networks”. In: (Jan. 1, 2016). URL: https://www.academia.edu/79307242/Techno_Economic_Assessment_of_Thermal_Energy_Storage_integration_into_Low_Temperature_District_Heating_Networks (visited on 06/23/2023).

[13] European Commission. Joint Research Centre., ILF Consulting Engineers Austria GmbH., and AIT Austrian Institute of Technology GmbH. *Long term (2050) projections of techno-economic performance of large-scale heating and cooling in the EU.* LU: Publications Office, 2017. URL: https://data.europa.eu/doi/10.2760/24422 (visited on 07/07/2023).

[14] Clemens Forman et al. “Estimating the global waste heat potential”. In: *Renewable and Sustainable Energy Reviews* 57 (May 1, 2016), pp. 1568–1579. ISSN: 1364-0321. DOI: 10.1016/j.rser.2015.12.192. URL: https://www.sciencedirect.com/science/article/pii/S1364032115015750 (visited on 02/20/2023).

[15] Guido Francesco Frate, Lorenzo Ferrari, and Umberto Desideri. “Analysis of suitability ranges of high temperature heat pump working fluids”. In: *Applied Thermal Engineering* 150 (Mar. 5, 2019), pp. 628–640. ISSN: 1359-4311. DOI: 10.1016/j.applthermaleng.2019.01.034. URL: https://www.sciencedirect.com/science/article/pii/S1359431118353602 (visited on 02/23/2023).

[16] Guido Francesco Frate, Lorenzo Ferrari, and Umberto Desideri. “Multi-criteria investigation of a pumped thermal electricity storage (PTES) system with thermal integration and sensible heat storage”. In: *Energy Conversion and Management* 208 (Mar. 15, 2020), p. 112530. ISSN: 0196-8904. DOI: 10.1016/j.enconman.2020.112530. URL: https://www.sciencedirect.com/science/article/pii/S0196890420300662 (visited on 11/21/2022).

[17] Guido Francesco Frate, Lorenzo Ferrari, and Umberto Desideri. “Rankine Carnot Batteries with the Integration of Thermal Energy Sources: A Review”. In: *Energies* 13.18 (Jan. 2020). Number: 18 Publisher: Multidisciplinary Digital Publishing Institute, p. 4766. ISSN: 1996-1073. DOI: 10.3390/en13184766. URL: https://www.mdpi.com/1996-1073/13/18/4766 (visited on 02/28/2023).

[18] Guido Francesco Frate et al. “Thermally integrated pumped thermal energy storage for multi-energy districts: Integrated modelling, assessment and comparison with batteries”. In: *Journal of Energy Storage* 61 (May 1, 2023), p. 106734. ISSN: 2352-152X. DOI: 10.1016/j.est.2023.106734. URL: https://www.sciencedirect.com/science/article/pii/S2352152X23001317 (visited on 02/28/2023).

[19] Solomos Georgiou, Nilay Shah, and Christos N. Markides. “A thermo-economic analysis and comparison of pumped-thermal and liquid-air electricity storage systems”. In: *Applied Energy* 226 (Sept. 15, 2018), pp. 1119–1133. ISSN: 0306-2619. DOI: 10.1016/j.apenergy.2018.04.128. URL: https://www.sciencedirect.com/science/article/pii/S0306261918306627 (visited on 03/30/2023).

[20] Liliana Andreia Morais Gomes. “Evaluation of the Technical and Economic Feasibility of Carnot Batteries”. In: ().

[21] *Heat Roadmap Europe*. URL: https://heatroadmap.eu/ (visited on 03/30/2023).

[22] Shuozhuo Hu et al. "Thermo-economic analysis of the pumped thermal energy storage with thermal integration in different application scenarios". In: *Energy Conversion and Management* 236 (May 15, 2021), p. 114072. ISSN: 0196-8904. DOI: 10.1016/j.enconman.2021.114072. URL: https://www.sciencedirect.com/science/article/pii/S019689042100248X (visited on 01/02/2023).

[23] Susan Kraemer. *Chile Considers Converting 30 Coal Plants into "Carnot" Batteries*. SolarPACES. June 2, 2021. URL: https://www.solarpaces.org/chile-considers-converting-30-coal-plants-into-carnot-batteries/ (visited on 08/11/2023).

[24] Robert B. Laughlin. "Pumped thermal grid storage with heat exchange". In: *Journal of Renewable and Sustainable Energy* 9.4 (July 2017). Publisher: American Institute of Physics, p. 044103. DOI: 10.1063/1.4994054. URL: https://aip.scitation.org/doi/10.1063/1.4994054 (visited on 03/30/2023).

[25] Sanne Lemmens. "Cost Engineering Techniques and Their Applicability for Cost Estimation of Organic Rankine Cycle Systems". In: *Energies* 9.7 (July 2016). Number: 7 Publisher: Multidisciplinary Digital Publishing Institute, p. 485. ISSN: 1996-1073. DOI: 10.3390/en9070485. URL: https://www.mdpi.com/1996-1073/9/7/485 (visited on 02/12/2023).

[26] Ting Liang et al. "Key components for Carnot Battery: Technology review, technical barriers and selection criteria". In: *Renewable and Sustainable Energy Reviews* 163 (July 1, 2022), p. 112478. ISSN: 1364-0321. DOI: 10.1016/j.rser.2022.112478. URL: https://www.sciencedirect.com/science/article/pii/S1364032122003823 (visited on 12/12/2022).

[27] Gauthier Limpens et al. "EnergyScope TD: A novel open-source model for regional energy systems". In: *Applied Energy* 255 (Dec. 1, 2019), p. 113729. ISSN: 0306-2619. DOI: 10.1016/j.apenergy.2019.113729. URL: https://www.sciencedirect.com/science/article/pii/S0306261919314163 (visited on 03/01/2023).

[28] Seyed Hossein Madaeni, Ramteen Sioshansi, and Paul Denholm. "How Thermal Energy Storage Enhances the Economic Viability of Concentrating Solar Power". In: *Proceedings of the IEEE* 100.2 (Feb. 2012). Conference Name: Proceedings of the IEEE, pp. 335–347. ISSN: 1558-2256. DOI: 10.1109/JPROC.2011.2144950.

[29] F. Marguerre. "Ueber ein neues Verfahren zur Aufspeicherung elektrischer Energie". In: 354.55 (1924), pp. 27–35.

[30] Joshua D. McTigue et al. "Techno-economic analysis of recuperated Joule-Brayton pumped thermal energy storage". In: *Energy Conversion and Management* 252 (Jan. 15, 2022), p. 115016. ISSN: 0196-8904. DOI: 10.1016/j.enconman.2021.115016. URL: https://www.sciencedirect.com/science/article/pii/S0196890421011924 (visited on 12/01/2022).

[31] Joshua D. McTigue et al. "Techno-economic analysis of recuperated Joule-Brayton pumped thermal energy storage - Supplementary information". In: *Energy Conversion and Management* 252 (Jan. 2022), p. 115016. ISSN: 01968904. DOI: 10.1016/j.enconman.2021.115016. URL: https://linkinghub.elsevier.com/retrieve/pii/S0196890421011924 (visited on 12/28/2022).

[32] Matteo Morandin et al. “Conceptual design of a thermo-electrical energy storage system based on heat integration of thermodynamic cycles – Part A: Methodology and base case”. In: *Energy*. The 24th International Conference on Efficiency, Cost, Optimization, Simulation and Environmental Impact of Energy, ECOS 2011 45.1 (Sept. 1, 2012), pp. 375–385. ISSN: 0360-5442. DOI: 10.1016/j.energy.2012.03.031. URL: https://www.sciencedirect.com/science/article/pii/S0360544212002228 (visited on 03/04/2023).

[33] Vaclav Novotny et al. “Review of Carnot Battery Technology Commercial Development”. In: *Energies* 15.2 (Jan. 2022). Number: 2 Publisher: Multidisciplinary Digital Publishing Institute, p. 647. ISSN: 1996-1073. DOI: 10.3390/en15020647. URL: https://www.mdpi.com/1996-1073/15/2/647 (visited on 10/24/2022).

[34] Henrik Öhman and Per Lundqvist. “Comparison and analysis of performance using Low Temperature Power Cycles”. In: *Applied Thermal Engineering* 52.1 (Apr. 5, 2013), pp. 160–169. ISSN: 1359-4311. DOI: 10.1016/j.applthermaleng.2012.11.024. URL: https://www.sciencedirect.com/science/article/pii/S1359431112007375 (visited on 03/01/2023).

[35] Ugo Pelay et al. “Thermal energy storage systems for concentrated solar power plants”. In: *Renewable and Sustainable Energy Reviews* 79 (Nov. 1, 2017), pp. 82–100. ISSN: 1364-0321. DOI: 10.1016/j.rser.2017.03.139. URL: https://www.sciencedirect.com/science/article/pii/S1364032117304021 (visited on 02/19/2023).

[36] Ramana G. Reddy. “Molten Salts: Thermal Energy Storage and Heat Transfer Media”. In: *Journal of Phase Equilibria and Diffusion* 32.4 (Aug. 1, 2011), pp. 269–270. ISSN: 1863-7345. DOI: 10.1007/s11669-011-9904-z. URL: https://doi.org/10.1007/s11669-011-9904-z (visited on 08/03/2023).

[37] D. Salomone-González et al. “Pumped heat energy storage with liquid media: Thermodynamic assessment by a Brayton-like model”. In: *Energy Conversion and Management* 226 (Dec. 15, 2020), p. 113540. ISSN: 0196-8904. DOI: 10.1016/j.enconman.2020.113540. URL: https://www.sciencedirect.com/science/article/pii/S0196890420310694 (visited on 02/28/2023).

[38] P L Spath and M K Mann. *Life Cycle Assessment of a Natural Gas Combined Cycle Power Generation System*. NREL/TP-570-27715, 776930. Dec. 27, 2000, NREL/TP–570–27715, 776930. DOI: 10.2172/776930. URL: http://www.osti.gov/servlets/purl/776930/ (visited on 03/17/2023).

[39] *STRATEGO-WP2-Background-Report-7-Potenital-for-Excess-Heat.pdf*. URL: https://heatroadmap.eu/wp-content/uploads/2018/09/STRATEGO-WP2-Background-Report-7-Potenital-for-Excess-Heat.pdf (visited on 06/23/2023).

[40] *The EnergyScope model — EnergyScope_documentation 2.2 documentation*. URL: https://energyscope.readthedocs.io/en/latest/ (visited on 06/28/2023).

[41] Silvia Trevisan, Bjarke Buchbjerg, and Rafael Guedez. “Power-to-heat for the industrial sector: Techno-economic assessment of a molten salt-based solution”. In: *Energy Conversion and Management* 272 (Nov. 15, 2022), p. 116362. ISSN: 0196-8904. DOI: 10.1016/j.enconman.2022.116362. URL: https://www.sciencedirect.com/science/article/pii/S0196890422011402 (visited on 06/28/2023).

[42] Bao Truong and Benjamin Bollinger. *Repurposing Fossil-Fueled Assets For Energy Storage*. FINAL REPORT - DOE - MALTA INC -FE0032004. Malta Inc., June 28, 2022. DOI: 10.2172/1874051. URL: https://www.osti.gov/biblio/1874051 (visited on 12/30/2022).

[43] *US Dollar to Euro Spot Exchange Rates for 2022*. URL: https://www.exchangerates.org.uk/USD-EUR-spot-exchange-rates-history-2022.html (visited on 04/09/2023).

[44] Andrea Vecchi et al. "Carnot Battery development: A review on system performance, applications and commercial state-of-the-art". In: *Journal of Energy Storage* 55 (Nov. 30, 2022), p. 105782. ISSN: 2352-152X. DOI: 10.1016/j.est.2022.105782. URL: https://www.sciencedirect.com/science/article/pii/S2352152X22017704 (visited on 11/14/2022).

[45] Philipp Vinnemeier et al. "Integration of Pumped-Heat-Electricity-Storage into Water / Steam Cycles of Thermal Power Plants". In: ().

[46] Liang Wang et al. "Unbalanced mass flow rate of packed bed thermal energy storage and its influence on the Joule-Brayton based Pumped Thermal Electricity Storage". In: *Energy Conversion and Management* 185 (Apr. 1, 2019), pp. 593–602. ISSN: 0196-8904. DOI: 10.1016/j.enconman.2019.02.022. URL: https://www.sciencedirect.com/science/article/pii/S0196890419302043 (visited on 02/22/2023).

[47] Yongcan Wang et al. "Flexible Operation of Retrofitted Coal-Fired Power Plants to Reduce Wind Curtailment Considering Thermal Energy Storage". In: *IEEE Transactions on Power Systems* 35.2 (Mar. 2020). Conference Name: IEEE Transactions on Power Systems, pp. 1178–1187. ISSN: 1558-0679. DOI: 10.1109/TPWRS.2019.2940725.

[48] Alexander White, Geoff Parks, and Christos N. Markides. "Thermodynamic analysis of pumped thermal electricity storage". In: *Applied Thermal Engineering*. Includes Special Issue: PRO-TEM Special Issue 53.2 (May 2, 2013), pp. 291–298. ISSN: 1359-4311. DOI: 10.1016/j.applthermaleng.2012.03.030. URL: https://www.sciencedirect.com/science/article/pii/S1359431112002141 (visited on 02/22/2023).

[49] Qingqing Yong et al. "Retrofitting coal-fired power plants for grid energy storage by coupling with thermal energy storage". In: *Applied Thermal Engineering* 215 (Oct. 1, 2022), p. 119048. ISSN: 1359-4311. DOI: 10.1016/j.applthermaleng.2022.119048. URL: https://www.sciencedirect.com/science/article/pii/S1359431122009802 (visited on 06/28/2023).

[50] Han Zhang et al. "Combined cooling, heating, and power generation performance of pumped thermal electricity storage system based on Brayton cycle". In: *Applied Energy* 278 (Nov. 15, 2020), p. 115607. ISSN: 0306-2619. DOI: 10.1016/j.apenergy.2020.115607. URL: https://www.sciencedirect.com/science/article/pii/S0306261920311144 (visited on 02/19/2023).

Appendices

Appendix A

Heat pump costs

Heat pump name	Cost [euro/kw] (lower)	Cost [euro/kw] (upper)
Rotation Heat Pump ecop Technologies GmbH	700	700
Hydrocarbon Heat Pump / HS-compressor Mayekawa Europe NV	450	450
Hydrocarbon Heat Pump / FC-compressor Mayekawa Europe NV	720	720
GEA CO2 Heat Pump GEA Heating and Refrigeration Technologies	200	300
CO2 Heat Pump System for Hot Water Production Fenagy A/S	250	425
Screw compressor high-temperature heat pump Rank	200	400
HWW 2/9583I R1233zd(E) COMBITHERM GmbH	200	400
ThermBooster SPH Sustainable Process Heat GmbH	150	1000
High Temperature Heat Pump Hybrid Energy	200	600
TC-C920 ToCircle Industries	250	430
Weel & Sandvig	150	250
Reversed Stirling Cycle Olvondo Technology AS	1200	1200
HeatBooster Heaten AS	250	350
HoegTemp UHT heat pump Enerin AS	600	800
High Temperature Heat Pump	300	400
Spilling Steam Compressor Spilling Technologies GmbH	100	400
MVR-HP EPCON Evaporation Technology AS	200	400
Turboden Large Heat Pumps	300	700
ETES CO2 Heat pump	300	500
Compressors and blowers for open loop MVR cycle and steam heat pumps	850	850
Industrial Heat Pump	250	800
Qpinch Heat Transformer	1000	2000
SkaleUP	500	700
Mean price euro/kW	405.2	642.4

Table A.1: Heat pump costs from manufacturer data sheets

Appendix B

Reference scenario - Data used

Here, the data used to model the 2020 energy model are grouped together. These data do not include information on the CBs implemented.

B.1 Demand

The following table shows the demand considered in the year 2020.

Table B.1: 2020 Demand by category

Demand	Households	Services	Industrial	Units
Electricity	18.6756	19.857	36.244	[TWh]
High temperature heat	0.0	0.0	59.414	[TWh]
Space heating	59.77	27.875	15.455	[TWh]
Hot water	15.279	6.249	4.004	[TWh]
Non-energy	0.0	0.0	51.451	[TWh]
Demand	**Consumption**			**Units**
Freight	69186.2			[Mtkm]
Private mobility	109702.8			[Mpkm]

B.2 Technologies

The technologies are implemented using the following units depending on their supposed function (Storage, heat or electricity generator, car,...).

Name	Inv. cost	Maint. cost	GWP	lifetime
Units	[€/kW]	[€/kWy]	[**gCO_2/kW**]	[y]
Units	[€/kWh]	[€/kWhy]	[**gCO_2/kWh**]	[y]
Units	[€/(kmpass/h)]	[€/(kmpass/h)y]	[**gCO_2/(kmpass/h)**]	[y]
Units	[€/(tonkm/h)]	[€/(tonkm/h)y]	[**gCO_2/(tonkm/h)**]	[y]

The implemented technologies are the following :

Nuclear	4845.73	102.93	707.88	60
Combined cycle gas turbine	825.96	20.92	183.79	25
Ammonia combined cycle gas turbine	825.96	20.92	183.79	25
Ultra-supercritical coal power plant	2598.77	30.34	331.6	35
Integrated gasification combined cycle with coal	3351.65	50.00	331.6	35
Photovoltaic	1220.85	13.94	2081.43	25
Wind onshore	1141.96	13.28	622.85	30
Wind offshore	5357.30	37.27	622.85	30
Hydro river	5044.92	50.44	1262.82	40
Geothermal power plant	8764.36	162.82	24929.09	30
Cogeneration gas (industry)	1528.10	98.22	1024.32	25
Cogeneration wood (industry)	1172.95	42.94	165.33	25
Cogeneration waste (industry)	3182.91	117.34	647.82	25
Boiler gas (industry)	70.67	1.42	12.32	17
Boiler wood (industry)	138.22	2.76	28.87	17
Boiler oil (industry)	65.83	1.42	12.32	17
Boiler coal (industry)	138.22	2.76	48.18	17
Boiler waste (industry)	138.22	2.76	28.87	17
Electrical resistors (industry)	387.73	1.76	1.47	15
Heat pump (DHN)	395.73	13.42	174.79	25
Cogeneration gas (DHN)	1361.46	39.81	490.88	25
Cogeneration wood (DHN)	1172.95	42.94	165.33	25
Cogeneration waste (DHN)	3182.91	117.34	647.82	25
Cogeneration wet biomass (DHN)	1491.64	121.40	1024.00	25
Cogeneration hydrolysis (DHN)	4923.77	240.59	647.80	15
Boiler gas (DHN)	70.67	1.42	12.32	17
Boiler wood (DHN)	138.22	2.76	28.87	17
Boiler oil (DHN)	65.83	1.42	12.32	17
Geothermal (DHN)	1611.94	60.40	808.76	30
Solar thermal (DHN)	381.37	0.45	221.22	30
Electrical heat pump (decentralised)	564.78	23.55	164.89	18
Thermal heat pump gas (decentralised)	362.35	10.59	381.93	20
Cogeneration gas (decentralised)	1528.10	98.22	1024.32	20
Cogeneration oil (decentralised)	1416.89	86.93	1024.32	20
Advanced cogeneration (Fuel cell) gas (decentralised)	9185.33	171.18	2193.45	20
Bioler gas (decentralised)	190.24	5.71	21.09	17
Boiler wood (decentralised)	554.93	19.42	21.09	17
Boiler oil (decentralised)	170.86	10.25	21.09	17
Solar thermal (decentralised)	757.56	8.41	221.22	20
Direct electrical heaters (decentralised)	43.61	0.19	1.47	15
Tram or metro	625.00	12.50	0.00	30
Bus diesel	577.94	30.56	0	15
Bus diesel hybrid	822.56	33.33	0	15
Bus gas	585.04	30.56	0	15
Bus fuel cell (H2)	1114.04	31.25	0	15
Train (passenger)	1506.02	54.35	0	40

Car gasoline	397.47	24.00	0	10
Car diesel	410.87	24.00	0	10
Car gas	411.06	24.00	0	10
Car methanol	397.47	24.00	0	10
Car hybrid (gasoline)	423.86	34.00	0	10
Car plug-in hybrid	473.46	34.00	0	10
Car electric	613.66	10.00	0	10
Car fuel cell (H2)	1062.10	10.00	0	10
Train (freight)	104.42	2.09	0	40
Boat diesel	72.24	3.82	0	40
Boat gas	73.13	3.82	0	40
Boat methanol	72.24	3.82	0	40
Trucks diesel	350.97	18.56	0	15
Truck methanol	350.97	18.56	0	15
Truck fuel cell (hydrogen)	430.17	12.07	0	15
Truck electric	878.38	23.13	0	15
Truck gas	355.28	18.56	0	15
Efficiency measures in energy system	5600.00	0.00	0	1
District heating network	825.88	0.00	0	60
Electrical grid cost	74919.06	0.00	0	80
Electrolysers	2784.81	76.58	0	15
Steam methane reforming	775.33	71.55	0	25
Biomass to hydrogen	4798.23	338.03	0	25
Wood gasification	4007.94	282.54	0	25
Hydrogen methanation	349.6	89.32	0	40
Biomass methanation	1122.22	15.55	0	20
Biomass hydrolysis	1811.76	123.53	0	15
Wood pyrolysis to gasoline and diesel	2554.01	116.08	0	25
Wood pyrolysis to LFO	2593.5	72.2	0	25
Carbon capture atmospheric	5342.73	132.62	0	40
Carbon capture from industry	2671.37	66.31	0	40
Hydrogen methanolation	2647.88	75.14	0	20
Methane to methanol	1511.16	66.08	0	25
Biomass methanolation	4788	73.15	0	20
Haber bosch (H2 to ammonia)	963.97	18.85	0	20
Ammonia to H2	775.33	71.55	0	25
Oil to HVC	449.55	2.39	0	15
Gas to HVC	907.75	22.69	0	25
Biomass to HVC	3311.7	98.8	0	20
Methanol to HVC	793.49	71.41	0	20
Batteries	501.3	0.78	61.3	15
Batteries of electric cars	0	0	0	1
Batteries of plug-in hybrid cars	0	0	0	1
Pumped hydro storage	58.8	0	8.33	50
Decentralised direct elec	18.97	0.13	0	20
Decentralised electrical heat pumps	18.97	0.13	0	20
Decentralised thermal heat pumps gas	18.97	0.13	0	20

Decentralised cogeneration gas	18.97	0.13	0	20
Decentralised cogenration oil	18.97	0.13	0	20
Decentralised fuel cell cogeneration gas	18.97	0.13	0	20
Decentralised fuel cell cogenration H2	18.97	0.13	0	20
Decentralised boiler gas	18.97	0.13	0	20
Decentralised boiler wood	18.97	0.13	0	20
Decentralised boiler oil	18.97	0.13	0	20
Centralised daily	3	0.01	0	40
Centralised seasonal	0.59	0.00	0	25
Thermal storage industries	28.03	0.30	0	25
Gas storage	0.05	0.00	0	50
Hydrogen storage	6.19	0.39	0	20
Diesel storage	0.01	0.00	0	20
Gasoline storage	0.01	0.00	0	20
LFO storage	0.01	0.00	0	20
Ammonia storage	0.01	0.00	0	20
Methanol storage	0.01	0.00	0	20
CO2 storage	49.5	0.50	0	30

B.3 Resources

The existing resources are the following :

Table B.3: Implemented resources

	Availability	**Direct and indirect emissions**	**Price**	**Direct emissions**
units	[GWh/y]	[ktCO2-eq./GWh]	[Meuro/GWh]	[ktCO2-eq./GWh]
ELECTRICITY	25205.63483	0.412971429	0.063732	0
GASOLINE	1E+15	0.3448	0.065566486	0.25
DIESEL	1E+15	0.3148	0.063479071	0.27
BIOETHANOL	1E+15	0	0.122502774	0.25
BIODIESEL	1E+15	0	0.131394244	0.27
LFO	1E+15	0.3115	0.047882136	0.26
GAS	1E+15	0.2666	0.033636659	0.2
GAS_RE	1E+15	0	0.132345636	0.2
WOOD	23400	0.0118	0.030123691	0.39
WET_BIOMASS	38900	0.0118	0.005285223	0.39
COAL	33354.99944	0.4014	0.015545445	0.36
URANIUM	1E+15	0.0039	0.003876456	0
WASTE	17800	0.1501	0.021187834	0.26
H2	1E+15	0.414044616	0.077642645	0
H2_RE	1E+15	0	0.137854413	0
AMMONIA	1E+15	0.285	0.071991938	0
METHANOL	1E+15	0.35	0.081184572	0.24570329
AMMONIA_RE	1E+15	0	0.092751343	0
METHANOL_RE	1E+15	0	0.122502774	0.24570329
ELEC_EXPORT	1E+15	0	0	0
CO2_EMISSIONS	1E+15	0	0	0
RES_WIND	1E+15	0	0	0
RES_SOLAR	1E+15	0	0	0
RES_HYDRO	1E+15	0	0	0
RES_GEO	1E+15	0	0	0
CO2_ATM	1E+15	0	0	0
CO2_INDUSTRY	0	0	0	0
CO2_CAPTURED	0	0	0	0

Appendix C

Environments

The changes made to environments to include technologies are detailed here.

C.1 Recuperated Brayton

To carry out this implementation, it is necessary to establish a singular electricity storage system. Subsequently, the task involves modifying the parameters of the CB in a code which runs the optimizations.

Table C.1: Modifications to storage characteristics

param :	storage_charge_time	storage_discharge_time	storage_availability	storage_losses
PHS	4.8309	4.2955	1	0
BATT_LI	4	4	1	0.0002
...	...	...	...	...
Recup_Brayton	10	x	1	0.0020833333

Table C.2: Modifications to storage Eff. in

param storage_eff_in :	ELECTRICITY	...	CO2_CAPTURED
PHS	0.866	...	0
BATT_LI	0.95	...	0
BEV_BATT	0.95	...	0
PHEV_BATT	0.95	...	0
Recup_Brayton	0.768115		0
...	...	...	...
CO2_STORAGE	0	...	1

Table C.3: Modifications to storage Eff. out

param storage_eff_out :	**ELECTRICITY**	**GASOLINE**	**...**	**...**	**...**
PHS	0.866				
BATT_LI	0.95	...	...	...	...
BEV_BATT	0.95	...	...	...	...
PHEV_BATT	0.95	...	...	...	...
Recup_Brayton	0.768114575	...	...	...	...
TS_DEC_DIRECT_ELEC	0	...	...	...	...
...	...	...	...	...	...

Table C.4: Modifications to technologies

Technologies param	**c__inv**	**c__maint**	**gwp__constr**	**lifetime**	**c__p**	**fmin__perc**	**fmax__perc**	**f__min**	**f__max**
NUCLEAR	4845.73	102.930986	707.88	60	0.843906	0	1	0	5.925
...	...	...	...	...	...	...	...	...	...
BATT_LI	501.3	0.775025166	61.3	15	1	0	1	0	1.00E+15
PHS	58.8	0	8.33	50	1	0	1	5	6.5
Recup_Brayton	x	x	6	25	1	0	1	0	1.00E+15
...	...	...	...	...	...	...	...	...	...

In this table, the x values are altered as the code goes through a loop, performing various optimizations.

C.2 Thermally integrated & Retrofit

Within this context, the x-values should be substituted with the respective values of technologies. The sole distinction between the retrofitted CB and the Thermally Integrated CB arises from the matrix that links layers to technologies and vice versa. In the case of the thermally integrated CB (specifically the charging cycle), it uses waste heat as an additional input alongside electricity in order to produce stored heat.

Table C.5: Added resources - Thermal storage layer and Waste heat layer

	Availability	Direct and indirect emissions	Price	Direct emissions
parameter name	avail	gwp_op	c_op	CO2_op
ELECTRICITY	25205.63	0.412971	0.063732	0
...	...	...	...	...
WASTE_HEAT	1.00E+15	0	0	0
LAYER_TES	0	0	0	0

Table C.6: Modifications to storage characteristics

param :	storage_charge_time	storage_discharge_time	storage_availability	storage_losses
PHS	4.8309	4.2955	1	0
BATT_LI	4	4	1	0.0002
...	...	...	...	...
TES	10	x	1	0.0020833333

Table C.7: Modifications to storage Eff. in

param storage_eff_in :	ELECTRICITY	...	WASTE_HEAT	LAYER_TES
PHS	0.866	...	0	0
BATT_LI	0.95	...	0	0
BEV_BATT	0.95	...	0	0
...	...	...	...	...
TES	0	...	0	1

Table C.8: Modifications to storage Eff. out

param storage_eff_in :	ELECTRICITY	...	WASTE_HEAT	LAYER_TES
PHS	0.866	...	0	0
BATT_LI	0.95	...	0	0
BEV_BATT	0.95	...	0	0
...	...	...	...	...
TES	0	...	0	1

Table C.9: Modifications to technologies

Technologies param	c_inv	c_maint	gwp_constr	lifetime	c_p	fmin_perc	fmax_perc	f_min	f_max
NUCLEAR	4845.73	102.931	707.88	60	0.843906	0	1	0	5.925
...	...	...	...	...	...	...	...	...	...
Charge cycle	x	x	x	x	1	0	1	0	1.00E+15
Discharge cycle	x	x	x	x	1	0	1	0	1.00E+15
TES	x	x	x	x	1	0	1	0	1.00E+15

Table C.10: Modifications to Layers_in_out

param layers_in_out:	ELECTRICITY		WASTE_HEAT	LAYER_TES
ELECTRICITY	1	...	0	0
WASTE_HEAT	0	...	1	0
LAYER_TES	0	...	0	1
NUCLEAR	1	...	0	0
...	...	...	...	...
Discharge cycle	1		0	-x
Charge cycle	-x		-x	1

Appendix D

Reference energy systems

D.1 System with $25\,\mathrm{MtCO_{2eq}}$ constraint

At a CO2 emission constraint of $25\,\mathrm{MtCO_{2eq}}$, the energy system continues to rely on fossil fuels, with gas being a significant fuel source alongside Uranium. Gas plays a crucial role in electricity production, heat generation, and transportation. However, the energy system is currently undergoing a transition phase, characterized by a substantial consumption of methanol for non-energy purposes and the increasing utilization of renewable energy sources like solar and wind for electricity generation. Additionally, biomass and non-renewable waste are used for heat production and fuel generation, particularly in the case of wet biomass where synthetic natural gas (SNG) is produced.

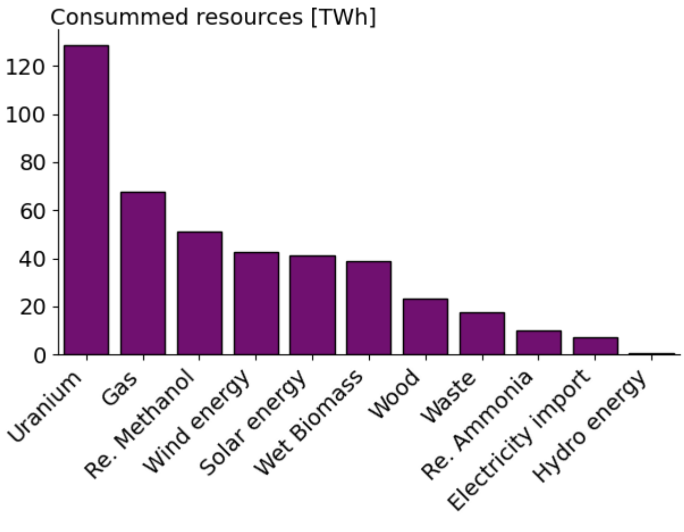

Figure D.1: Resource consumption in reference $25\,\mathrm{MtCO_{2eq}}$ energy system

From the following figure, it is shown that the energy system primarily generates electricity through PV panels, wind farms, and nuclear power, with the surplus energy stored in pumped hydro storage for early morning or evening electricity production. The CCGT is employed for electricity generation as needed, such as during nighttime or in winter. Heat production primarily relies on electricity, supplemented by gas, wood, and waste. Since this heat is generated during periods of high electricity demand, significant storage capacity is necessary to accommodate it.

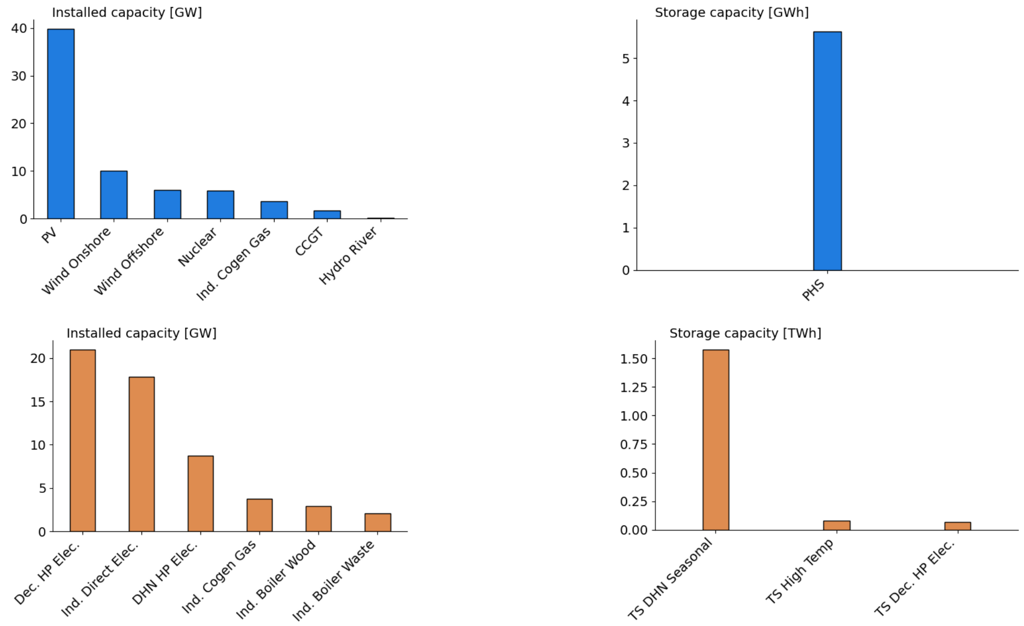

Figure D.2: Electricity and heat production and storage

As mentioned, the energy system produces a small amount of gas through bio-hydrolysis (Wet-biomass consumption)

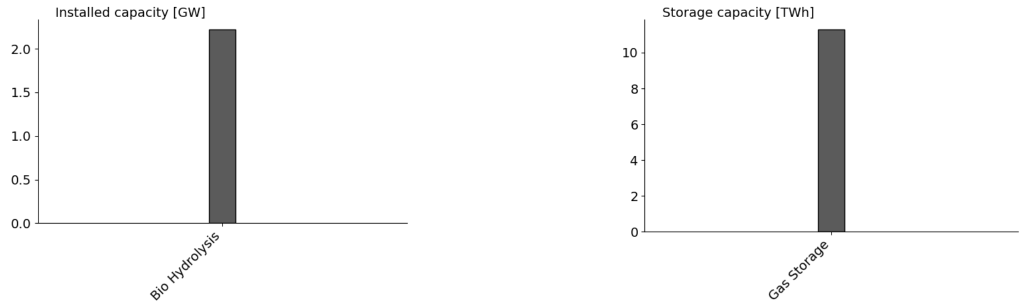

Figure D.3: Gas production and storage

Finally, as mentioned earlier, gas is mainly used for mobility assets.

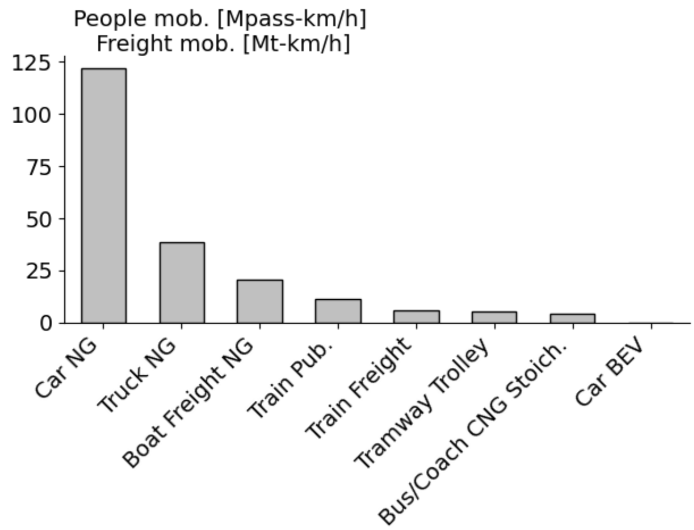

Figure D.4: Mobility assets

The energy system behavior is shown in the following figure.

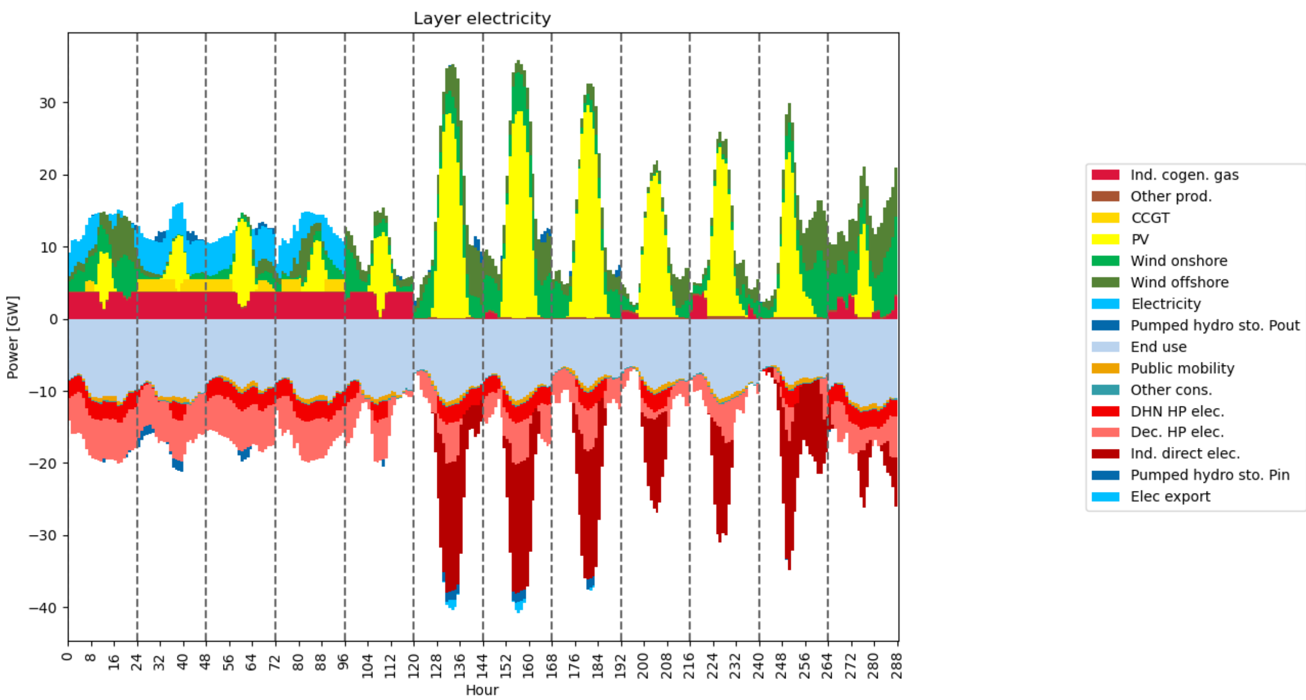

Figure D.5: Behavior of the energy system under the 25 $MtCO_{2eq}$ constraint

D.2 System with 10 $MtCO_{2eq}$ constraint

With the shift towards more stringent CO2 emission regulations, the energy system is undergoing a transition. Solar energy utilization is being expanded, accompanied by the adoption of Renewable Ammonia (Re. ammonia) for electricity generation, replacing the previous reliance on gas-fired

CCGTs). Additionally, there is an emergence of bio-diesel, employed for boat freight, while the diminishing use of gas is leading to a shift in the mobility sector towards electrified vehicles.

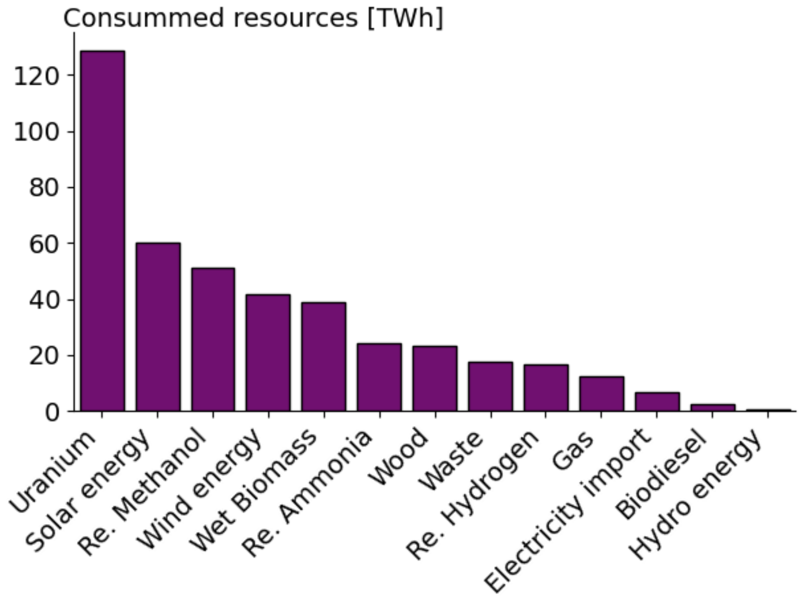

Figure D.6: Resource consumption in reference 10 $MtCO_{2eq}$ energy system

Figure D.7 illustrates notable changes in the energy system. There is a significant surge in PV utilization, accompanied by an increase in the utilization of ammonia-fired CCGTs, while the usage of traditional gas-fired CCGTs experiences a decline. The wind farm production has reached its maximum capacity, and we now rely on vehicle-to-grid technology for electricity storage, functioning similarly to pumped hydro storage. Similar to the previous energy system, heat generation primarily relies on electricity, with a slight rise in direct electricity-to-heat conversion and a reduction in gas cogeneration. We can also observe a large increase in seasonal HS.

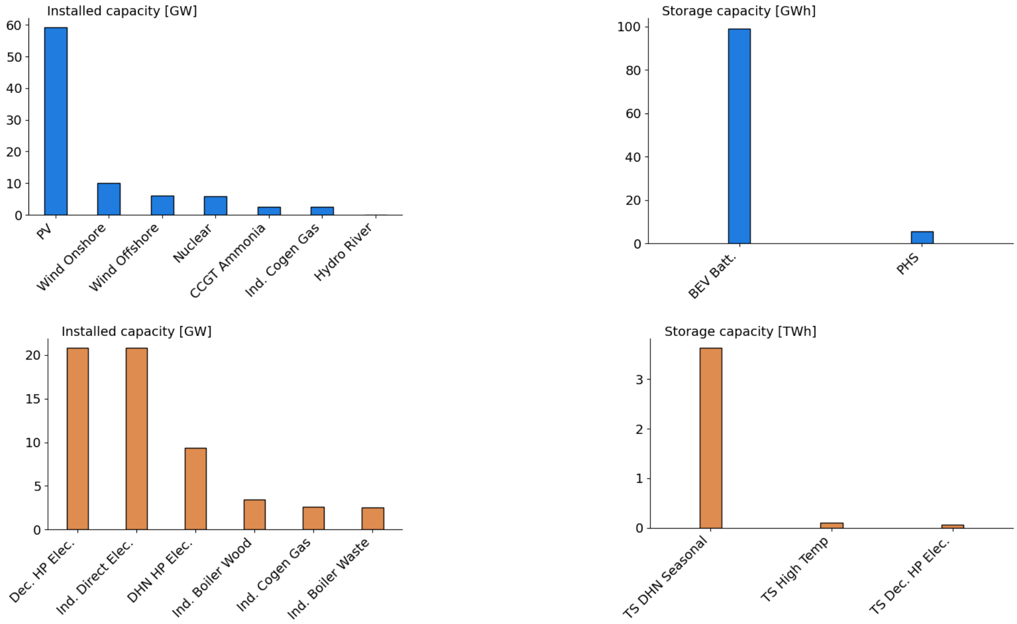

Figure D.7: Electricity and heat assets and respective storage

In the energy system, there is still a minor contribution of gas production from wet biomass. However, as the consumption of gas decreases, a corresponding reduction in gas storage is observed.

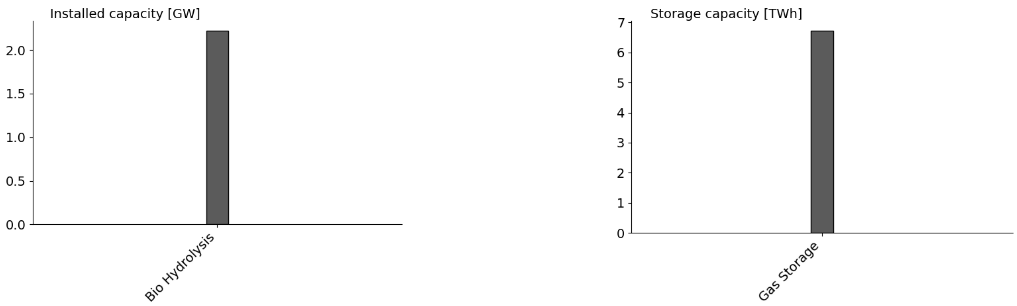

Figure D.8: Gas production and storage

As previously mentioned, the transition from natural gas vehicles to battery electric vehicles is taking place, along with the replacement of natural gas trucks with fuel cell trucks and boats with (bio)-diesel boats. However, due to the relatively lenient constraint on the system, natural gas cars are still present. This is shown in figure D.9

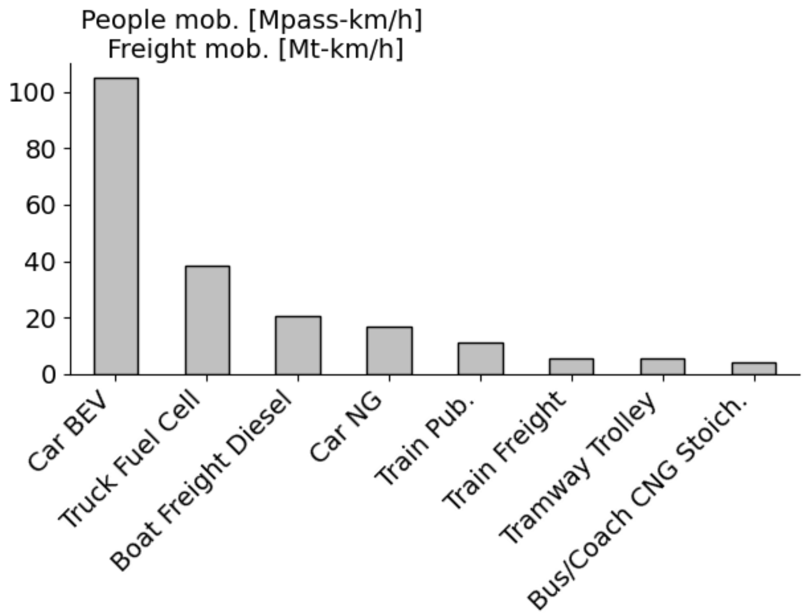

Figure D.9: Mobility assets

Finally, the energy system behavior is shown in the following figure.

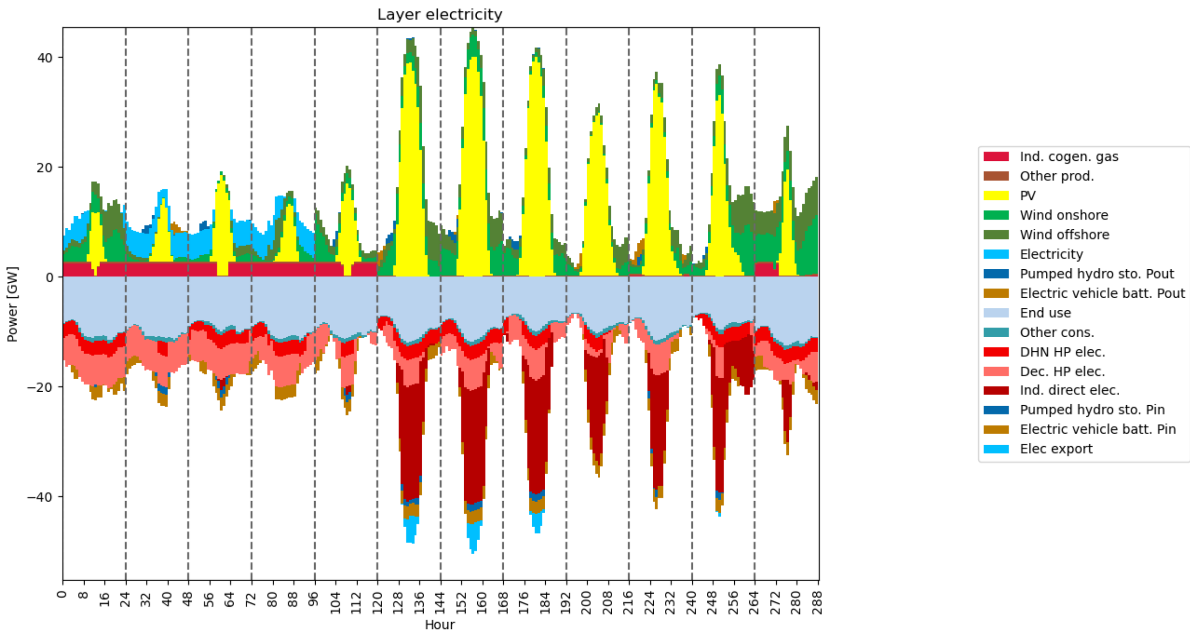

Figure D.10: Behavior of the energy system under the 10 $MtCO_{2eq}$ constraint

D.3 System with 5 $MtCO_{2eq}$ constraint

Lastly, as we reach the most constrained system, we observe the emergence of renewable hydrogen and renewable gas consumption, accompanied by a decrease in electricity imports.

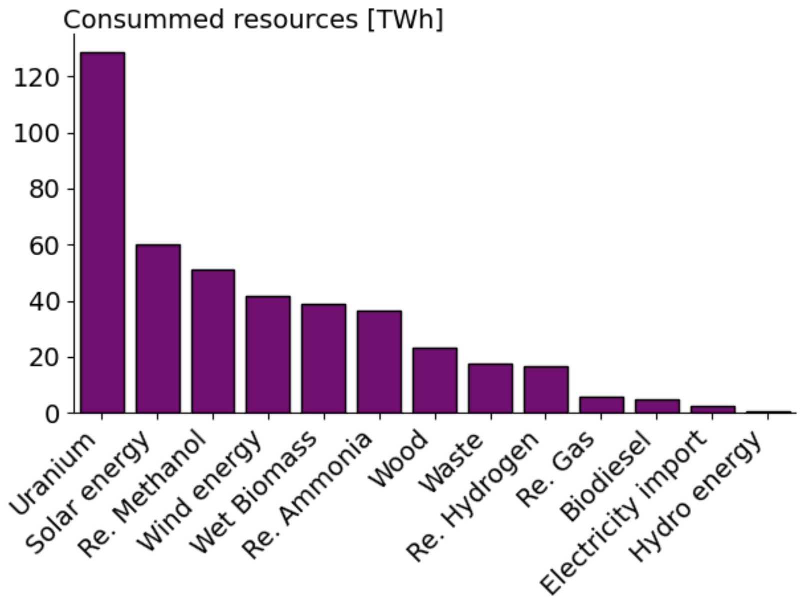

Figure D.11: Caption

In Figure D.12, it can be observed that the electricity and heat production assets remain relatively stable. However, with the ongoing electrification of the mobility sector, there is an increase in the storage capacity for electricity. Notably, there is a decrease in seasonal storage capacity, primarily driven by the expansion of electricity storage capacity and the rise in renewable fuel consumption.

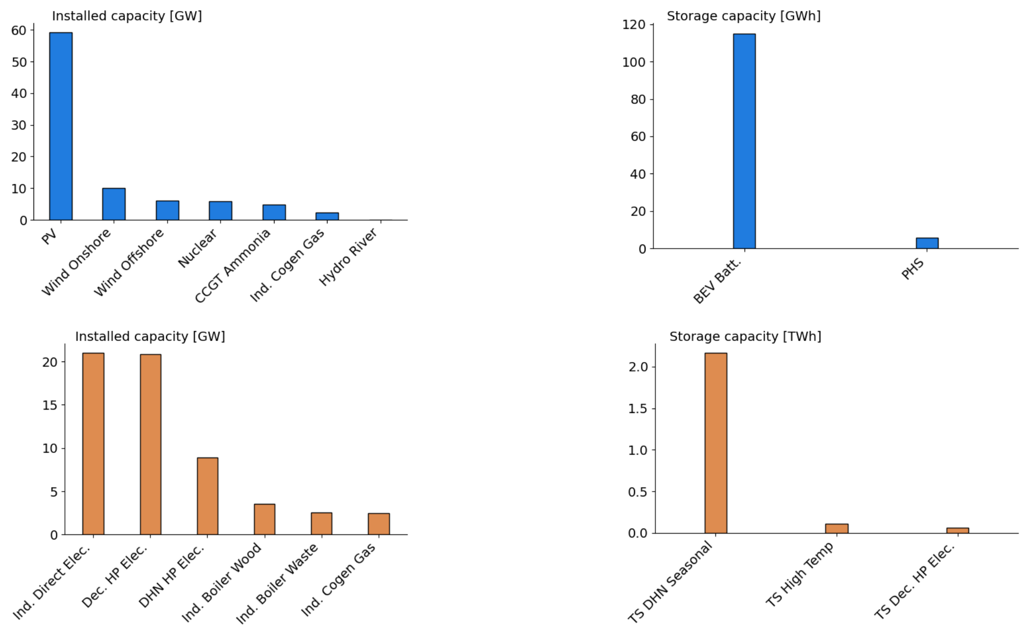

Figure D.12: Electricity and heat assets and respective storage

Once again, there is a reduction in gas storage capacity, although it is not completely eliminated as renewable gas is now being utilized. The production of gas from wet-biomass continues as part of the energy system.

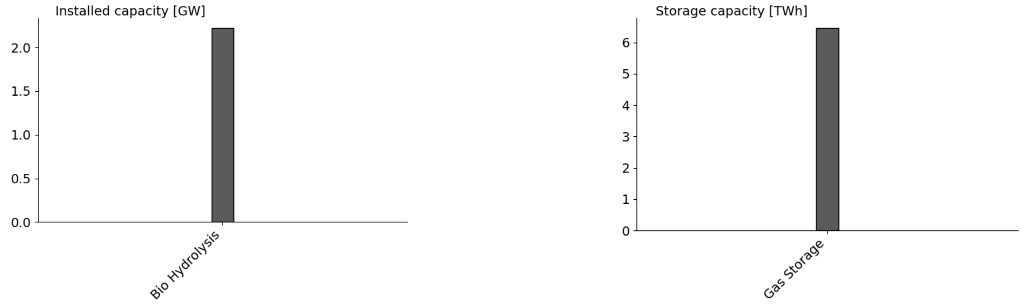

Figure D.13: Gas production and storage

In Figure D.14, we observe a dominance of battery electric vehicles, with other types of cars having disappeared entirely from the system.

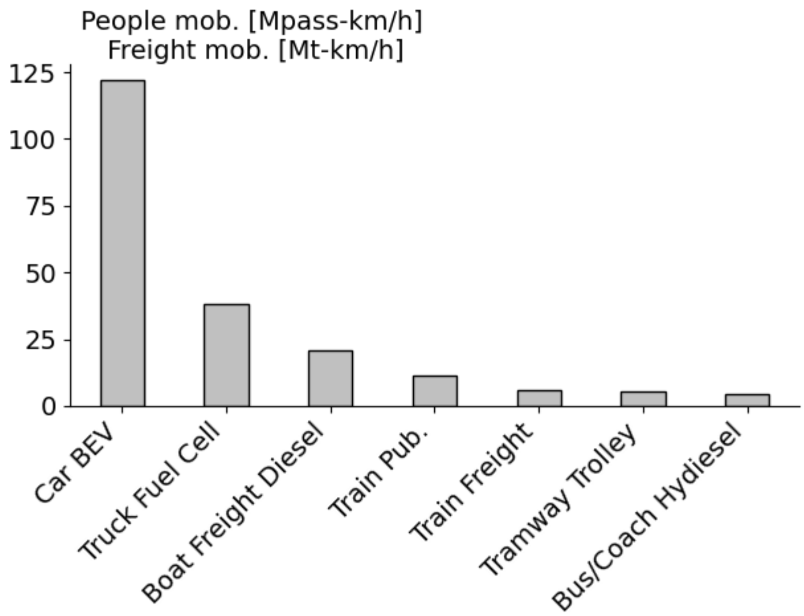

Figure D.14: Mobility assets

Finally, the energy system behavior is shown in the following figure.

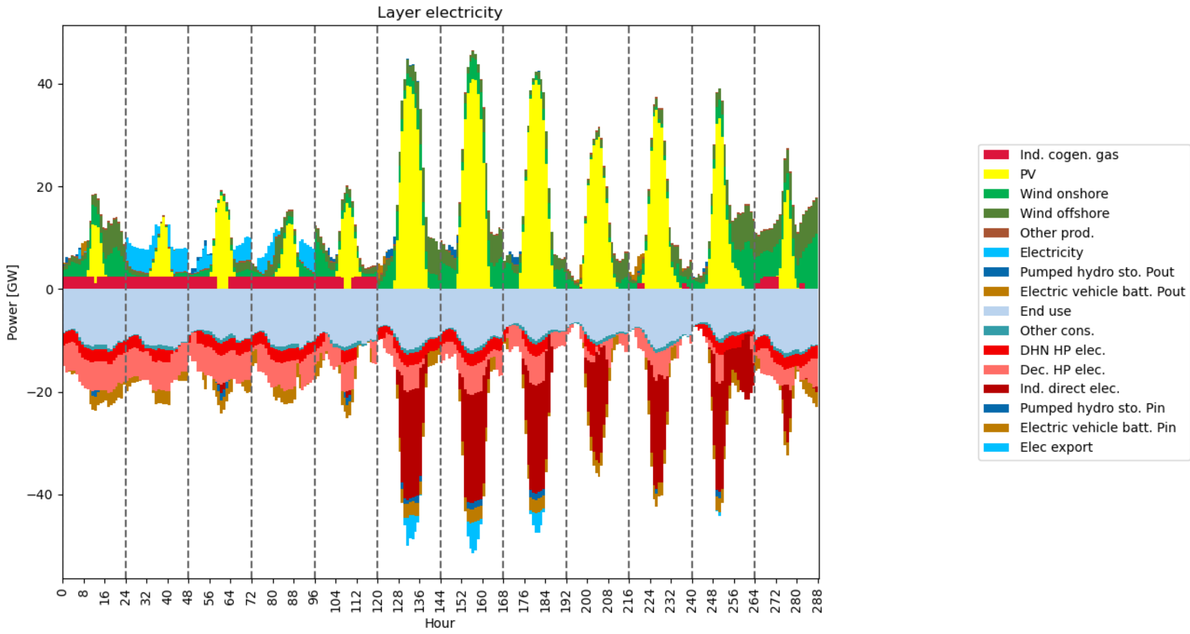

Figure D.15: Behavior of the energy system under the 5 $MtCO_{2eq}$ constraint

Appendix E

Discrepancy in costs per unit

The aim of this appendix is to explain why a CB with a lower efficiency would be deployed with a higher investment cost per unit of storage and power. The following figure shows a selection of points that highlight this characteristic.

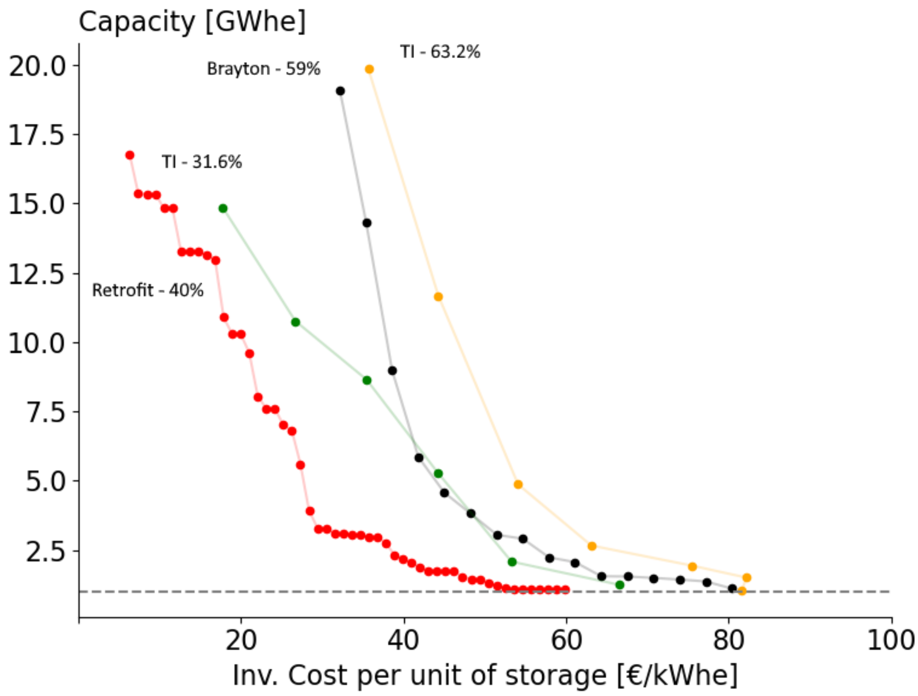

Figure E.1: Cost per unit of storage of deployed Carnot batteries

So we're going to work by elimination, and follow a first path that attempts to look at the number of cycles and the capacity factor of the two CBs in question. These two characteristics are presented in the following figures:

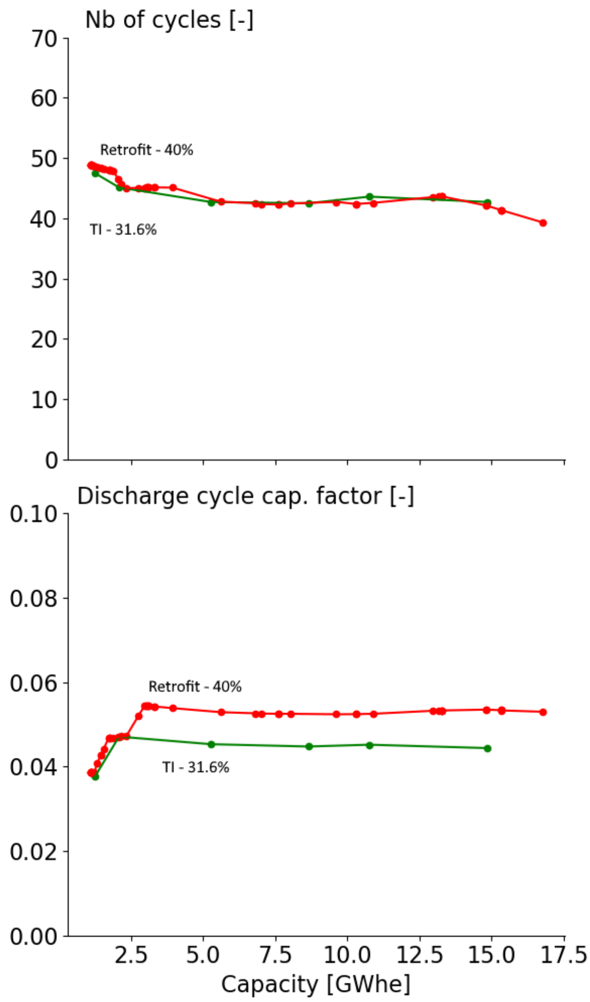

Figure E.2: Caption

The first graph shows that the number of cycles for the two systems is fairly similar for different capacities. The second graph shows that, for both systems, the discharge cycle operates between 4 and 5% of the time at maximum power, with the retrofit battery operating more often at higher power. These two graphs therefore do not specifically show an advantage for the thermally integrated battery.

Next, the costs of the specific components of each battery are inspected, and this time we notice a reason that could explain the deployment of the thermally integrated battery. In the figure E.3 below, we can see the costs per unit of each component.

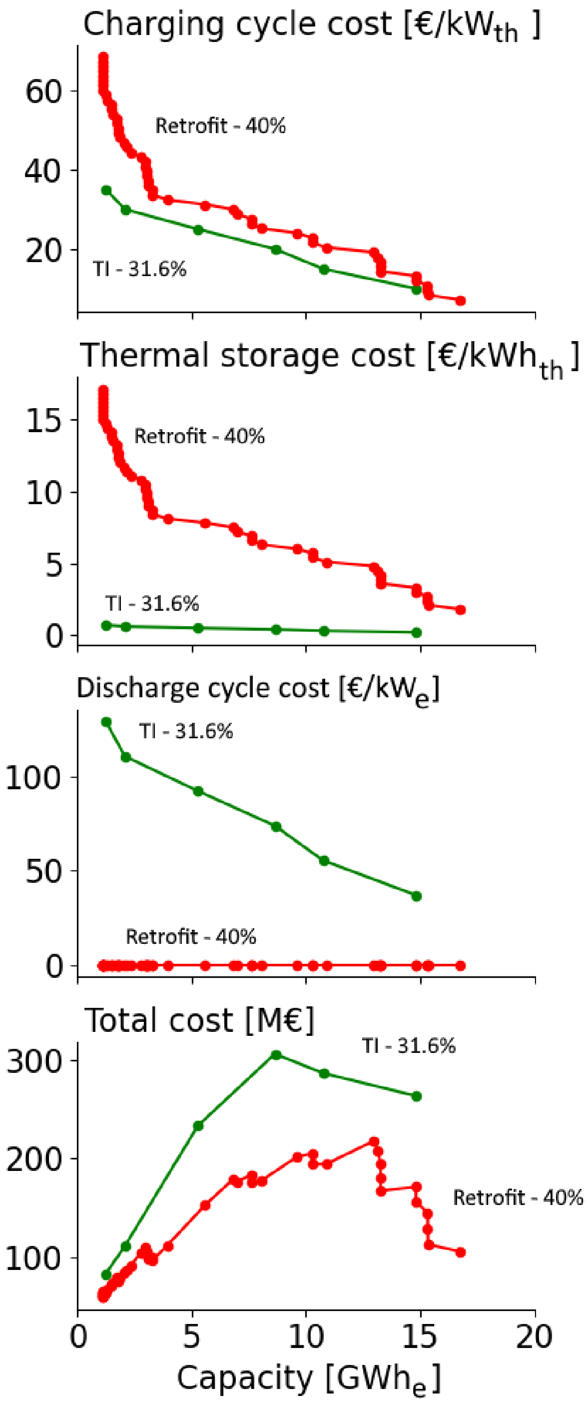

Figure E.3: Specific components costs

For the retrofit battery, investment costs for the charge cycle and storage are higher than for the thermally integrated battery. On the other hand, the opposite trend can be observed for the discharge cycle. We should therefore find ourselves with higher energy-to-power ratios in the case of the thermally-integrated battery. (since the power developed should, logically, be lower). However, this is not what is observed, as shown in figure E.4 below. In particular, the first figure shows that the power of the thermally integrated battery is higher than that of the retrofit battery. The reason for this is given in the following figure. This figure shows the evolution of maintenance costs for the thermally integrated battery and the retrofit battery. Because of its constant maintenance cost, the retrofit battery has rising maintenance costs, whereas the thermally integrated battery has very low maintenance costs. This prevents the deployment of more output power. Part of the system's costs are therefore obscured by these maintenance costs, and we therefore find ourselves with comparison issues when it comes to comparing the retrofit battery with other technologies.

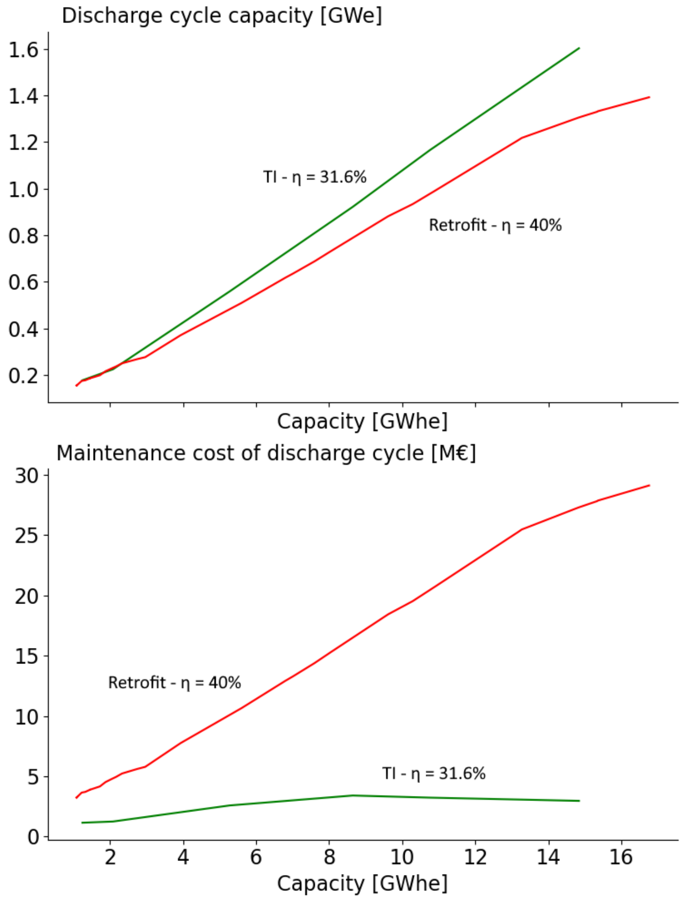

Figure E.4: Reason for discrepancy

We can therefore see that the technology is poorly positioned due to an implementation that does not reduce the costs associated with discharge cycle maintenance costs. The results linked to this battery should therefore, if we change the way we treat maintenance costs, give us more sensible results and increase the cost at which the retrofit battery is deployed (making it 'more interesting' from the point of view taken by this study).

We will first show the impact of a reduction in maintenance cost with the fraction of cost applied, the costs concerning the retrofitted CB will be formulated as follows, with x the applied cost fraction:

$$\begin{aligned} c_{inv} &= 0[€/kW] \\ c_{maint} &= 20.92 \times x[€/kWy] \end{aligned}$$

The results of this change are shown in the following figureE.5:

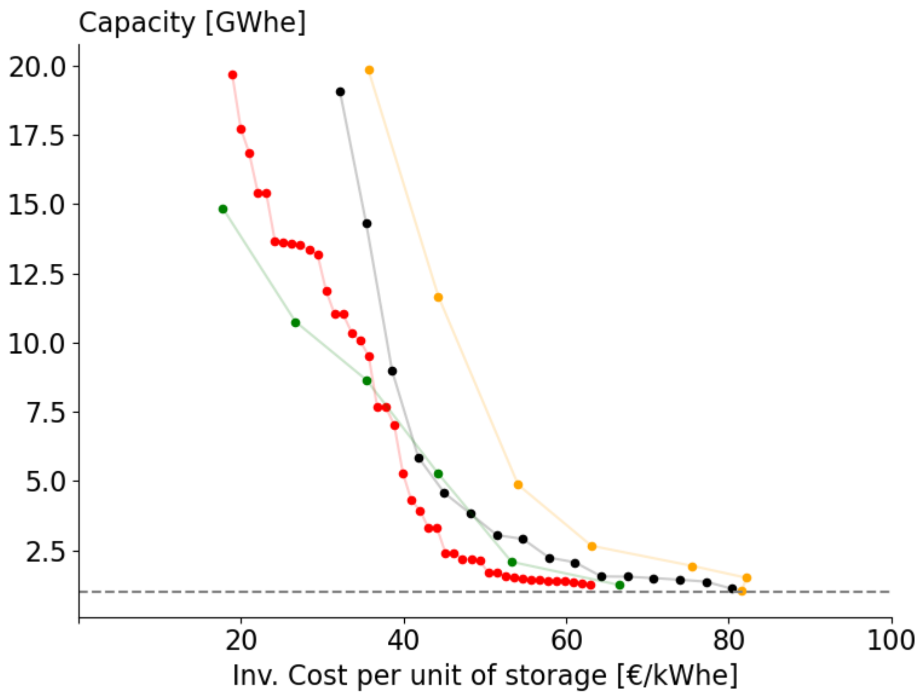

Figure E.5: Cost per unit of storage of Deployed Carnot batteries - Decreased retrofit maintenance costs

Despite this, we can see that the maintenance cost of the renovation battery's discharge cycle is an obstacle to its deployment, and that as this cost decreases, installed capacity increases.

Finally, if we're really looking for 'perfect' results, we can make the same assumption for all batteries. In other words, we can impose that maintenance costs are all strictly equal to 5% of investment costs. In this case the maintenance costs are written as follows for all CBs:

$$c_{maint} \quad = 5\% \times c_{inv}[€/kWy]$$

And we obtain the figure E.7:

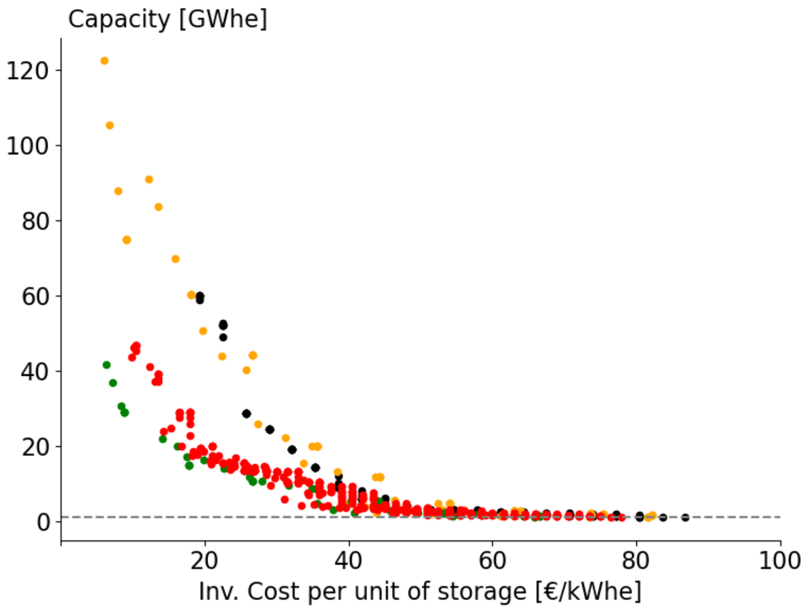

Figure E.6: Cost per unit of storage of Deployed Carnot battery - Maintenance cost is 5% of investment costs for all technologies

With this assumption, the deployment of the CB has a deployment that makes more physical sense. However, these results come with the assumption that the maintenance cost of the renovation battery's discharge cycle is zero, since its investment cost is itself zero.

A similar figure is provided for the costs per unit of power of the batteries where we can now observe that the retrofitted coal-fired powerplant battery is deployed earlier than all the other technologies since its discharge cycle is now free.

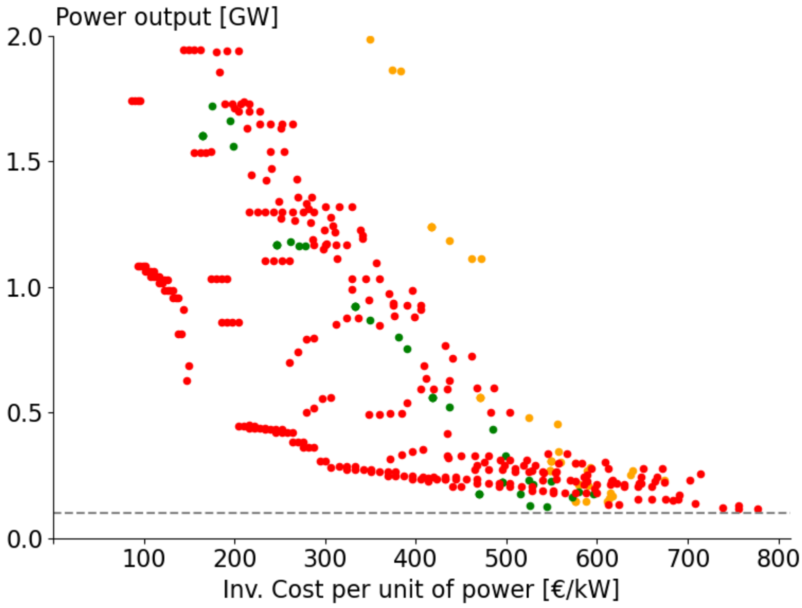

Figure E.7: Cost per unit of power of Deployed Carnot batteries - Maintenance cost is 5% of investment costs for all technologies

This appendix is very lengthy, and highlights the fact that uncertainty and the impossibility of finding data on investment costs, maintenance costs and correct cost projections lead to results that are highly dependent on the assumptions made by the author. The author of this work acknowledges that the methodology employed is not perfect and shows flaws, but these results can still be used, taking into account the hypothesis and the lessons that have been learned from this appendix.

Appendix F

Additional figures

This section is intended to add graphs that describe similar behaviors when analyzing energy systems. This section will first show the graphs for the system with a constraint of 10 $MtCO_{2e}q$ and then move on to the system with a constraint of 5 $MtCO_{2e}q$.

F.1 Energy system with 10 $MtCO_{2e}q$ constraint

In Chapter 3, we looked at the changes in system behavior following the insertion of the CB with regard to heat production. These changes are as follows:

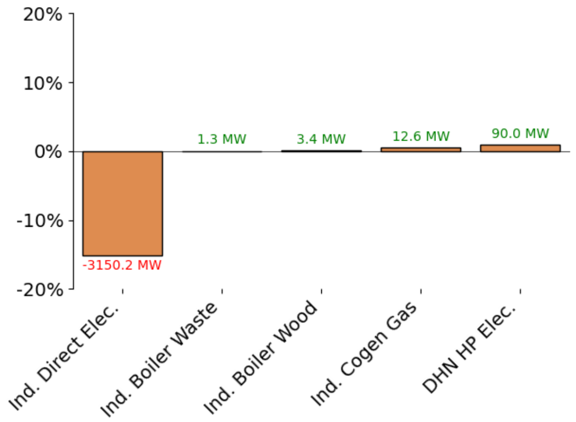

Figure F.1: (a) Retrofit - $\eta = 40\%$

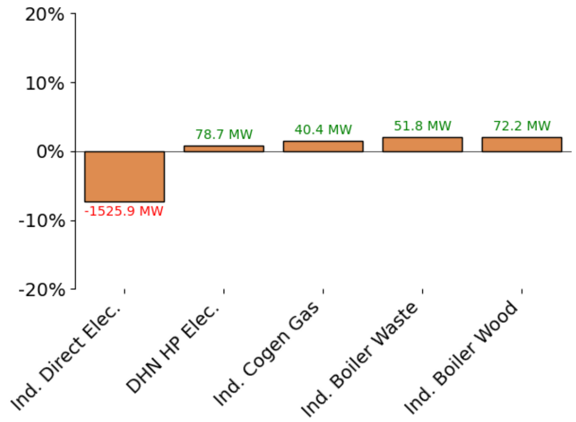

Figure F.2: (b) Brayton - $\eta = 59\%$

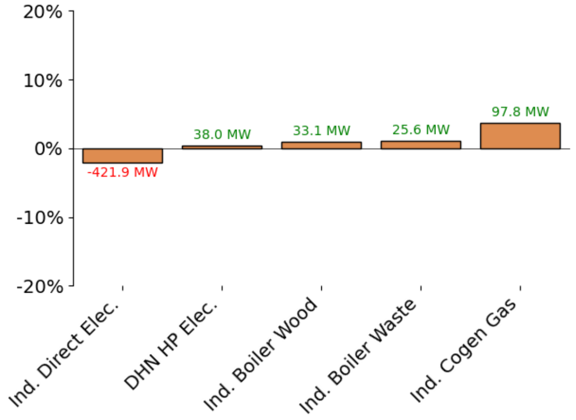

Installed capacity < 1 GWhe

Figure F.3: (c) TI - $\eta = 63.2\%$

Figure F.4: (d) TI - $\eta = 31.6\%$

Figure F.5: Difference in heating technology capacities due to Carnot battery insertion

As stated earlier, we see a change in industrial heat production, with a large decrease in installed capacity for industrial heat production through electric resistance, as well as small adjustments in production through industrial boilers. Finally, an adjustment in district heating network production is visible in all scenarios (similar to what we saw in the case where the constraint was 25 $MtCO_{2e}q$). Finally, for this constraint, the variation in heat production is accompanied by a variation in HS, as shown in the figure F.10 below.

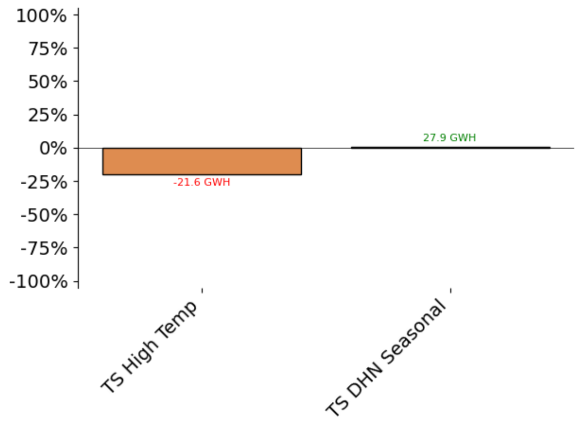

Figure F.6: (a) Retrofit - $\eta = 40\%$

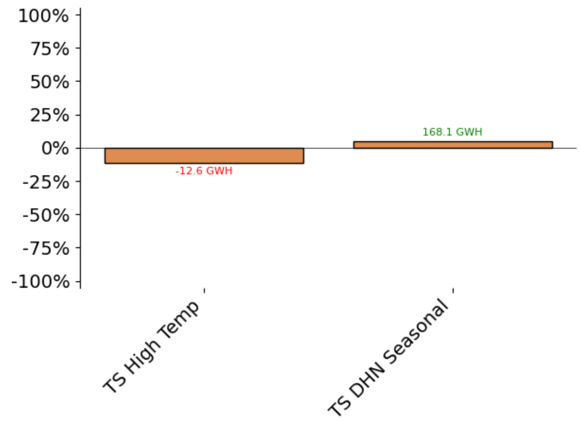

Figure F.7: (b) Brayton - $\eta = 59\%$

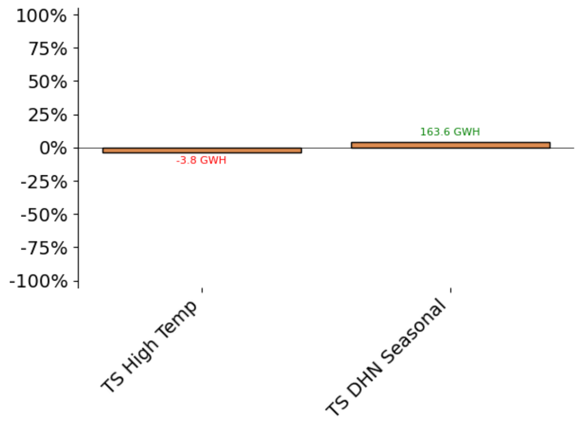

Figure F.8: (c) TI - $\eta = 63.2\%$

Installed capacity < 1 GWhe

Figure F.9: (d) TI - $\eta = 31.6\%$

Figure F.10: Difference in heating technology capacities due to Carnot battery insertion

F.2 Energy system with $5\,\mathrm{MtCO_{2e}q}$ constraint

As mentioned in Chapter 3, here are the figures for the electricity and heat generation as well as the HS.

This time, we can see that installed CCGT capacities are practically the same, due to the system's increased reliance on electricity. With this, we also see an increase in production due to cogeneration.

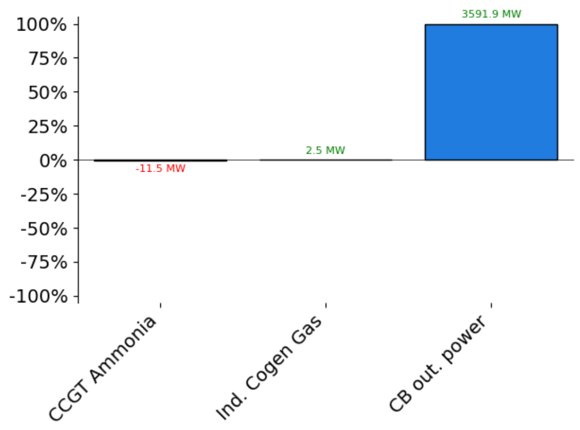

Figure F.11: (a) Retrofit - $\eta = 40\%$

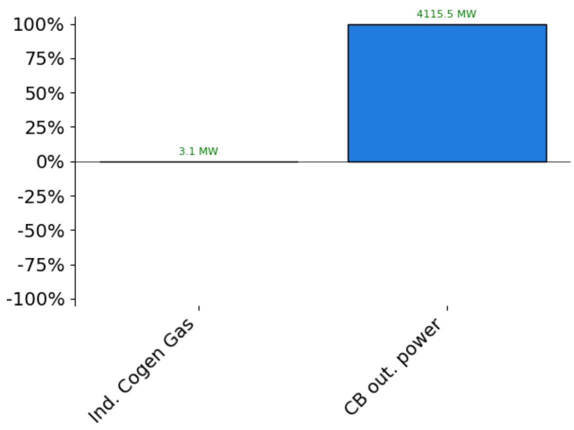

Figure F.12: (b) Brayton - $\eta = 59\%$

Figure F.13: Difference in electricity technology capacities due to Carnot battery insertion

On the heat generation side, shown in figure F.19, the variations shown in this graph are similar to those observed previously. There is a decrease in the capacity to produce process heat using electrical resistance. This is accompanied by small changes in wood-fired process heat production and a slight increase in (renewable) gas-fired cogeneration. Finally, a decrease in the installed capacity of electric heat pumps in district heating networks is observed, but this is offset by an increase in seasonal storage, as can be seen in the figure F.19 below:

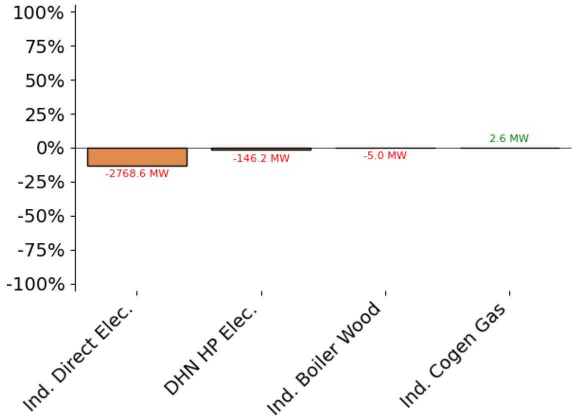

Figure F.14: (a) Retrofit - $\eta = 40\%$

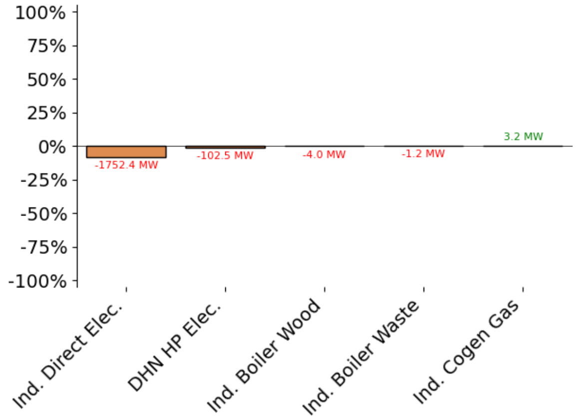

Figure F.15: (b) Brayton - $\eta = 59\%$

Figure F.16: Difference in heating technology capacities due to Carnot battery insertion

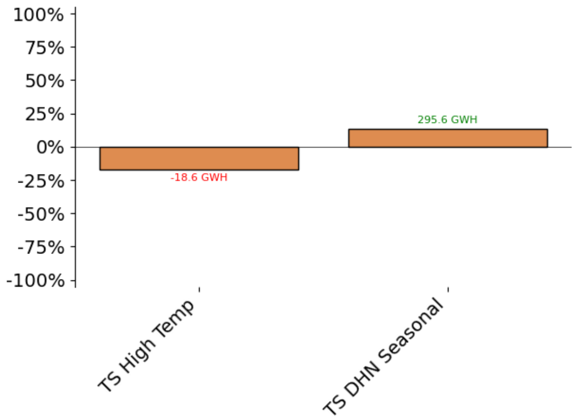

Figure F.17: (a) Retrofit - $\eta = 40\%$

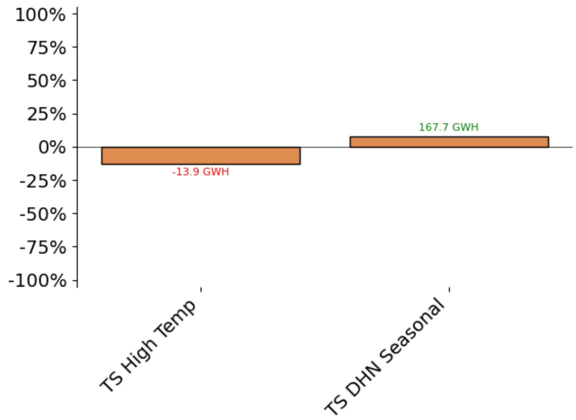

Figure F.18: (b) Brayton - $\eta = 59\%$

Figure F.19: Difference in heat storage capacities due to Carnot battery insertion

F.3 Number of cycles

Here are the numbers of cycles for the other CBs studied. As this number is similar, the figures have been appended so as not to overload readers.

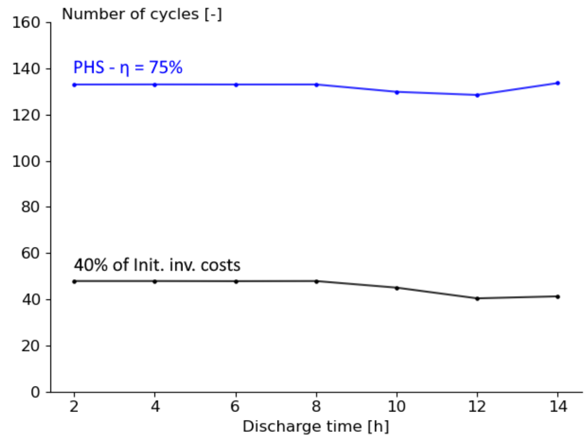

Figure F.20: (a) Retrofit - $\eta = 40\%$

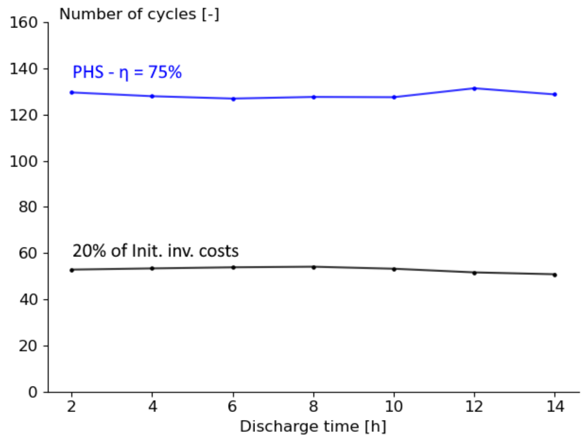

Figure F.21: (b) Brayton - $\eta = 59\%$

Figure F.22: Number of cycles for Retrofit and Brayton Carnot batteries

F.4 Discharge time - Comparison

This appendix compares two systems with a CB. The first system has a minimum discharge time of 6 hours, while the second has a discharge time of 14 hours. We can see a reduction in the power of the discharge cycles and the addition of certain components that go beyond everyday behavior, enabling night-time and early-morning discharges. (Circled in dotted red on figure .)

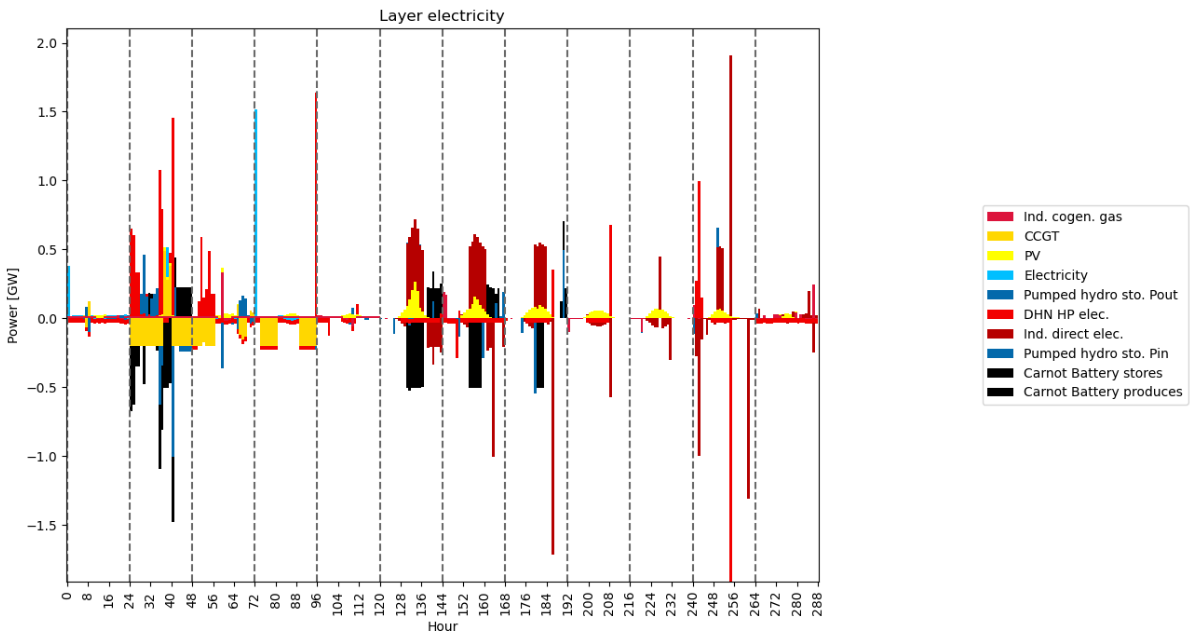

Figure F.23: Carnot battery behavior with $\tau_{disch} = 6\,\text{h}$

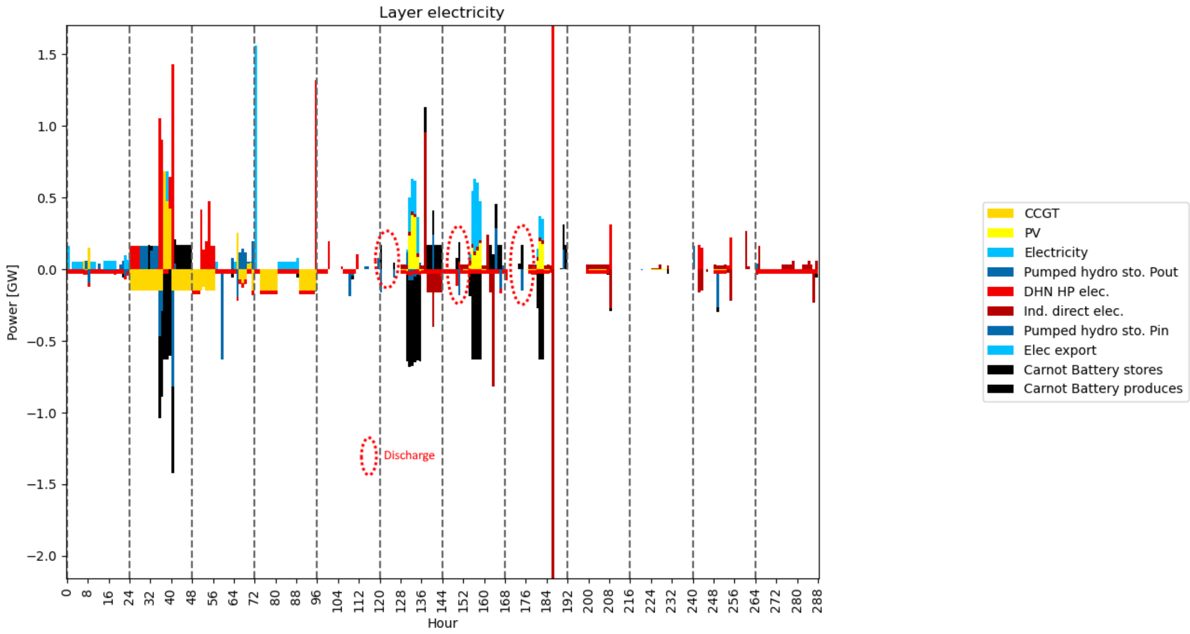

Figure F.24: Carnot battery behavior with $\tau_{disch} = 14\,\text{h}$

UNIVERSITÉ CATHOLIQUE DE LOUVAIN
École polytechnique de Louvain
Rue Archimède, 1 bte L6.11.01, 1348 Louvain-la-Neuve, Belgique | **www.uclouvain.be/epl**